

4.21 One View of the Geochemistry of Subduction-Related Magmatic Arcs, with an Emphasis on Primitive Andesite and Lower Crust

PB Kelemen, Columbia University, Palisades, NY, USA

K Hanghøj, Lamont-Doherty Earth Observatory of Columbia University, Palisades, NY, USA

AR Greene, University of British Columbia, Vancouver, BC, Canada

© 2014 Elsevier Ltd. All rights reserved.

This article is reproduced from the previous online update, volume 3, pp. 1–70, © 2007, Elsevier Ltd.

4.21.1	Introduction	749
4.21.1.1	Definition of Terms Used in This Chapter	750
4.21.2	Arc Lava Compilation	750
4.21.3	Characteristics of Arc magmas	751
4.21.3.1	Comparison with MORBs	751
4.21.3.1.1	Major elements	752
4.21.3.1.2	We are cautious about fractionation correction of major elements	756
4.21.3.1.3	Distinctive, primitive andesites	757
4.21.3.1.4	Major elements in calc-alkaline batholiths	757
4.21.3.2	Major and Trace-Element Characteristics of Primitive Arc Magmas	762
4.21.3.2.1	Primitive basalts predominate	765
4.21.3.2.2	Are some low Mg# basalts primary melts? Perhaps not	766
4.21.3.2.3	Boninites, briefly	766
4.21.3.2.4	Primitive andesites: a select group	766
4.21.3.2.5	Three recipes for primitive andesite	767
4.21.3.3	Trace Elements, Isotopes, and Source Components in Primitive Magmas	772
4.21.3.3.1	Incompatible trace-element enrichment	772
4.21.3.3.2	Tantalum and niobium depletion	776
4.21.3.3.3	U-series isotopes	778
4.21.3.3.4	Geodynamic considerations	781
4.21.4	Arc Lower Crust	782
4.21.4.1	Talkeetna Arc Section	783
4.21.4.1.1	Geochemical data from the Talkeetna section	784
4.21.4.1.2	Composition, fractionation, and primary melts in the Talkeetna section	788
4.21.4.2	Missing Primitive Cumulates: Due to Delamination	791
4.21.4.3	Garnet Diorites and Tonalites: Igneous Garnet in the Lower Crust	795
4.21.5	Implications for Continental Genesis	795
4.21.5.1	Role of Lower Crustal Delamination in Continental Genesis	795
4.21.5.2	Additional Processes are Required	796
4.21.5.2.1	Andesitic arc crust at some times and places	796
4.21.5.2.2	Arc thickening, intracrustal differentiation, and mixing	796
4.21.6	Conclusions	796
Acknowledgments		797
References		797

4.21.1 Introduction

This chapter has four main aims. We wish to provide a comprehensive picture of the composition of volcanic rocks from subduction-related magmatic arcs. There are several recent reviews of the geochemistry of arc basalts. This chapter differs in including andesites as well as basalts, in focusing on major elements, as well as trace elements and isotopes, and in using elemental abundance in ‘primitive’ lavas, rather than trace-element ratios, to investigate enrichments of incompatible elements in arc magmas relative to primitive mid-ocean ridge basalts (MORBs).

1. We review evidence in favor of the existence of andesitic, as well as basaltic primary magmas in arcs. While we have recently reviewed evidence for this in the Aleutian arc, in this chapter we broaden our data set to arcs worldwide, and concentrate on whether mixing of lower crustal melts with primitive basalts offers a viable alternative to the hypothesis that there are ‘primary’ andesites, i.e., andesites in Fe/Mg equilibrium with mantle olivine, passing from the mantle into the crust beneath arcs.
2. We present new data on the composition of arc lower crust, based mainly on our ongoing work on the Talkeetna arc section in south-central Alaska. To our knowledge, this is

the first complete ICP-MS data set on an arc crustal section extending from the residual mantle to the top of the volcanic section.

3. We summarize evidence from arc lower crustal sections that a substantial proportion of the dense, lower crustal pyroxenites and garnet granulites produced by crystal fractionation are missing. These lithologies may have been removed by diapirs descending into less dense upper mantle.

To achieve these aims and limit the length of the chapter, we have not provided a detailed review of theories regarding the origin of primitive arc basalts, the mixing of magmatic components derived from the upper mantle, aqueous fluids, and sediment melts, or open-system processes in the crust including mixing and assimilation. For a more complete view of these theories, we refer the reader to the many excellent review papers and individual studies that are, all too briefly, cited below.

4.21.1.1 Definition of Terms Used in This Chapter

The following terms are used extensively throughout this chapter, and/or in the recent arc literature. We have tried to define each term where it first arises in the text. However, we realize that not all readers will read every section. Thus, we include the following brief definitions here.

Accumulated minerals. These are crystals in lavas that are in excess of the amounts that could crystallize from a melt in a closed system. Similar to cumulates, some cases of accumulated crystals may be impossible to detect, but others stand out because they result in rock compositions different from all or most terrestrial melts.

Adakite. This term is justly popular, but unfortunately it means many different things to different people, so we try not to use it. It is generally used for andesites and dacites with extreme light rare-earth element (REE) enrichment (e.g., La/Yb > 9), very high Sr/Y ratios (e.g., Sr/Y > 50), and low yttrium and heavy REE concentrations (e.g., Y < 20 ppm, Yb < 2 ppm).

Andesite. For the purposes of this chapter, andesites are simply lavas (or bulk compositions) with >54 wt% SiO₂. For brevity, we have not subdivided relatively SiO₂-rich magmas into dacite, rhyodacite, etc.

Basalt. In this chapter, basalt means lavas or bulk compositions with <54 wt% SiO₂. Note that we have eliminated alkaline lavas (nepheline or kalsilite normative) from the data compilation. In a few places, we use terms picrite and komatiite to refer to basaltic melts with more than 15 and 18 wt% MgO, respectively.

Boninite. By boninites, we mean andesites with TiO₂ < 0.5 wt%, plus lavas identified as boninites in the original papers presenting geochemical data (includes some basalts).

Calc-alkaline. These are magmas having both high Na + K at high Mg# (Irvine and Baragar, 1971) and high SiO₂ at high Mg# (i.e., high SiO₂ at low Fe/Mg; Miyashiro, 1974); 'tholeiitic magmas' have lower SiO₂ and Na + K at the same Mg#, when compared with calc-alkaline magmas.

Compatible element. An element with equilibrium solid/melt partition coefficient > 1. In garnet (and zircon), heavy REE,

scandium, vanadium, and yttrium are compatible. These elements are incompatible in all other rock-forming minerals involved in igneous fractionation processes discussed in this chapter.

Cumulate. A rock formed by partial crystallization of a melt, after which the remaining melt is removed. While some cumulates may be difficult to recognize, others are evident because the cumulate mineral assemblage has major and/or trace-element contents distinct from all or most terrestrial melts, easily understood as the result of crystal/melt partitioning.

Eclogite facies. This term represents high-pressure and relatively low-temperature, metamorphic parageneses with omphacitic clinopyroxene and pyrope-rich garnet.

EPR. East Pacific Rise.

Evolved. Lavas, melts, and liquids with Mg# < 50.

JDF. Juan de Fuca Ridge.

High Mg#. Lavas, melts, liquids with Mg# from 50 to 60.

Incompatible element. Equilibrium solid/melt partition coefficient < 1.

LILEs. Large ion lithophile elements, rubidium, radium, barium, potassium (and cesium – but we do not use cesium data in this chapter). Although they are not, strictly speaking, LILE, we sometimes group thorium and uranium with the LILE when referring to elements that are highly incompatible.

Mantle wedge. 'Triangular' region underlying arc crust, overlying a subduction zone, extending to perhaps 400 km depth.

Mg#. 100 × molar MgO/(MgO + FeO), where all iron is treated as FeO.

MORB. Mid-ocean ridge basalt.

Primary. Lavas, melts, and liquids derived solely via melting of a specific, homogeneous source. In practice, it is hard to recognize or even conceive of a truly primary melt. Strictly speaking, even mantle-derived MORBs may be mixtures of primary melts derived from a variety of sources, including polybaric melts of variably depleted peridotites and/or 'basaltic veins.' For brevity, we have used the term 'primary' in a few cases in this chapter. Where it is used without qualification, we refer to melts that are, or could be, in equilibrium with mantle olivine with Mg# of 90–93.

Primitive. Lavas, melts, and liquids with Mg# > 60. Primitive cumulates have Mg# > 85.

REE groups. Light – lanthanum to samarium; middle – europium to dysprosium; heavy – holmium to lutetium.

Subduction-related magmatic arc (or simply, arc). Chains of volcanoes on the overthrust plate parallel to, and ~100–200 km horizontally away from, the surface expression of a subduction zone, together with coeval, underlying plutonic rocks.

4.21.2 Arc Lava Compilation

Data in this and subsequent sections are from the [Georoc database \(2006\)](#) (arcs worldwide), our Aleutian arc compilation, including all data available from the database compiled by James Myers and Travis McElfrish and available at the [Aleutian arc website \(2006\)](#), supplemented by additional data cited in [Kelemen et al. \(2003b\)](#), a new Costa Rica and Panama compilation ([Abratis and Worner, 2001](#); [Carr et al.,](#)

1990; Cigolini et al., 1992; de Boer et al., 1991, 1988, 1995; Defant et al., 1991a,b, 1992; Drummond et al., 1995; Hauff et al., 2000; Herrstrom et al., 1995; Patino et al., 2000; Reagan and Gill, 1989; Tomascek et al., 2000), and Central American data compiled by Mike Carr and available at <http://www.rci.rutgers.edu/carr/index>. We also included a very complete data set on lavas from Mt. Shasta in the southern Cascades (Baker et al., 1994; Grove et al., 2001). We compare compositions of arc lavas to data on MORB glasses downloaded from the *PetDB* website (2006).

Lava data come from intra-oceanic arcs (Tonga, $n=704$; Kermadec, 189; Bismark/New Britain, 165; New Hebrides, 252; Marianas, 834; Izu-Bonin, 878; oceanic Aleutians, 1082; South Sandwich, 328; Lesser Antilles, 356) and arcs that are, or may be, emplaced within older continental material or thick sequences of continentally derived sediment (Philippines, 221; Indonesia, 380; Papua New Guinea, 78; SW Japan, 92; NW Japan, 2314; Kuriles, 721; Kamchatka, 447; Cascades, 202; Central America, 857; the Andes, 1156; Greater Antilles, 175). Notably missing are data from New Zealand, the Alaska Peninsula, and Mexico. We apologize to authors whose work is not cited here, but whose analyses we compiled using large, online databases. It is simply not practical to cite the sources of all the data compiled for this chapter. We urge readers to contact us, and to visit the online databases, to check on the provenance of specific data.

In comparing arc lavas to MORB glasses, it is important to keep in mind that none of our arc data sets discriminates between true liquid compositions, and compositions of lavas potentially including abundant, accumulated phenocrysts. Many of the lavas in our complete compilation had MgO contents >20 wt% at 100 MgO/(MgO + FeO), or $Mg\# > 65$. Samples with more than 20 wt% MgO have been eliminated from all our plots; we believe these, and possibly many other lavas with 10–20 wt% MgO, reflect the effect of accumulated olivine. In addition, many high-Mg# lavas with lower MgO contents contain abundant phenocrysts of clinopyroxene and/or olivine. The high Mg# of such samples could be due to accumulated clinopyroxene or olivine, at least in part. High-Mg# andesites play a large role in the interpretive sections of this chapter, and thus this problem should be kept in mind. With this said, the high SiO_2 and alkali contents and the low MgO and CaO contents of these samples, and the similarity of nearly aphyric primitive andesites from Mt. Shasta (Baker et al., 1994; Grove et al., 2001) to other similar compositions worldwide does not allow for much accumulated olivine and clinopyroxene. Finally, abundant accumulated plagioclase probably accounts for some lava compositions with very high Al_2O_3 contents (e.g., Brophy, 1989; Crawford et al., 1987). However, because this may remain controversial, we did not eliminate lavas on the basis of Al_2O_3 content.

Another issue is that when relying on compiled information from databases, one has to be aware of the possibility that data may have been incorrectly entered, transferred, or normalized. Thus, for visual clarity, we eliminated some outliers, including lavas with more than 80 wt% SiO_2 and $Mg\# > 50$, lavas with more than 70 wt% SiO_2 and $Mg\# > 60$, lavas with <10 wt% MgO and $Mg\# > 80$, and lavas with <5 wt% MgO and $Mg\# > 75$. We also eliminated alkali basalts (normative nepheline or kalsilite), especially in data compilations for the

Sunda and Honshu arcs, and placed boninitic lavas (>54 wt% SiO_2 , <0.5 wt% TiO_2 , plus samples described in the original data sources as boninites) in a group separate from other lavas.

A third issue in using large numbers of compiled data is quality. Analytical methods have varied over time, and some labs are more reliable than others. Outliers appear on many of our plots, particularly those involving trace elements. In some cases, where outliers are orders of magnitude different from the bulk of the data, we have adjusted axis limits in plots so that outliers are no longer visible but the variation in the bulk of the data is easily seen. However, other than this, we have not made any attempt in this chapter to discriminate between ‘good’ and ‘bad’ data. This approach is deliberately different from other recent reviews of arc data (e.g., Elliott, 2003; Plank, 2003). We are not critical of these other reviews, but we think an alternative, more inclusive approach may be useful until a truly large number of high-quality ICP-MS data become available for a fully representative set of arc magma compositions worldwide. In particular, a focus of this chapter – on the origin of primitive andesites and calc-alkaline magma series – would be all but impossible if we restricted attention to data sets including ICP-MS analyses. We urge readers to be cautious in interpreting our data plots, and to check key points for themselves. Also, we believe this chapter indicates several areas in which additional data would be very valuable.

Finally, a substantial limitation of our compilation is that it includes very sparse data on chlorine, fluorine, boron, beryllium, and lithium, and essentially no data on volatile contents (H_2O , CO_2 , sulfur, and noble gases). While data on H_2O in glass inclusions are beginning to become available, it is not yet clear, for example, to what extent H_2O contents in primitive arc magmas correlate with other compositional characteristics. We look forward to learning more about these topics.

4.21.3 Characteristics of Arc magmas

4.21.3.1 Comparison with MORBs

In this section, we compare arc lava compositions (on an anhydrous basis) with compositions of MORB glasses; also see Chapter 4.13. The contrasts are remarkably distinct (Figure 1). Before we go on to describe these contrasts, it is convenient to define ‘primitive andesites’ (lavas with $SiO_2 > 54$ wt% and $Mg\# > 60$, exclusive of boninites) and ‘high-Mg# andesites’ ($SiO_2 > 54$ wt% and $Mg\# > 50$). These classifications include primitive and high-Mg# lavas that are dacites and even rhyolites, as well as true andesites. However, we group them all for brevity.

Implicit in our definition of lavas with $Mg\# > 60$ as ‘primitive’ and those with lower $Mg\#$ as ‘evolved’ is the assumption that crystallization processes always produce a lower $Mg\#$ in derivative liquids, as compared with parental liquids. As far as we know, this assumption is justified on the basis of all available experimental data on crystallization/melting of igneous rocks with $Mg\#$ higher than 40 (see compilation in Kelemen 1995) at oxygen fugacities within 2 log units of Ni–NiO (typical for arcs, Blatter and Carmichael 1998; Brandon and Draper, 1996; Gill, 1981; Parkinson and Arculus, 1999), or lower. Oxygen fugacity more than 2 log units above Ni–NiO may facilitate early and abundant crystallization of FeTi oxides,

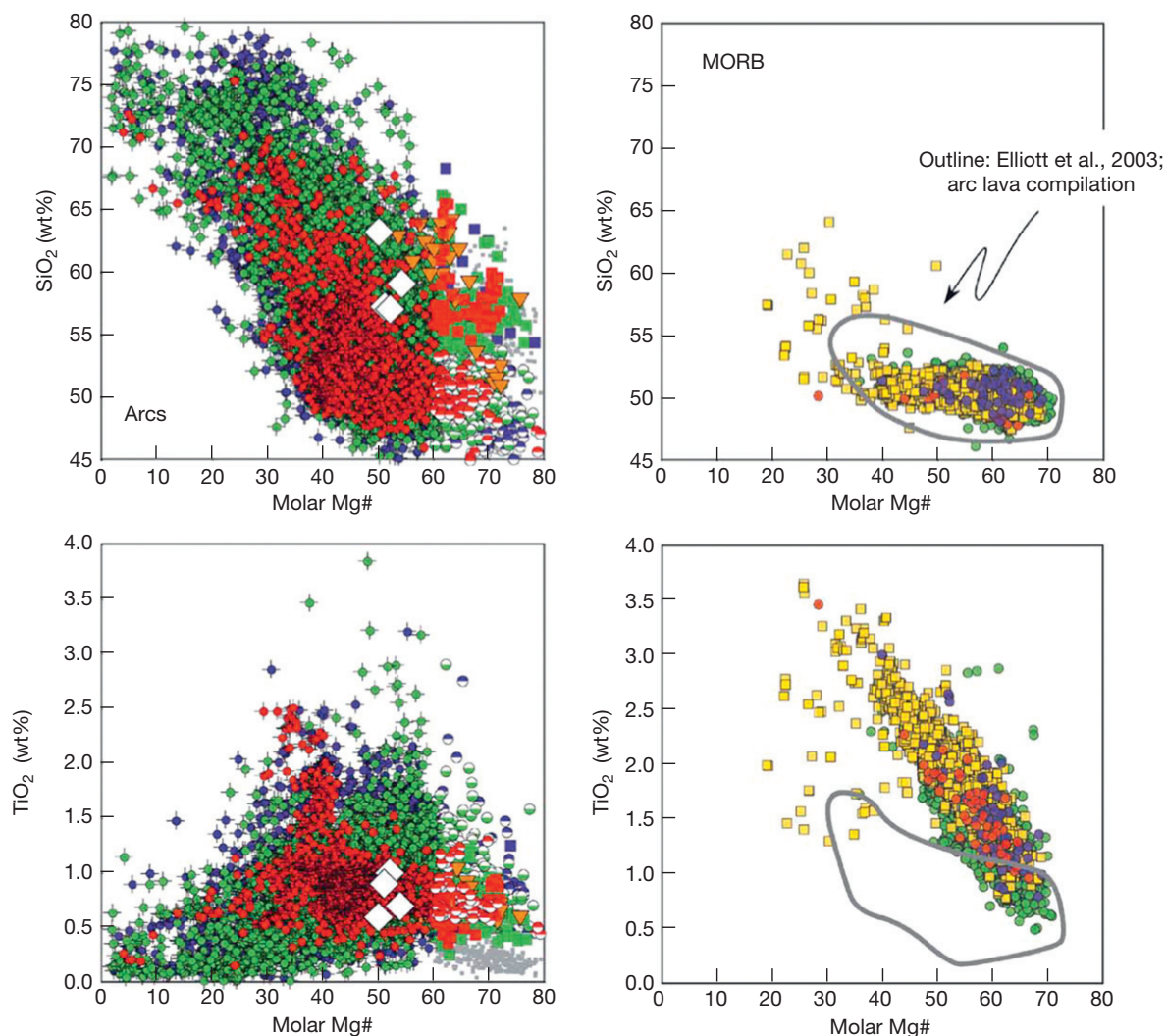


Figure 1 Molar Mg# versus concentrations of major-element oxides, in weight percent, in arc lavas (left) and MORB glasses (right), both on an anhydrous basis. Outlined fields on the right-hand diagrams show the range of variation in arc lava compilation of Elliott (2003). Arc and MORB data sources are described in text. For MORB, yellow squares are EPR, green circles are Atlantic, red JDF, and blue Indian. For primitive arc lavas with Mg# > 60, half-filled circles are basalts and squares andesites; evolved lavas with Mg# < 60 are circles with barbs. Blue symbols are for oceanic arcs, green for continental arcs, and red for the oceanic Aleutian arc. Boninites are shown with small gray squares. Inverted orange triangles are for primitive andesites and basalts from Mt. Shasta, southern Cascades (Grove et al., 2001). Intra-oceanic arcs in our data set are from Tonga, Kermadec, Bismark/New Britain, New Hebrides, Marianas, Izu-Bonin, South Sandwich, and the Lesser Antilles. Samples from arcs in our compilation which are, or may be, emplaced within older continental material or thick sequences of continentally derived sediment are from the Philippines, Indonesia, Papua New Guinea, SW Japan, NW Japan, Kuriles, Kamchatka, Cascades, Central America, the Andes, and the Greater Antilles. Large filled diamonds are estimated compositions of the continental crust from Christensen and Mooney (1995), McLennan and Taylor (1985), Rudnick and Fountain (1995), and Weaver and Tarney (1984), including Archean estimate of Taylor and McLennan.

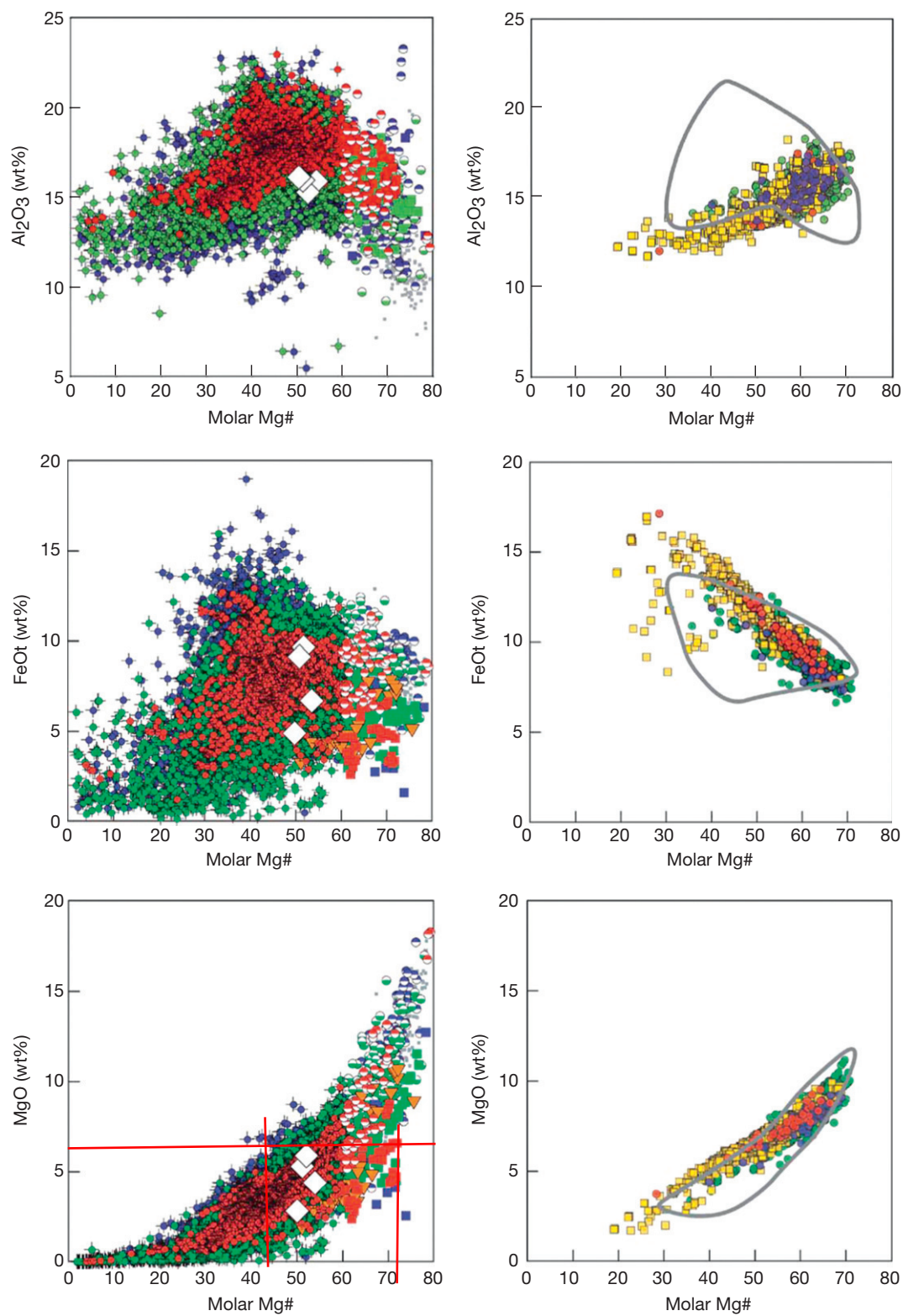
(Continued)

and thus nearly constant Mg# with decreasing temperature and liquid mass (Kawamoto, 1996). However, this is unlikely beneath most arcs.

4.21.3.1.1 Major elements

We first examine major elements as a function of Mg# (Figure 1). A very small fraction of MORB glasses have Mg# < 35, whereas lavas with Mg# < 35 are common in arcs. While SiO₂ in primitive (Mg# > 60) MORB is restricted to

48–52 wt%, primitive arc lavas range from 45 wt% to more than 60 wt% SiO₂. The contrast for evolved (Mg# < 60) compositions is even more striking. Overall, Mg# versus SiO₂ for MORB glasses closely approximates a single liquid line of descent, involving olivine + plagioclase + clinopyroxene, with cumulate SiO₂ ~ liquid SiO₂ (see Chapter 4.13). The arc lavas show a much broader trend of Mg# versus SiO₂, consistent with crystallization of SiO₂-poor assemblages (less plagioclase, added hornblende and/or FeTi oxides) from a range of parental

**Figure 1** (Continued)

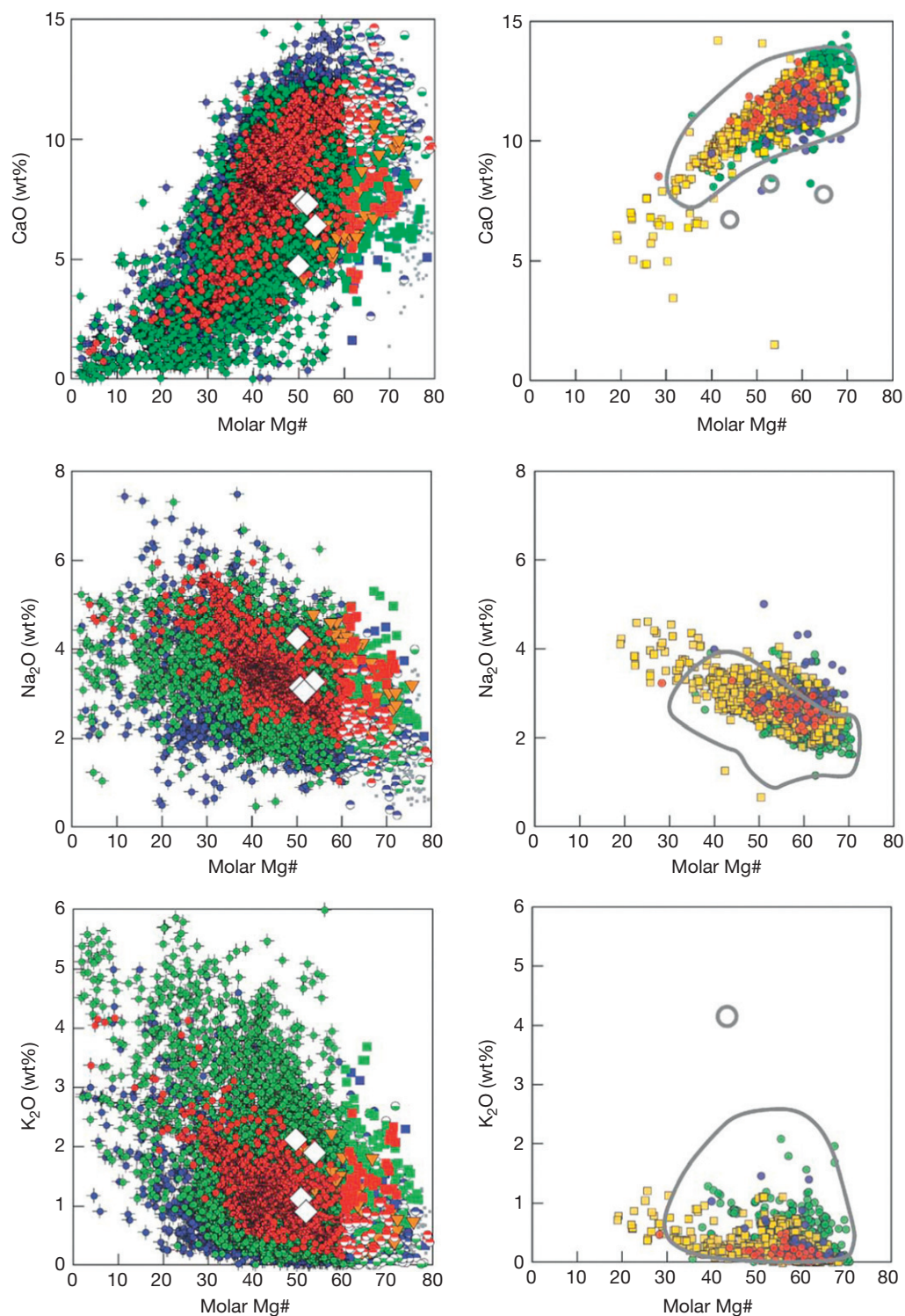


Figure 1 (Continued)

melts with SiO_2 contents of 45 to >60 wt%. SiO_2 contents from 45 to >60 wt% are found in arc lavas with an Mg# of 70 (close to Fe/Mg exchange equilibrium with residual mantle peridotite having an olivine Mg# of 90–91). This is not the result of crystal fractionation from basalts with Mg# ~ 70 .

However, the manner in which these parental melts acquire their differing SiO_2 contents is uncertain and controversial (see [Sections 4.21.3.2.4](#) and [4.21.3.2.5](#)).

TiO_2 contents of arc magmas are generally lower than in MORB glasses. TiO_2 versus Mg# in the entire arc lava

compilation, and in most individual suites, shows a sharp transition from increasing TiO_2 with decreasing Mg\# , for $\text{Mg\#} > \sim 50$, to decreasing TiO_2 with decreasing Mg\# , for $\text{Mg\#} < \sim 50$, which is due to fractionation of FeTi oxides from evolved melts. It is probably safe to conclude that primitive arc magmas have not undergone FeTi oxide fractionation, and thus their low TiO_2 , compared to MORB, is a primary feature or the result of magma mixing. Primitive andesites and boninites have the lowest TiO_2 contents in our compilation.

Al_2O_3 contents of primitive arc lavas range from 10 to 19 wt%, extending to much lower and higher values than primitive MORB glasses. Al_2O_3 contents of arc lavas increase with decreasing Mg\# , for lavas with $\text{Mg\#} > \sim 50$, for the entire data set, and for most individual arc suites. For $\text{Mg\#} < \sim 55$, Al_2O_3 decreases with decreasing Mg\# , reflecting plagioclase fractionation. This suggests that plagioclase fractionation may play a minor role in differentiation of most arc melts from Mg\# of 70 or more to Mg\# of ~ 55 . Instead, olivine, pyroxene, and/or hornblende fractionation may predominate. Given that primitive arc lavas are generally H_2O -rich compared to anhydrous mantle melts at arc Moho depths (e.g., Anderson, 1974; Falloon and Danyushevsky, 2000; Kamenetsky et al., 1997; Macdonald et al., 2000; Pichavant et al., 2002; Roggensack et al., 1997; Sisson and Layne, 1993; Sobolev and Chaussidon, 1996), many primary mantle melts are probably in a reaction relationship with olivine (e.g., Müntener et al., 2001), forming by reactions such as orthopyroxene + clinopyroxene + spinel = olivine + melt. Such melts are in equilibrium with olivine, but will not crystallize olivine upon isobaric cooling, and instead will crystallize websterites (two pyroxene pyroxenites). Other primitive, hydrous arc magmas are olivine-saturated; these commonly produce olivine clinopyroxene cumulates (e.g., Conrad and Kay, 1984; Conrad et al., 1983). In addition, primitive arc magmas probably have temperatures $> 1100^\circ\text{C}$ (e.g., Elkins Tanton et al., 2001; Gill, 1981; Kelemen et al., 2003b), above the thermal stability of hornblende, although this might be uncertain for very H_2O -rich compositions. Thus, pyroxenite (clinopyroxenite, websterite) fractionation is most likely responsible for the increase in Al_2O_3 with decreasing Mg\# , for liquid Mg\# of more than 70 to ~ 55 (e.g., Conrad and Kay, 1984; Conrad et al., 1983).

Pyroxenites have seismic velocities similar to or only slightly less than residual mantle peridotites. The temperature and melt content of the sub-arc mantle are poorly constrained, and seismologists commonly report sub-Moho P-wave velocities $< 8 \text{ km s}^{-1}$ (e.g., Flidner and Klemperer, 1999; Holbrook et al., 1999; Suyehiro et al., 1996). Thus, the igneous crust may extend well below the seismic Moho in arcs. However, by the same token, seismic data certainly do not require abundant pyroxenite. Pyroxenites, while well represented among arc plutonic xenoliths, comprise a very small proportion of exposed arc crustal sections (e.g., DeBari and Coleman, 1989; Miller and Christensen, 1994). Thus, pyroxenites may be removed by viscous 'delamination' during or after arc magmatism (e.g., Arndt and Goldstein, 1989; DeBari and Sleep, 1991, 1996; Herzberg et al., 1983; Kay and Kay, 1988, 1991, 1993, 1985; Turcotte, 1989). We will return to this topic in Sections 4.21.4.2 and 4.21.5.1.

Rare primitive arc lavas, including well-studied compositions that almost certainly represent liquid compositions, have

Al_2O_3 higher than primitive MORB. These are generally interpreted as products of equilibration of nearly anhydrous basaltic melts with residual mantle peridotite at 1–1.2 GPa, just beneath the base of the arc crust in the Cascades and Indonesia (e.g., Bartels et al., 1991; Elkins Tanton et al., 2001; Sisson and Bronto, 1998; see also Turner and Foden, 2001). Although these compositions are not common (Figure 1), they are nonetheless of great importance because wellknown phase equilibria for nearly anhydrous melt/mantle equilibration allows these lavas to be used to place fairly tight constraints on sub-arc temperature at specific depths in the mantle wedge (e.g., Elkins Tanton et al., 2001).

Al_2O_3 contents in evolved arc magmas range up to more than 20 wt%, much higher than in evolved MORB. Interpretation of Al_2O_3 contents of evolved arc lavas is notoriously difficult, because of the potential for incorporation of accumulated plagioclase in porphyritic lavas (Brophy, 1989; Crawford et al., 1987). However, some carefully studied 'high-alumina basalts' are probably liquid compositions (Baker and Eggler, 1983, 1987; Sisson and Grove, 1993a,b). In addition, some authors have maintained that high- Al_2O_3 arc lavas with $\text{Mg\#} < 0.5$ might represent primary melts from diapirs of subducted basalt that rise into the mantle wedge, but do not chemically equilibrate with residual mantle peridotite (e.g., Brophy and Marsh, 1986; Johnston and Wyllie, 1988; Marsh, 1976; Myers et al., 1986a,b, 1985). This topic is visited again in Section 4.21.3.2.3. Alternatively, moderate Mg\# lavas may be derived via crystal fractionation from primitive melts, or may be partial melts of arc lower crust. From this perspective, Al_2O_3 increases due to crystallization of plagioclase-free cumulates, where plagioclase saturation is suppressed by abundant H_2O (greater than $\sim 2 \text{ wt\% H}_2\text{O}$) in primitive arc melts (e.g., Baker and Eggler, 1983, 1987; Kelemen et al., 1990a; Müntener et al., 2001; Sisson and Grove, 1993a,b).

In this review, using compiled data on arc lava compositions, it is impossible to improve upon previous estimates of oxygen fugacity or $\text{Fe}^{3+}/\text{Fe}^{2+}$ in arc magmas (generally close to Ni–NiO; e.g., Blatter and Carmichael, 1998; Brandon and Draper, 1996; Gill, 1981; Parkinson and Arculus, 1999). Thus, here we concentrate on total Fe as FeO (FeOt). Both primitive and evolved arc magmas extend to FeOt contents much lower than in MORB glasses. While some of this difference among evolved compositions results from FeTi oxide fractionation in relatively oxidizing arc magmas, the differences between primitive arc lavas and primitive MORB are clear, and are not attributable to FeTi oxide fractionation because FeTi oxides are not saturated in primitive arc lavas. Instead, this reflects a difference in the FeOt content of primary magmas, and/or the effects of magma mixing.

MgO contents among arc lavas show a much broader range than in MORB glasses. Arc lava MgO contents higher than MORB glasses may be due, in part, to incorporation of compositions with accumulated clinopyroxene and/or olivine into our data set. However, boninite suites clearly include high-MgO liquids (e.g., Falloon and Green, 1986; Sobolev and Danyushevsky, 1994), and some picritic and ankaramitic arc lava compositions are also believed to be liquid compositions (e.g., Eggins, 1993; Nye and Reid, 1986; Ramsay et al., 1984). Primitive arc lavas also extend to MgO contents much lower than primitive MORB glasses. These have MgO too low to be

derived from high-MgO primitive arc lavas via olivine fractionation. Alternatively, primitive andesites could be derived via olivine fractionation from picritic or komatiitic primary melts. However, as we will show in Sections 4.21.3.2 and 4.21.3.3, primitive andesites generally have trace-element characteristics that are distinct from primitive basalts, so the two cannot be related by crystal fractionation alone. Instead, similar to low FeO, low MgO in primitive arc andesites reflects either low MgO in primary melts equilibrated with residual mantle peridotite, or the effects of magma mixing.

Similar to FeO and MgO, CaO contents in both primitive and evolved arc lavas are much lower than in primitive and evolved MORB glasses, and andesites are the low CaO end-member among primitive lavas. It is ironic that low CaO is one of the characteristics of these end-member 'calc-alkaline' lavas; this suggests that the 'tholeiitic' versus 'calc-alkaline' terminology should be changed.

Na₂O, K₂O, and, to a lesser extent, P₂O₅ in both primitive and evolved arc lavas extend to higher and lower concentrations than in primitive and evolved MORB glasses. Again, primitive andesites stand out, having the highest Na₂O, K₂O, and P₂O₅ among primitive compositions. As for the other elements discussed above, these characteristics are not due to crystal fractionation but must be characteristics of primary magmas or arise via magma mixing.

4.21.3.1.2 We are cautious about fractionation correction of major elements

Na₂O concentration in basalts, corrected to 6 wt% MgO, has been used as an indicator of the relative degree of mantle melting in the arc mantle source (e.g., Plank and Langmuir, 1988, 1993). This method involves two explicit assumptions. First, it is assumed that primary melts have a common MgO content. While it is beyond the scope of this chapter to investigate this assumption on a volcano-by-volcano basis, in Figure 2, we show that this assumption seems questionable for Aleutian lavas, which show a wide variation in MgO at high Mg#. Lavas from the Piip volcano with 6 wt% MgO are primitive, so that their Na₂O contents may be close to those of the 'primary' magma, whereas lavas from the Okmok and Seguam volcanoes with 6 wt% MgO are fractionated, with Na₂O contents higher than in corresponding primary melts in equilibrium with mantle olivine. Since the trends of Na₂O versus Mg# for the Okmok and Seguam volcanoes cross, correction to 6 wt% MgO yields higher Na₂O in Okmok compared to Seguam, whereas primary Okmok melts (Mg# ~ 70) probably have lower Na₂O compared to primary Seguam melts.

Second, it is assumed that Na₂O in arc magmas is derived primarily from the mantle, without a significant contribution from subducting sediment and oceanic crust. We think this also is uncertain, because fluids and melts in equilibrium with subducting, eclogite facies metasediment and metabasalt contain abundant dissolved sodium. This dissolved sodium could be carried into the mantle wedge together with H₂O and other components derived from subducting material (see Chapter 4.19, and references therein). For example, primitive andesites in the Aleutians that have exceptionally high Na₂O also have exceptionally high La/Yb, Sr/Nd, Dy/Yb, and ¹⁴³Nd/¹⁴⁴Nd, and exceptionally low lead and strontium isotope ratios (Kelemen et al., 2003b), which likely reflects

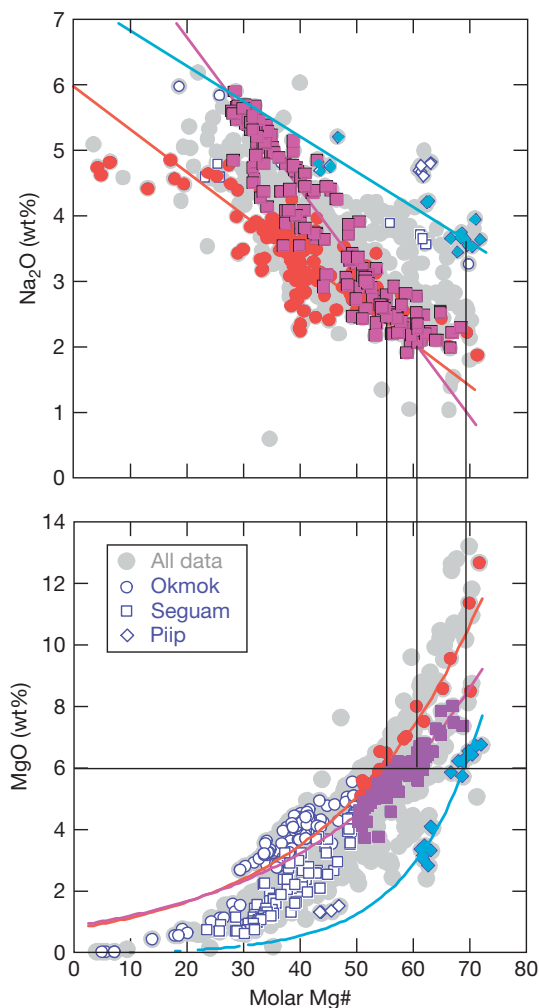


Figure 2 Molar Mg# versus wt% Na₂O for Aleutian lavas (compiled by Kelemen et al., 2003b), illustrating that variation trends have different slopes for different volcanoes, and that these trends cross. As a result, it would be unwise to infer Na₂O concentrations in primary Aleutian magmas using an 'average' fractionation trend and the compositions of evolved lavas. Data for Seguam volcano mainly from Singer et al. (1992a,b) and data compiled by James Myers and Travis McElfrish and available at the Aleutian arc website (2006). Data for Okmok volcano are mainly from Class et al. (2000), Miller et al. (1992, 1994), Nye (1983), and Nye and Reid (1986, 1987). Okmok data with Mg# ~ 80 are omitted. Data for Piip volcano are from Yogodzinski et al. (1994). Light grey circles, all Aleutian data (compiled by Kelemen et al., 2003). Other shapes are for individual volcanoes, as shown in the legend. Darker symbols used in fits (linear in top panel, exponential in bottom panel); open symbols omitted from fits.

incorporation of an eclogite melt component. We will return to this point in Section 4.21.3.2.

If partial melts of eclogite have ~5 wt% Na₂O (Rapp et al., 1999; Rapp and Watson, 1995), addition of 5% eclogite melt to some part of the mantle wedge adds 0.25 wt% Na₂O to that region. This can be compared to, for example, 0.4 wt% Na₂O in fertile 'pyrolite' (Ringwood, 1966) or ≤0.05 wt% in depleted oceanic peridotites (Dick, 1989). Thus, it is plausible that a 'slab melt' component might add significant and potentially variable amounts of sodium to the mantle 'source' of arc

magmas, particularly if the arc mantle has been previously depleted by melt extraction beneath a mid-ocean ridge and/or a back-arc basin.

To more quantitatively constrain the relative contributions of sodium from melt or fluid derived from subducting material versus the preexisting peridotite in the mantle wedge, it would be useful to know the degree of depletion of the preexisting peridotite, due to previous melt extraction events prior to arc magmatism. One can try to use the concentration of 'immobile' elements such as niobium, together with mantle/melt distribution coefficients, to estimate the degree of depletion of the mantle 'source' of each arc magma, assuming that 'immobile' elements are not added by fluids or melts of subducting material (Langmuir, personal communication, 2003). However, in addition to sodium, eclogite melts also contain ~5 ppm niobium (Rapp and Watson, 1995), while primitive mantle is estimated to contain <1 ppm niobium (Hofmann, 1988; Sun and McDonough, 1989). Therefore, determining the extent of prior depletion in the mantle wedge is also problematic for systems open to eclogite melt.

Third, use of Na_2O as an indicator of mantle melting processes involves the implicit assumption that Na_2O contents in arc magmas have not been affected by open-system processes in the crust, such as magma mixing and assimilation. Again, this assumption is violated in some cases, particularly when considering evolved rather than primitive lava compositions (e.g., Grove et al., 1982, 1988; Hildreth and Moorbath, 1988; McBirney et al., 1987).

4.21.3.1.3 Distinctive, primitive andesites

As will be seen throughout this chapter, despite limited data, primitive andesites define an end-member on almost all compositional variation diagrams. The primitive andesite end-member is distinct from primitive MORB glasses in ways that epitomize the overall difference between arc lavas and MORB (Table 1 and Figure 3).

High-Mg# andesites and their plutonic equivalents are end-member calc-alkaline lavas, distinct from the tholeiitic magma series. Here we define calc-alkaline magmas as having both high $\text{Na} + \text{K}$ at high Mg# (Irvine and Baragar, 1971) and high SiO_2 at high Mg# (i.e., high SiO_2 at low Fe/Mg, Miyashiro, 1974); tholeiitic magmas have lower SiO_2 and $\text{Na} + \text{K}$ at the same Mg#, when compared with calc-alkaline magmas. (Note that in this chapter we do not consider alkaline lavas, i.e., nepheline or kalsilite normative compositions.) While primitive basalts and evolved tholeiitic lavas are found in a variety of plate tectonic settings, it is plain that calc-alkaline andesite lavas are found almost exclusively in arcs (Gill, 1981). Thus, one could argue that the genesis of primitive andesite is the defining process of arc magmatism.

While high-Mg# andesites are clearly less voluminous than tholeiitic lavas in most arcs (Figure 4; see also, e.g., White and McBirney (1978)), we consider them very important in other ways. Explaining the difference between calc-alkaline and tholeiitic magma series has been one of the central topics of igneous petrology for almost a century (e.g., Baker et al., 1994; Bowen, 1928; Brophy, 1987; Fenner, 1929, 1937; Green, 1976; Grove et al., 1982; Green and Ringwood, 1967, 1966; Grove and Kinzler, 1986, 2001; Kay, 1978, 1980; Kay and Kay, 1994; Kay et al., 1982; Kelemen, 1986, 1990; Kuno,

1950, 1968; Kushiro, 1969, 1974; Kushiro and Yoder, 1972; McBirney et al., 1987; Miller et al., 1992; Nicholls and Ringwood, 1973; Nicholls, 1974; Osborn, 1959; Sisson and Grove, 1993a,b; Tatsumi, 1981, 1982; Tatsumi and Ishizaka, 1981, 1982; Wilcox, 1944), and there is still no community-wide consensus on this.

Similarly, the estimated bulk composition of the continental crust (e.g., Christensen and Mooney, 1995; McLennan and Taylor, 1985; Rudnick and Fountain, 1995; Weaver and Tarney, 1984) is almost identical to some high-Mg# andesites in both major and trace-element concentrations, and some authors have proposed that the genesis of the continental crust involved processes similar to the generation of high-Mg# andesites today (e.g., Defant and Kepezhinskis, 2001; Drummond and Defant, 1990; Ellam and Hawkesworth, 1988b; Kelemen, 1995; Kelemen et al., 1993, 2003b; Martin, 1986, 1999; Rapp and Watson, 1995; Taylor, 1977). Again, however, there is no consensus on this.

Finally, plutonic rocks with high-Mg# andesite compositions probably form the bulk of the major calc-alkaline plutons in orogenic belts, such as the Mesozoic batholiths along the Pacific margins of North and South America. For example, the average composition of the Peninsular Ranges batholith in southern California is essentially identical to that of the continental crust (Gromet and Silver, 1987; Silver and Chappell, 1988). Similarly, the average composition of exposed Eocene to Miocene plutonic rocks in the Aleutian arc is that of high-Mg# andesite (Kelemen et al., 2003b). Thus, high-Mg# andesite magmas may be more commonly emplaced as plutonic rocks in the middle and upper crust (Kay et al., 1990; Kelemen, 1995), and may be under-represented among erupted lavas. For these reasons, and because this topic has not received a recent comprehensive review, one emphasis in this chapter is documentation of the difference between primitive arc basalts and andesites, and evidence bearing on its origin.

4.21.3.1.4 Major elements in calc-alkaline batholiths

... there is no reason to suppose that the relative amounts of magmas of different compositions erupted on the surface should be proportional to their amounts ... at depth.

Kuno (1968, p. 168)

This section is based on a limited compilation of plutonic rock compositions from 'intermediate, calc-alkaline batholiths,' such as are common among Mesozoic and Early Tertiary exposures associated with circum-Pacific arcs. Section 4.21.4 describes the composition of plutonic rocks from exposed arc sections that extend into the lower crust, including a much larger proportion of mafic gabbros.

Our data include the few data available in Georoc, our previous compilation of Aleutian plutonic rock compositions (Kelemen et al., 2003b), plutonic rocks from the Tanzawa complex, interpreted as accreted mid-crustal rocks from the Izu-Bonin arc (Kawate and Arima, 1998), and a compilation of limited data from highly 'calc-alkaline' batholiths such as the Mt. Stuart and Chilliwack batholiths in the North Cascades (Erikson, 1977; Kelemen and Ghiorso, 1986; Tepper et al.,

Table 1a Average primitive MORB and arc basalts (molar Mg# > 60)

	MORB	Average oceanic	Average continental	Kermadec	Lesser Antilles	Marianas	New Hebrides	Scotia	Tonga	Aleutian	Andean	Cascades	Central America	Greater Antilles	Honshu	Kamchatka	Luzon																	
N	203	503	497	36	84	168	65	41	70	66	56	60	78	21	137	78	24																	
SiO ₂	50.51	50.46	51.33	51.12	48.25	51.04	50.26	51.50	50.57	50.50	52.58	51.62	50.27	50.23	51.13	52.22	50.85																	
TiO ₂	1.22	0.91	0.98	0.81	0.85	1.01	0.69	1.06	0.94	0.79	1.03	0.87	1.02	1.04	1.03	0.92	0.78																	
Al ₂ O ₃	15.97	15.72	15.70	15.65	14.48	16.64	13.67	16.97	15.59	16.51	16.66	16.83	14.60	15.54	16.14	14.76	14.20																	
FeO(T)	8.85	8.52	8.72	8.77	9.17	8.02	8.74	8.05	8.60	8.58	8.11	7.89	9.50	9.20	8.79	8.78	8.92																	
MnO	0.16	0.17	0.17	0.16	0.17	0.15	0.19	0.15	0.17	0.16	0.15	0.15	0.17	0.20	0.16	0.17	0.18																	
MgO	8.57	9.84	9.48	9.07	13.69	8.57	11.33	7.74	9.39	9.22	8.28	9.12	10.63	10.57	9.29	9.39	10.86																	
CaO	11.85	11.44	9.93	11.50	10.79	11.51	11.96	11.34	11.99	11.09	8.80	9.86	10.49	9.57	9.68	9.96	10.75																	
Na ₂ O	2.57	2.35	2.61	2.27	2.01	2.62	2.06	2.72	2.16	2.39	2.97	2.93	2.31	2.50	2.53	2.73	2.24																	
K ₂ O	0.16	0.45	0.88	0.53	0.45	0.31	0.90	0.32	0.43	0.61	1.19	0.54	0.77	0.91	0.99	0.87	0.99																	
P ₂ O ₅	0.14	0.15	0.22	0.12	0.15	0.13	0.18	0.15	0.16	0.14	0.21	0.18	0.23	0.23	0.26	0.19	0.22																	
Molar Mg#	63.23	66.29	65.24	64.48	70.97	65.05	69.53	63.06	65.81	64.96	64.12	67.17	64.49	67.64	65.00	65.09	66.05																	
La	4.13	<i>n</i> 59	7.01	<i>n</i> 168	11.85	<i>n</i> 159	6.69	<i>n</i> 10	8.72	<i>n</i> 50	5.00	<i>n</i> 46	8.38	<i>n</i> 21	6.49	<i>n</i> 14	8.95	<i>n</i> 12	5.98	<i>n</i> 27	18.79	<i>n</i> 28	11.29	<i>n</i> 24	14.75	<i>n</i> 29	5.60	<i>n</i> 16	<i>n</i> 6.92	<i>n</i> 41	15.99	<i>n</i> 13		
Ce	11.46	62	15.67	181	25.87	157	15.27	10	18.94	56	11.73	51	19.26	20	15.19	16	18.11	12	14.39	27	41.23	26	24.22	24	30.54	29	14.06	16	16.89	41	32.76	13		
Pr	1.84	6	2.11	55	2.85	65	0.72	7	0.72	21	2.28	11	2.21	5	7.10	10	1.90	5	1.35	17	1.70	6	2.64	23	2.64	29	9.88	16	12.60	41	18.26	12		
Nd	9.30	60	10.14	168	14.88	152	10.76	10	10.93	55	9.10	40	11.82	21	9.88	16	10.83	12	8.80	27	20.60	26	13.74	24	15.83	29	9.88	16	12.60	41	18.26	12		
Sm	2.96	66	2.70	172	3.43	155	2.61	10	2.68	57	2.72	40	2.79	21	2.86	16	2.74	12	2.33	27	4.37	28	3.16	24	3.42	29	2.80	16	3.33	41	2.80	9		
Eu	1.13	66	0.95	181	1.07	157	0.88	10	0.91	56	1.01	51	0.90	21	1.03	16	1.00	11	0.80	27	1.24	28	1.02	24	1.08	29	0.93	16	1.09	39	0.94	13		
Gd	4.04	27	3.10	134	3.55	107	2.98	45	3.47	36	2.86	20	3.34	15	3.49	5	2.28	12	4.79	10	3.37	11	3.46	29	3.09	6	3.49	41	3.38	8				
Tb	0.68	42	0.52	97	0.51	122	0.48	10	0.43	18	0.55	16	0.47	20	0.61	11	0.49	9	0.43	20	0.60	26	0.49	20	0.43	17	0.51	16	0.51	27	0.38	9		
Dy	4.70	25	3.31	133	3.32	91	2.93	41	3.86	37	2.77	21	3.87	16	3.41	6	2.81 ^a	25	4.04	10	2.93	5	3.29	29	2.39	6	3.51	31	2.76	8				
Ho	0.93	6	0.62	58	0.68	65	0.40	10	0.58	20	0.83	11	0.58	5	0.52	5	0.75	10	0.65	5	0.60	17	0.74	6	0.70	17	0.74	6	0.70	23				
Er	3.00	29	2.00	136	1.95	84	1.69	43	2.38	37	1.65	21	2.33	16	2.20	6	1.36	11	2.14	10	1.79	5	1.88	29	2.15	6	2.02	24	1.62	8				
Tm	0.47	4	0.28	33	0.29	63	0.20	11	0.24	6	0.36	11	0.31	9	0.29	5	0.25	17	0.32	6	0.29	22	0.29	22	0.29	6	0.29	22	0.29	22				
Yb	2.72	62	1.86	171	1.82	159	1.88	10	1.59	56	2.29	40	1.57	21	2.27	16	1.62	12	1.40	27	1.83	28	1.88	24	1.68	29	1.95	16	1.89	41	1.38	13		
Lu	0.41	40	0.27	97	0.28	138	0.30	10	0.25	42	0.37	7	0.23	6	0.35	11	0.19	8	0.21	19	0.28	26	0.27	24	0.25	17	0.29	16	0.30	40	0.22	7		
Sc	36.75	45	36.37	112	32.51	110	35.80	10	34.76	44	33.64	15	38.00	14	34.45	11	44.58	9	38.71	20	26.54	28	34.24	5	33.20	13	33.21	14	35.33	40	36.32	5		
V	245.77	39	254.01	119	246.59	107	255.10	10	235.38	39	245.57	21	336.00	16	237.00	11	222.60	10	294.38	8	198.36	22	224.00	5	268.53	29	253.20	15	186.65	20	260.45	31		
Cr	357.10	48	575.68	132	397.96	145	317.10	10	974.55	47	322.50	22	420.11	18	266.33	15	716.67	9	449.93	27	344.42	26	358.75	24	491.51	29	269.13	15	507.53	45	442.26	39	339.57	7
Co	41.76	33	44.17	56	41.20	80	61.22	13	34.79	14	44.67	6	35.94	10	45.07	6	44.09	16	41.06	9	43.08	22	57.13	15	41.72	36	35.63	7	57.13	15	41.72	36	35.63	7
Ni	135.24	46	239.67	135	158.74	146	110.00	10	442.69	52	128.30	20	131.72	18	34.67	15	182.22	9	130.08	26	130.49	28	151.29	24	245.05	29	141.53	15	191.52	57	135.08	40	96.57	7
Cu	69.87	30	84.86	74	91.91	40	82.40	10	78.21	34	126.00	6	65.30	10	78.50	4	46.80	5	46.80	5	118.17	13	108.86	7	75.00	9	108.86	7	75.00	9	75.00	9		
Zn	67.27	30	72.22	97	81.30	68	77.60	10	74.59	40	60.08	12	72.17	6	77.06	16	91.86	7	83.86	22	63.00	5	81.89	9	83.52	27	81.89	9	83.52	27	83.52	27		
Rb	2.93	33	9.89	179	18.63	140	8.30	10	10.22	57	5.61	50	14.83	20	7.24	16	24.96	10	9.88	21	29.23	28	16.42	23	10.63	29	12.48	12	22.10	39	14.45	33	37.07	11
Sr	141.42	55	306.74	181	425.70	153	274.90	10	314.97	57	231.78	51	499.81	21	202.00	16	451.64	11	445.09	23	532.34	28	469.38	24	437.96	29	284.60	16	715.20	38	345.68	41	566.18	11
Y	27.48	46	19.47	145	18.69	141	20.40	10	17.45	54	24.14	21	17.86	21	23.29	16	16.64	11	12.90	18	19.74	28	20.91	22	18.67	29	13.15	16	22.54	21	19.54	32	16.10	10
Zr	92.63	54	62.21	145	92.70	144	65.90	10	59.65	53	65.14	22	51.58	21	86.22	16	50.91	11	54.94	18	118.96	28	105.96	24	79.94	29	63.38	16	122.55	22	87.14	32	96.00	11
Nb	6.04	20	3.99	129	6.23	135	2.30	10	4.79	52	3.81	14	1.83	20	6.71	16	5.88	6	4.05	17	11.76	24	6.70	21	7.03	29	3.51	14	11.80	21	2.90	32	5.05	11
Cs	0.05	6	0.32	54	0.71	87	0.32	12	0.08	10	0.14	6	0.11	11	1.34	5	0.46	21	1.00	19	0.38	22	0.22	10	0.43	2	0.43	2	0.49	27				
Ba	30.70	44	132.96	175	295.04	155	124.00	10	137.67	54	65.47	48	257.24	21	84.23	16	274.91	11	195.54	26	317.81	28	271.33	24	315.53	29	284.88	16	498.13	24	279.70	40	335.80	12
Hf	2.31	41	1.65	87	2.14	133	1.73	10	1.54	13	1.61	14	1.58	18	2.15	11	1.53	9	1.58	22	2.76	26	2.22	22	1.53	25	1.70	15	2.39	32	1.88	6		
Ta	0.31	28	0.24	64	0.45	83	0.26	10	0.26	11	0.14	12	0.16	6	0.50	11	0.04	5	0.25	12	0.99	20	0.48	17	0.29	17			0.13	22	0.16	5		
Pb	0.38	14	2.48	109	3.36	83	2.80	10	2.40	32	1.08	26	4.12	10	1.63	12	5.99	8	3.95	10	7.21	19	2.26	10	1.40	26	3.20	5	2.77	22				
Th	0.28	34	1.52	111	2.03	139	1.11	10	2.96	38	0.41	12	1.19	20	0.89	12	0.78	8	1.21	23	3.77	26	1.33	22	1.08	26	0.75	15	0.88	32	5.80	13		
U	0.23	26	0.59	105	0.53	102	0.28	8	1.07	39	0.17	11	0.41	20	0.23	11	0.51	5	0.58	19	1.35	11	0.39	22	0.37	26			0.43	31	0.62	7		
⁸⁷ Sr/ ⁸⁶ Sr	0.70274	104	0.70389	141	0.70401	133	0.70419	19	0.70482	46	0.70303	45	0.70392	4	0.70337	14	0.70406	7	0.70315	19	0.70515	11	0.70382	27	0.70388	25	0.70432	1	0.70437	27	0.70344	28	0.70442	4
¹⁴³ Nd/ ¹⁴⁴ Nd	0.51310	90	0.51298	124	0.51292	104	0.51293	11	0.51291	42	0.51306	41	0.51300	4	0.51301	5	0.51292	3	0.51303	16	0.51262	6	0.51285	27	0.51301	25	0.51293	1	0.51277	9	0.51307	26		

Table 1b Average primitive arc andesites (molar Mg# > 60)

	<i>Continental</i>		<i>Oceanic</i>		<i>Aleutian</i>		<i>Boninites</i>	
<i>n</i> majors	142		32		47		348	
SiO ₂	58.05		57.72		59.03		56.83	
TiO ₂	0.79		0.64		0.69		0.25	
Al ₂ O ₃	15.96		15.16		16.61		13.22	
FeO(T)	6.14		6.69		5.22		7.93	
MnO	0.12		0.14		0.10		0.15	
MgO	6.56		7.95		5.65		10.64	
CaO	7.20		7.32		7.35		8.35	
Na ₂ O	3.31		2.95		3.64		2.02	
K ₂ O	1.67		1.27		1.50		0.56	
P ₂ O ₅	0.22		0.14		0.20		0.06	
Molar Mg#	65.18		66.29		65.62		69.50	
		<i>n</i>		<i>n</i>		<i>n</i>		<i>N</i>
La	18.89	59			16.02	28	1.88	74
Ce	37.44	53			37.27	28	4.44	73
Pr	5.38	13					0.92	23
Nd	20.89	42			20.20	28	2.79	63
Sm	3.92	56			3.95	28	0.77	71
Eu	1.08	59			1.12	28	0.28	76
Gd	3.92	26			3.61	5	0.92	55
Tb	0.51	47			0.43	23	0.17	38
Dy	3.09	23			3.06*	28	1.01	60
Ho	0.55	15					0.31	21
Er	1.63	22			1.77	7	0.70	55
Yb	1.54	57			1.32	28	0.80	69
Lu	0.23	51			0.19	27	0.14	53
Li	6.73	3					7.61	14
Be	0.87	3					0.26	16
Sc	20.98	41	26.14	18	17.55	25	36.45	54
V	158.27	19	196.66	21	170.00	2	188.01	70
Cr	326.83	55	260.75	21	252.76	27	696.03	76
Co	31.36	36	30.69	8	22.07	21	43.10	38
Ni	137.89	52	118.63	22	95.14	28	191.76	75
Cu	91.75	8	75.44	18	63.67	3	65.28	25
Zn	74.43	14	69.02	18	72.33	3	57.13	31
Rb	45.66	47	29.52	25	20.52	21	9.47	76
Sr	586.66	48	358.80	25	1035.88	27	141.84	77
Y	17.13	37	20.34	25	14.85	22	7.59	68
Zr	137.19	41	91.04	25	115.33	15	39.05	74
Nb	7.94	34	4.08	20	4.95	21	2.17	31
Cs	2.27	20	1.61	4	0.44	23	0.19	14
Ba	501.74	41	273.27	27	309.62	28	54.53	73
Hf	3.56	32	1.83	5	3.06	23	0.70	43
Ta	0.85	22	0.08	4	0.25	20	0.13	22
Pb	8.45	20	6.00	13	4.70	13	1.83	15
Th	4.51	35	3.90	16	1.99	23	0.42	28
U	1.57	29	0.37	6	0.82	24	0.26	19
⁸⁷ Sr/ ⁸⁶ Sr	0.70469	31	0.70493	14	0.70291	13	0.70423	55
¹⁴³ Nd/ ¹⁴⁴ Nd	0.51277	27	0.51288	6	0.51308	18	0.51294	50
²⁰⁶ Pb/ ²⁰⁴ Pb	18.53	11	18.81	4	18.30	18	18.68	37
²⁰⁷ Pb/ ²⁰⁴ Pb	15.56	11	15.58	4	15.47	18	15.53	37
²⁰⁸ Pb/ ²⁰⁴ Pb	38.36	11	38.54	4	37.76	18	38.31	37

Major-element oxides in wt%, trace elements in ppm. Trace-element averages are calculated as in Table 1a, except for oceanic andesites, where REE averages are not calculated (too few and variable analyses) and where all analyses are included for other trace elements.

1993), the Peninsular Ranges batholith in Baja California (Gromet and Silver, 1987; Larsen, 1948; Silver and Chappell, 1988), and the Ladakh batholith in northwestern India (Honegger et al., 1982). Unfortunately, because this data set is small, it is not clear to what extent the compiled

compilations are representative of intermediate arc plutons in general.

A second problem in interpreting plutonic rock compositions is determining the extent to which they represent liquid versus 'cumulate' compositions, where 'cumulate' is taken to

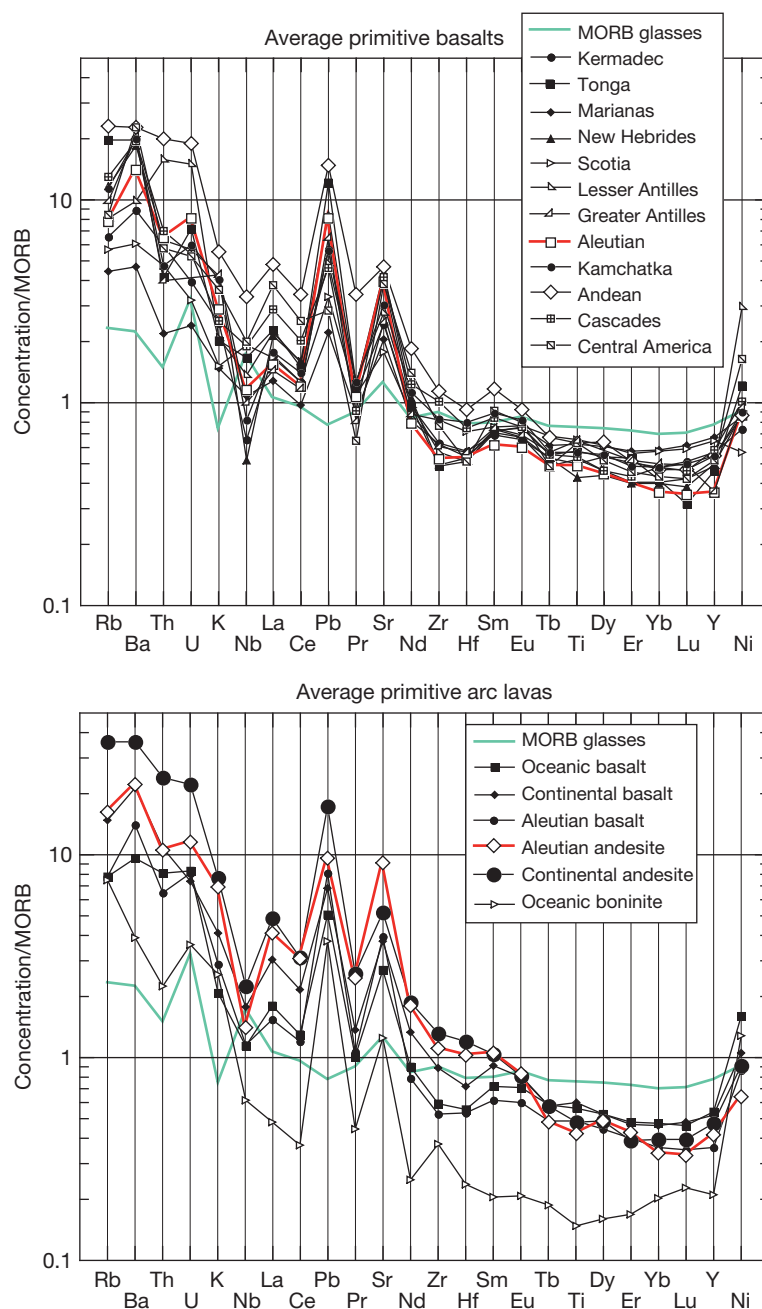


Figure 3 Extended trace-element diagrams for average arc lavas (Table 1). Concentrations are normalized to N-MORB (Hofmann, 1988). Primitive arc basalts are remarkably similar from one arc to another, and consistently distinct from MORB. In the oceanic Aleutian arc, and in continental arcs, primitive andesites are more enriched than primitive basalts. For plotting purposes, some REE abundances are extrapolated from neighboring REEs with more analyses (Pr in Lesser Antilles, Dy in Greater Antilles, and Er in Aleutian).

mean a component formed by partial crystallization of a melt, after which the remaining melt was extracted from the system of interest. A wide array of possible plutonic compositions can be envisioned, lying between these two extremes. For example, some plutonic rocks may be cumulates plus a small amount of 'trapped melt.' Others may be cumulates affected by interaction with unrelated migrating melts.

Cumulates with abundant plagioclase should generally have high Sr/Nd, since strontium is much more compatible

than neodymium in plagioclase, and Eu/Sm, since europium is generally much more compatible than samarium in plagioclase (depending on oxygen fugacity). In general, plutonic rocks with more than 55–60 wt% SiO₂ closely resemble liquid compositions in many ways, often containing abundant incompatible elements and lacking anomalously high Sr/Nd and Eu/Sm. We quantify this for intermediate to felsic plutonic rocks from the Jurassic Talkeetna arc section in Section 4.21.4.1.1.

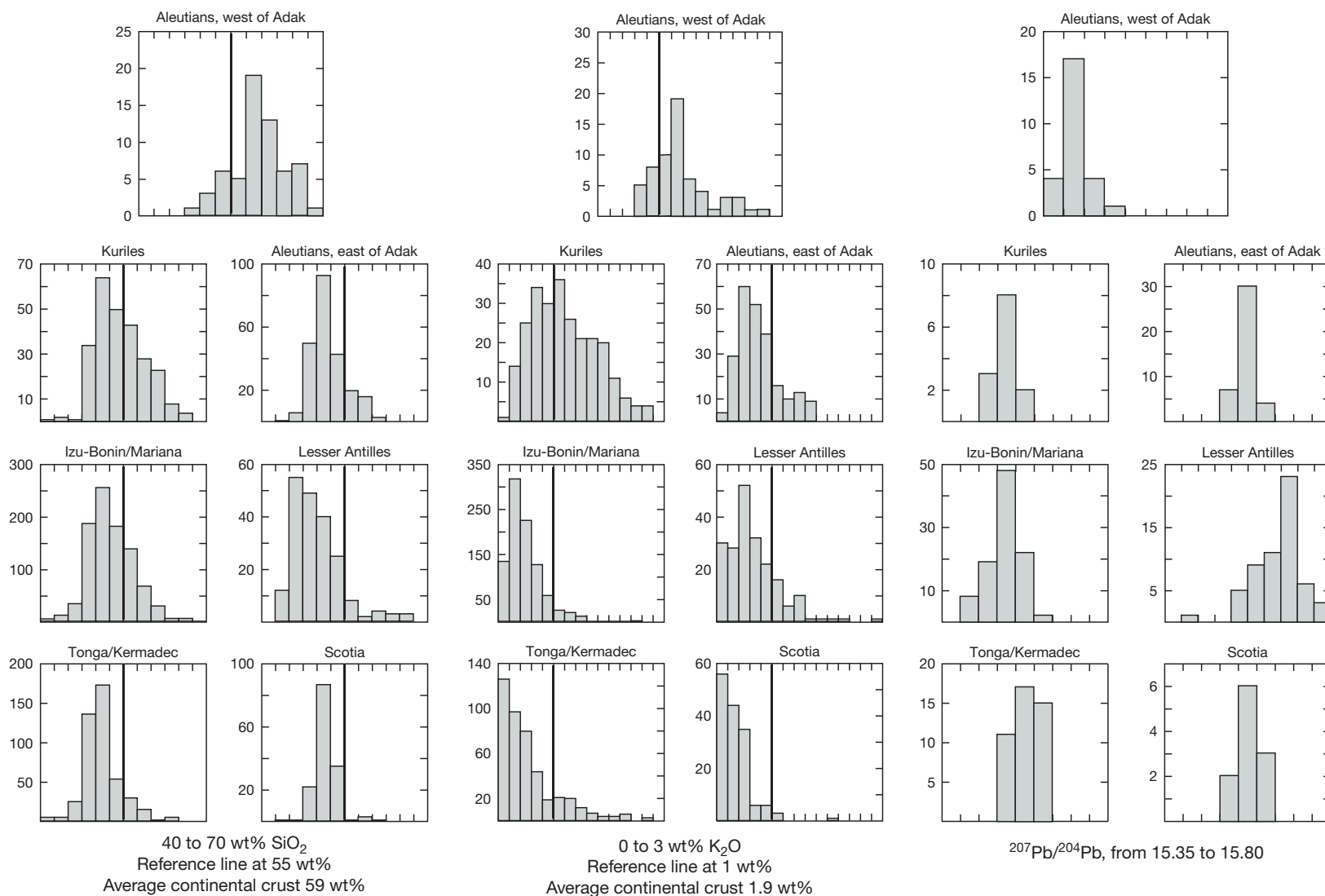


Figure 4 Histograms of wt% SiO₂, wt% K₂O, and ²⁰⁷Pb/²⁰⁴Pb for intra-oceanic arc lavas in our compilation. SiO₂ and K₂O are for lavas with Mg# > 50, while Pb isotopes are for all lavas. This diagram shows that relatively low K basalts predominate over relatively K-rich, high-Mg# andesites in all intra-oceanic arcs except the western Aleutians. The western Aleutian arc also has the least radiogenic Pb isotopes of any intra-oceanic arc. Thus, the predominance of primitive andesites in the western Aleutians is probably not due to recycling of components from subducting continental sediment or crustal contamination involving preexisting continental material.

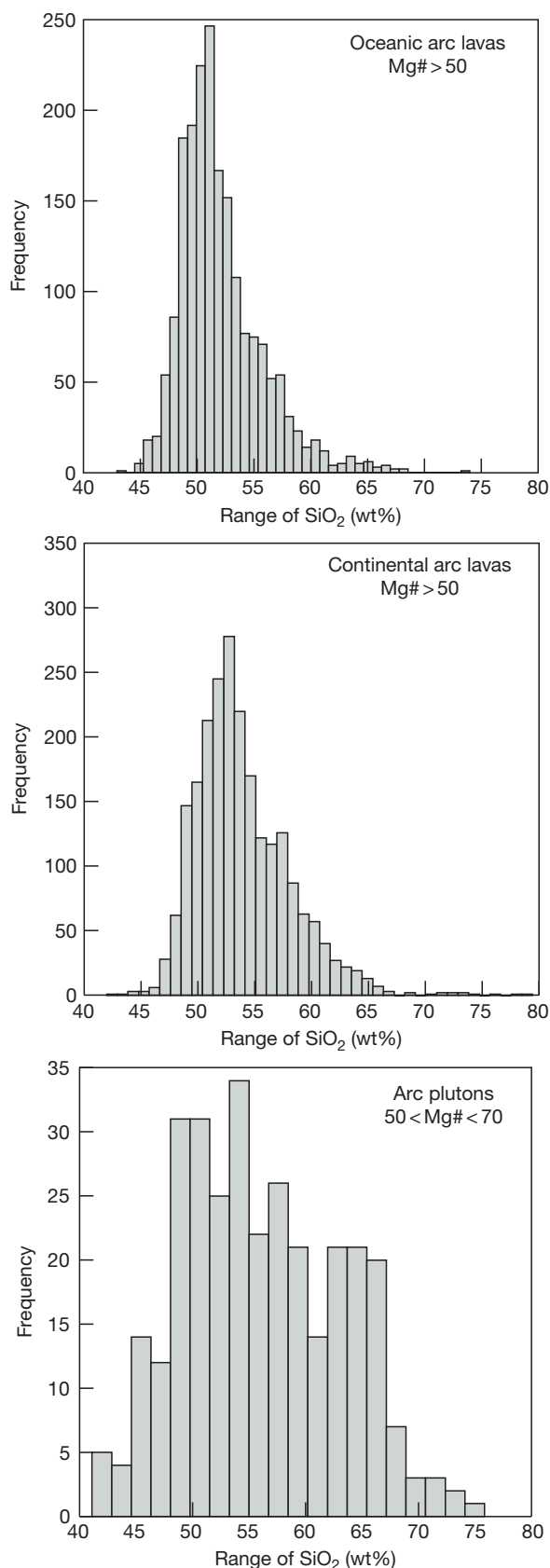


Figure 5 Histograms of wt% SiO₂ for arc lavas and a limited compilation of samples from arc plutons and batholiths. In general, arc plutonic rocks have higher SiO₂ content at similar Mg#. Data sources as in [Figure 1](#).

Our compiled plutonic rock compositions are generally more SiO₂-rich at a given Mg# than the compiled arc lavas ([Figure 5](#)). This is particularly clear in comparing Aleutian lavas to Aleutian plutons ([Kelemen et al., 2003b](#)). TiO₂ is highest in plutonic rocks with Mg# of ~60. Al₂O₃ is low in plagioclase-poor, high-Mg# pyroxenites, and then – generally – similar to the lower Al₂O₃ arc lavas at a given Mg#. Arc plutons have lower FeO, MgO, and CaO, at a given Mg#, than the bulk of arc lavas. Although some primitive cumulates in our compilation have very low alkali contents, in general, Na₂O contents in arc plutons and lavas are comparable while K₂O contents are higher in arc plutons compared to arc lavas at the same Mg#. To summarize, in all their major-element characteristics, the samples in our compilation of arc plutons are more strongly calc-alkaline, and include more high-Mg# andesite compositions, than typical arc lavas.

It seems that high-Mg# andesite liquids may be better represented among intermediate plutonic rocks than among arc lavas. This is certainly the case for exposed Aleutian plutons compared to Aleutian lavas. To explain this, following [Kay et al. \(1990\)](#), we have suggested that this difference arises due to the relatively high viscosity of intermediate to felsic magmas as they lose H₂O by degassing in the mid- and upper crust ([Kelemen, 1995](#); [Kelemen et al., 2003b](#)). Lower H₂O, low-SiO₂ basaltic melts continue to rise to the surface and erupt, whereas higher SiO₂ magmas, with initially higher H₂O, rise more slowly and crystallize faster.

4.21.3.2 Major and Trace-Element Characteristics of Primitive Arc Magmas

[A few scientists] seem to want to cling to the possibility that andesites are primary mantle-derived melts despite overwhelming evidence from experimental petrology, trace-element geochemistry, mineral chemistry, petrography, textural, and field relations to the contrary. It would be hard to find very many students of arc petrology who would argue ... that andesites, even Mg-rich ones, are ... primary mantle melts.

Anonymous (2003, personal communication)

... primitive magnesian andesites and basaltic andesites from the Mt. Shasta region, N. California ... form by hydrous mantle melting

[Grove et al. \(2003\)](#)

We turn now to the chemical characteristics of primitive arc lavas (Mg# > 60). First, we examine major-element variation as a function of Na₂O and TiO₂ contents. Although Na₂O contents of primitive basalts and andesites overlap, plots of Na₂O versus TiO₂, FeO, MgO, and CaO clearly discriminate between boninites (very low TiO₂ and Na₂O), primitive basalts (high TiO₂, FeO, MgO, and CaO at a given Na₂O), and primitive andesites (low TiO₂, FeO, MgO, and CaO at a given Na₂O) ([Figure 6](#)). It is evident from the trends of these elements versus Mg# ([Figure 1](#)) that these variations do not arise from crystal fractionation. For example, arc lavas with Mg# of ~70 or more, in Fe/Mg equilibrium with mantle olivine having Mg# of 90–91 or more, have SiO₂ contents ranging from 45 to 63 wt%. These cannot be related by fractional crystallization. The antithetical behavior of sodium and titanium (high sodium and

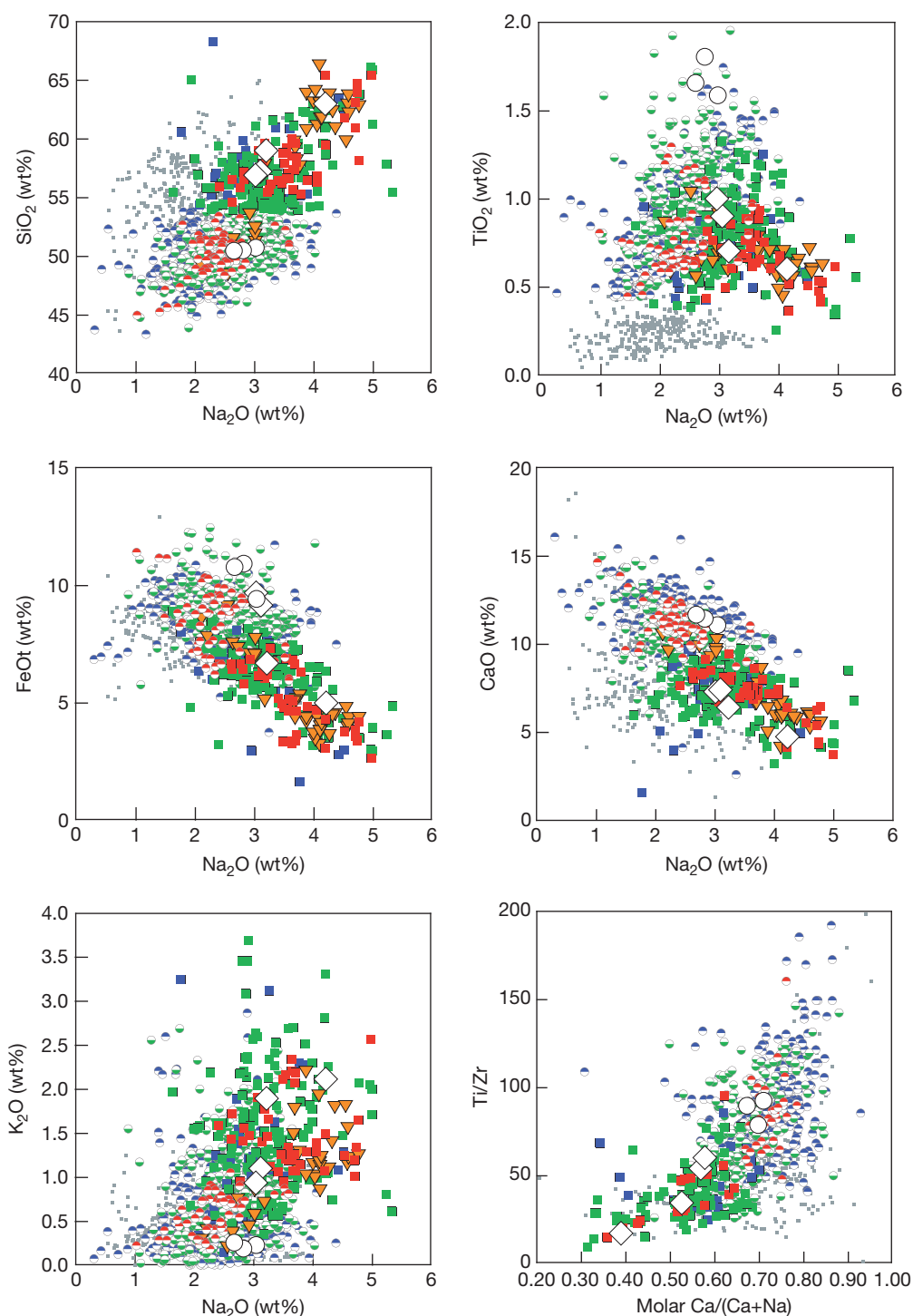


Figure 6 Weight% Na₂O versus other major-element oxides (in wt%) plus molar Ca/(Ca + Na) versus ppm Ti/Zr, for primitive arc lavas (Mg# > 60). Many of these plots clearly show distinct compositional fields for primitive basalts, primitive andesites, and boninites. While most of the primitive andesites are from 'continental' arcs, they plot together with western Aleutian primitive andesites, which are from an intra-oceanic arc and have MORB-like Sr, Pb, and Nd isotope ratios. Thus, assimilation of older, continental material is not essential to producing the distinctive composition of primitive andesites. Large circles show values for average MORB glasses from the East Pacific Rise, Juan de Fuca Ridge, and Indian Ocean. Other symbols and data as for Figure 1.

low titanium in primitive andesites, high titanium and low sodium in primitive basalts; ~2 wt% Na₂O in both primitive MORB and primitive arc basalts, but 0.3–1 wt% TiO₂ in primitive arc basalts compared to 1.2 wt% in

primitive MORB, Table 1) suggests that sodium contents of arc magmas may not be a good indicator of the degree of partial melting in the sub-arc mantle. (Also see Figure 2, and the last three paragraphs of Section 4.21.3.1.1.)

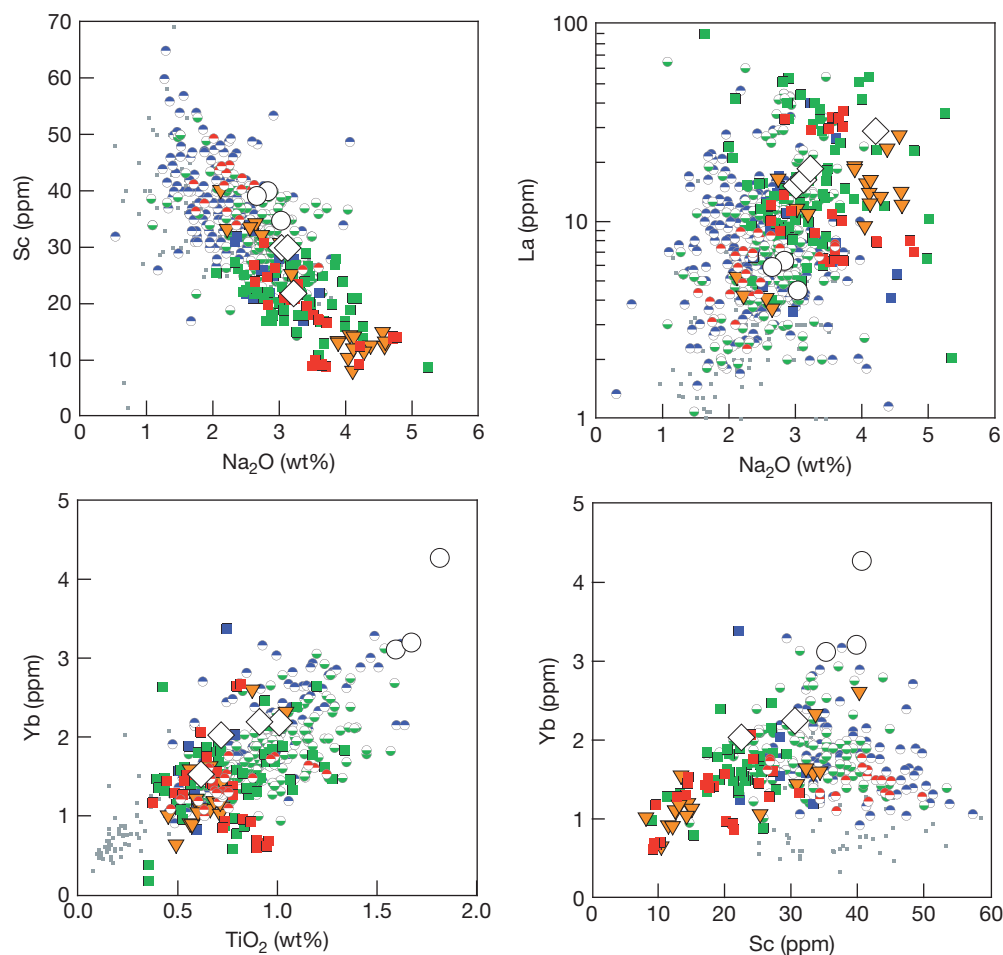


Figure 7 Weight% Na_2O , wt% TiO_2 , and ppm Sc versus other trace-element concentrations in ppm, for primitive arc lavas. Again, these plots clearly separate andesites from basalts. Primitive andesites from the oceanic, western Aleutians plot with other primitive andesites from continental arcs. Combined heavy REE, Y, Sc, Ti, and V depletion are indicative of either an important role for garnet fractionation, or a more depleted mantle source, in the genesis of primitive andesites as compared to primitive basalts. Data and symbols as for [Figure 6](#).

Although there is some overlap, plots of rubidium, barium, thorium, strontium, lead, zirconium, hafnium, and light REE versus Na_2O also discriminate between these groups (e.g., lanthanum versus Na_2O , [Figure 7](#)) with high LILEs, light REEs, and other highly incompatible elements in primitive andesites as compared to primitive basalts at a given Na_2O concentration. Middle REE concentrations are similar in both andesites and basalts, while heavy REE and related elements (holmium, erbium, thulium, ytterbium, lutetium, yttrium, scandium, and vanadium) are lower in andesites than in basalts at a given Na_2O concentration (e.g., scandium and ytterbium versus Na_2O , [Figure 7](#)). Low heavy REE and titanium contents in arc magmas have sometimes been considered to be indicative of a highly refractory mantle source and/or high degrees of melting beneath arcs, and scandium may be more compatible than sodium during mantle melting. However, it seems to us that either heavy REE, yttrium, titanium, and vanadium are poor indicators of the extent of mantle melting in the source of primitive lavas, or Na_2O is a poor indicator, or neither is a good proxy for the extent of mantle melting.

Positive correlation between FeO, scandium, vanadium, and titanium, and negative correlations of each of these with SiO_2 for all primitive arc lavas raises once again the question of whether the concentrations of all these elements are related to FeTi oxide fractionation. However, the plot of TiO_2 versus Mg# shows that the concentration of titanium increases with decreasing Mg# in primitive lavas ([Figure 1](#)), in accord with experimental studies showing that primitive lavas at oxygen fugacities typical for arcs are not saturated in FeTi oxides. In addition, heavy REE concentrations are correlated with TiO_2 in primitive arc lavas. Heavy REE are incompatible in FeTi oxides and silicates other than garnet (e.g., [EarthRef database, 2006](#) and references therein). These two observations almost certainly rule out an important role for FeTi oxide fractionation in controlling the major-element compositions of primitive lavas. Instead, the similar behavior of vanadium, titanium, and heavy REE suggests either high degrees of mantle melting, or an important role for garnet fractionation, in the genesis of primitive andesites (see [Section 4.21.3.2.5](#)).

4.21.3.2.1 Primitive basalts predominate

Primitive arc basalts have trace-element characteristics that are very distinct from primitive MORB (Figure 3). Figure 4 shows that primitive basalts are more commonly sampled than any other primitive magma type in most oceanic arcs. Biased sampling of picturesque and dangerous strato-volcanoes composed of calc-alkaline andesite, rather than low-lying basaltic shields, may have complicated this picture for continental arcs, but basalts may predominate among primitive lavas in continental arcs as well (e.g., White and McBirney, 1978). The geochemical characteristics of primitive basalts have been the subject of numerous recent reviews (Elliott, 2003; Davidson, 1996; Elliott et al., 1997; Hawkesworth et al., 1993a,b, 1997; Pearce and Peate, 1995; Plank, 2003; Plank and Langmuir, 1988, 1993, 1998; Tatsumi and Eggins, 1995; Turner et al., 2003, 2001).

Considerable uncertainty remains regarding the relative importance of various processes in producing primitive arc basalts. For example, in some arcs the presence of nearly anhydrous, primitive basalts suggests a large role for decompression melting (Bartels et al., 1991; Draper and Johnston, 1992; Elkins Tanton et al., 2001; Sisson and Bronto, 1998), although see also Turner and Foden (2001), with major and trace-element systematics that might be similar to those beneath mid-ocean ridges (e.g., Plank and Langmuir, 1988, 1993). Possible mechanisms for decompression melting include near vertical, diapiric upwelling of low-density mixtures of melt + mantle peridotite (e.g., Davies and Stevenson, 1992; Iwamori, 1997) or diagonal upwelling of peridotite in return flow due to viscous entrainment of the mantle wedge with the subducting plate (Conder et al., 2002; Furukawa, 1993a,b; Kelemen et al., 2003a; Kincaid and Sacks, 1997; van Keken et al., 2002).

Other evidence implies that decompression may be minor or absent, and 'fluxed melting' of the mantle is controlled mainly by addition of H₂O and other fluxes from subducting material into the mantle wedge. This has generally been modeled as 'fluid-fluxed melting,' resulting from addition of an aqueous fluid to initially solid, but hot peridotite (Abe et al., 1998; Eiler et al., 2000; Grove et al., 2001, 2003; Ozawa, 2001; Ozawa and Shimizu, 1995; Stolper and Newman, 1992). Thus, static or even descending mantle peridotite in the wedge could partially melt if sufficient aqueous fluid were added, provided aqueous fluid reached parts of the mantle where temperature exceeded the fluid-saturated peridotite solidus. Substantial H₂O contents in primitive arc basalts, commonly ~3 wt% (Anderson, 1974; Baker and Eggler, 1987; Falloon and Danyushevsky, 2000; Kamenetsky et al., 1997; Kelemen et al., 1990b; Macdonald et al., 2000; Müntener et al., 2001; Pichavant et al., 2002; Roggensack et al., 1997; Sisson and Grove, 1993b; Sisson and Layne, 1993; Sobolev and Chaussidon, 1996), but more than 4.5 wt% in primitive andesites (Grove et al., 2003) are often taken as evidence for addition of H₂O-rich fluid to the mantle wedge, and for fluxed melting.

A variant on the flux melting hypothesis is the idea of 'melt-fluxed melting,' in which reaction between hydrous partial melts of subducting sediment and/or basalt and overlying mantle peridotite leads to increasing melt mass, producing a hybrid 'primary melt' in which more than 90% of the compatible elements, such as magnesium, iron, and nickel, are derived from the mantle, while most of the alkalis and other

incompatible trace elements come from the initial, melt of subducted material (e.g., Kelemen, 1986, 1990, 1995; Kelemen et al., 1993, 2003b; Myers et al., 1985; Yogodzinski et al., 1995; Yogodzinski and Kelemen, 1998). If this process occurs, it would be facilitated by the fact that melts migrating upward in the mantle wedge must heat as they decompress; under such circumstances, even anhydrous melts will be able to dissolve solid mantle minerals comprising tens of percent of the initial liquid mass (Kelemen, 1986, 1990, 1995; Kelemen et al., 1993). Similarly, Grove and co-authors propose that fluid-saturated partial melts of peridotite form at ~950 °C, very close to the subducting plate, and then these fluid-saturated peridotite melts cause melt-fluxed melting higher in the wedge (Grove et al., 2003). Aqueous-fluid-saturated melts of eclogite facies sediment or basalt, and fluid-saturated melts of mantle peridotite, would have 25–50 wt% H₂O at 3–5 GPa (Dixon and Stolper, 1995; Dixon et al., 1995; Kawamoto and Holloway, 1997; Mysen and Wheeler, 2000). In this regard, they would be efficient fluxing agents, causing additional melt to form via melt/rock reaction in the mantle wedge (Eiler et al., 2000). In principle, addition of such H₂O-rich melts to the mantle wedge could explain the substantial water contents in primitive arc magmas, without additional H₂O from a fluid.

It is worth noting that melt-fluxed melting is distinct from most open-system processes proposed to explain melting beneath mid-ocean ridges, including batch melting (e.g., Gast, 1968; Presnall and Hoover, 1984; Shaw, 1970), fractional melting (e.g., Gast, 1968; Johnson et al., 1990; Langmuir et al., 1977; Richardson and McKenzie, 1994; Shaw, 1970), incremental melting (e.g., Johnson et al., 1990; Kinzler and Grove, 1992, 1993; Klein and Langmuir, 1987; Langmuir et al., 1977), and continuous melting (Iwamori, 1994; Johnson and Dick, 1992; Langmuir et al., 1977; Sobolev and Shimizu, 1992), because in the latter processes melt forms due to decompression, not as a result of reaction between solid phases and migrating melt. In zone refining (e.g., Harris, 1957; Langmuir et al., 1977), melt mass is constant, so this too is different from melt-fluxed melting. Models of melt generation beneath mid-ocean ridges that include increasing melt mass due to reactive porous flow (e.g., Asimow and Stolper, 1999; Iwamori, 1994; Jull et al., 2002; Lundstrom et al., 1995, 2000; Spiegelman and Elliot, 1992; Spiegelman et al., 2001) are similar to proposed processes of melt-fluxed melting beneath arcs. (Note that Langmuir et al., 1977 mentioned but did not model this process for MORB genesis.) However, beneath arcs – unlike ridges – melt-fluxed melting may be extensive, even in regions that are not simultaneously undergoing decompression melting.

Understanding the different mantle melting processes and determining their relative importance in the generation of primary arc basalts is an active area of research, with much sponsorship from the US National Science Foundation's MARGINS initiative. We anticipate rapid developments in increasingly refined theories on this topic.

Another very active area of recent research is the identification of several different source components in primary arc basalts, including (1) fluids derived by dehydration of subducting metabasalt, (2) fluids derived by dehydration of subducting metasediment, (3) partial melts of subducting basalt, (4) partial melts of subducting sediment, (5) fertile mantle peridotite similar to the MORB source, (6) mantle peridotite depleted

by melt extraction beneath a mid-ocean ridge and/or a back-arc basin, and (7) enriched mantle similar to the source of ocean island basalt. We return to this topic in [Section 4.21.3.3](#).

Nonetheless, as we show in previous and subsequent sections of this chapter, focusing exclusively on arc basalts risks missing end-members whose characteristics epitomize the difference between arc versus mid-ocean ridge magmas. Thus, in the following sections we focus on other types of primitive arc lavas. However, some detailed characteristics of primitive arc basalts, together with other primitive arc magmas, are described in [Section 4.21.3.3](#).

4.21.3.2.2 Are some low Mg# basalts primary melts? Perhaps not

Hypothetical derivation of primary low Mg# basalts and andesites from partial melting of subducted basalt – without major-element equilibration with the overlying mantle – remains controversial for arcs (e.g., [Brophy and Marsh, 1986](#); [Johnston and Wyllie, 1988](#); [Marsh, 1976](#); [Myers et al., 1986a,b, 1985](#)), as well as hotspots (e.g., [Chauvel and Hemond, 2000](#); [Hauri, 1995](#); [Korenaga and Kelemen, 2000](#); [Lassiter and Hauri, 1998](#); [Sobolev et al., 2000](#)) and even mid-ocean ridges (e.g., [Schiano et al., 1997](#)). On the basis of the criteria outlined by [Gill \(1981, 1974, 1978\)](#), we see no evidence for direct partial melts of subducted, eclogite facies sediment or basalt in our data compilation. It may be that diapirs of melting basalt always rise to depths at which garnet is no longer stable, prior to separation of melt from residue ([Brophy and Marsh, 1986](#)), but there seems to be no direct evidence for this. Instead, arc lavas with a trace-element signature consistent with derivation via partial melting of eclogite (e.g., high middle/heavy REE ratios) are primitive, with Mg# > 60 (e.g., [Grove et al., 2001](#); [Kay, 1978](#); [Kelemen et al., 2003b](#); [Yogodzinski et al., 1995](#); [Yogodzinski and Kelemen, 1998](#)). Thus, in this chapter we make the simplifying assumptions that lavas with Mg# < 60 are derived from primitive melts via crustal differentiation, and that all melts passing from the mantle wedge into arc crust have Mg# > 65 (depending on $\text{Fe}^{3+}/\text{Fe}^{2+}$), and are close to Fe/Mg exchange equilibrium with mantle peridotite (Mg# ~ 70).

Related to this topic are questions about the genesis of tonalites, trondhjemites, and granodiorites (TTGs), that are common in Archean cratons (see [Kemp and Hawkesworth, 2003](#)). Although it is difficult to be certain, we believe that TTGs are probably not ‘primary’ melts of subducting eclogite as has been proposed ([Defant and Kepezhinskis, 2001](#); [Martin, 1986, 1999](#); [Rapp and Watson, 1995](#); [Rapp et al., 1991](#)), simply because it does not seem likely that H_2O -rich low-temperature melts could traverse the high-temperature mantle wedge without substantial reaction with peridotite. Instead, we infer that TTGs are probably the products of intracrustal differentiation, with felsic melts rising to the upper crust, and mafic residues remaining in the lower crust. (Note that while seismic and petrologic data on continental crust clearly establish that it is differentiated, the intracrustal differentiation process could have modified an initially andesitic ‘or’ basaltic bulk composition.) They may have evolved by crystal fractionation from a parental, primitive andesite melt. However, because the process of intracrustal differentiation may have involved residual garnet, it is difficult to discern which TTGs with heavy REE depletion inherited

their trace-element characteristics from primitive andesites, and which reflect crustal garnet fractionation.

4.21.3.2.3 Boninites, briefly

In determining the characteristics of ‘primary’ arc magmas – melts that pass from residual mantle into the overlying, igneous crust – most recent reviews of geochemistry have concentrated on the characteristics of primitive basaltic magmas. In doing so, these reviews have implicitly incorporated the assumption that primary arc magmas are invariably basaltic. In our view, there are two types of ‘andesitic’ primitive magmas in arcs, boninites, and primitive andesites. These two types of magmas extend to end-members having Mg# > 0.7, and carry olivine phenocrysts with Mg# > 90 (typical mantle values). While these are less common than primitive basalts, we think they are important for the reasons enumerated in [Section 4.21.3.1.3](#).

While there are many far more detailed definitions and subdivisions of boninite lava compositions (e.g., [Crawford, 1989](#)), we found it convenient to simply define boninites as lavas with >54 wt% SiO_2 , <0.5 wt% TiO_2 (plus samples described in the original data sources as boninites, including some basalts). As can be seen in [Figures 1, 6, and 7](#), lavas defined in this way share many other distinctive characteristics, including high MgO and low alkali contents at a given SiO_2 and Mg#. Boninites are largely restricted to western Pacific island arcs, and in those arcs they are apparently more abundant in the early stages of magmatism (e.g., [Bloomer and Hawkins, 1987](#); [Falloo et al., 1989](#); [Stern and Bloomer, 1992](#)). Their high MgO contents (some >10 wt%) and the presence of clinopyroxene phenocrysts probably reflect both high temperatures and high water contents in the mantle wedge, with a highly depleted, harzburgite residue, consistent with generally low REE concentrations and flat to light REE depleted patterns (e.g., [Falloo and Green, 1986](#); [Falloo et al., 1989](#); [Pearce et al., 1992](#); [Sobolev and Danyushevsky, 1994](#)). Most authors accept that most boninites are derived by crystal fractionation from primary andesite melts derived by high degrees of relatively low-pressure melting, with a harzburgite residue. However, some lavas termed boninites could conceivably be derived via substantial olivine \pm low calcium pyroxene fractionation from very high-Mg# incompatible-element-depleted primary picrites or komatiites.

The abundance of boninites in early stages of western Pacific arc magmatism, combined with the high magmatic fluxes inferred for the early stages of magmatism in those arcs, may have led to bulk crustal compositions that remain dominantly boninitic. Relatively low bulk crustal seismic velocities in the Izu–Bonin arc ([Suyehiro et al., 1996](#)), compared to the central Aleutian arc (e.g., [Holbrook et al., 1999](#)), might reflect higher SiO_2 in the Izu–Bonin crust. Nonetheless, boninitic crust with >54 wt% SiO_2 would be depleted in alkalis and light REEs, and thus very different from continental crust, and from calc-alkaline magma series.

4.21.3.2.4 Primitive andesites: a select group

We turn now to primitive andesites (Mg# > 0.6) and high-Mg# andesites (Mg# > 0.5). High-Mg# andesites have been the subject of much attention in recent years because of their unique major and trace-element characteristics (e.g., [Baker et al., 1994](#);

Defant et al., 1991a; Defant and Drummond, 1990; Defant et al., 1992, 1989, 1991b; Defant and Kepezzhinskias, 2001; Grove et al., 2001, 2003; Kay, 1978; Kelemen, 1995; Kelemen et al., 2003b; Rogers et al., 1985; Shimoda et al., 1998; Stern and Kilian, 1996; Tatsumi, 1981, 1982, 2001a; Tatsumi and Ishizaka, 1981, 1982; Yogodzinski and Kelemen, 1998, 2000; Yogodzinski et al., 1995, 2001, 1994).

Some high-Mg# andesites – particularly some lavas on Adak Island in the Aleutians (Kay, 1978) – have been called ‘adakites’ (e.g., Defant and Drummond, 1990) as well as ‘sanukitoids,’ ‘high-Mg andesites,’ and ‘bajaites.’ The term ‘adakite’ is used in a variety of contexts by different investigators, but generally refers to andesites and dacites with extreme light REE enrichment (e.g., $\text{La/Yb} > 9$), very high Sr/Y ratios (e.g., $\text{Sr/Y} > 50$), and low yttrium and heavy REE concentrations (e.g., Y, 20 ppm, $\text{Yb} < 2$ ppm). In the Aleutians, all lavas with these characteristics are high-Mg# andesites and dacites. However, the *de facto* definition of ‘adakite’ does not specify a range of Mg#. Worldwide, many evolved lavas have been termed adakites. Thus, not all adakites are high-Mg# andesites. Similarly, most high-Mg# andesites, in the Aleutians and worldwide, have $\text{La/Yb} < 9$ and $\text{Sr/Y} < 50$, and so not all high-Mg# andesites are adakites. Finally, for some authors adakite has a genetic connotation. Some investigators infer that all andesites and dacites with extreme light REE enrichment, very high Sr/Y ratios, and low yttrium and heavy REE concentrations formed via partial melting of subducted basalt in eclogite facies are adakites, and use the term ‘adakite’ to refer to both composition and genesis interchangeably. While we believe that many high-Mg# andesites do indeed include a component derived from partial melting of eclogite, we feel it is important to separate rock names, based on composition, from genetic interpretations. For this reason, we do not use the term ‘adakite’ in this chapter.

4.21.3.2.5 Three recipes for primitive andesite

Loosely speaking, the difference between primitive basalts and primitive andesites might arise in several ways:

1. Both may arise from melting of different sources, with primitive andesites incorporating a relatively large proportion of melts of subducted basalt and/or sediment, compared to primitive basalts.
2. They might arise from the same mantle source, with different degrees of melting, related to different extents of enrichment via fluids derived from subducting sediment and/or oceanic crust.
3. High-Mg# andesites might arise via mixing of primitive basalts with evolved, high SiO_2 melts, or assimilation of ‘granitic’ rocks in primitive basalts.

We briefly expand one each of these in the next few paragraphs.

(1) *Primary andesite magma with an eclogite melt component.* High-Mg# andesites may incorporate a component formed by partial melting of subducted basalt or sediment in eclogite facies, which subsequently reacted with the overlying mantle peridotite to form a hybrid melt (Carroll and Wyllie, 1989; Kay, 1978; Kelemen, 1986, 1995; Kelemen et al., 1993, 2003b; Myers et al., 1985; Yogodzinski et al., 1995, 1994). In the hybrid melt, high incompatible-element contents reflect

eclogite melting, and major-element concentrations reflect melt/mantle equilibration. In this view, high H_2O , K_2O , and Na_2O contents stabilize high SiO_2 melt in equilibrium with mantle olivine at ~ 1 GPa, as demonstrated experimentally for simple systems (Hirschmann et al., 1998; Kushiro, 1975; Ryerson, 1985), peridotite melting experiments (Hirose, 1997; Kushiro, 1990; Ulmer, 2001), and phase equilibrium experiments on natural primitive andesite compositions (e.g., Baker et al., 1994; Grove et al., 2003; Tatsumi, 1981, 1982).

In some cases, the entire incompatible trace-element budget of these hybrid melts might be derived from eclogite melting, with only major elements and compatible trace elements (nickel and chromium) affected by interaction with peridotite. However, there are few primitive lavas in our compilation with a clear eclogite melting signature. Since heavy REEs and yttrium are compatible in garnet, concentrations of the same in eclogite melts should be low, and middle to heavy REE ratios in eclogite melts should be high (e.g., chondrite normalized $\text{Dy/Yb} > 1.5$). The few primitive lavas in our compilation that do have chondrite normalized $\text{Dy/Yb} > 1.5$ are mainly primitive andesites from the western Aleutian arc, at and west of Adak Island. Thus (Figure 8), not all light REE-enriched, high Sr/Nd arc lavas have high Dy/Yb.

Lack of a clear eclogite melting signature in heavy REE and yttrium contents does not rule out a role for eclogite melt in producing high-Mg# andesites. In hypothesis (1), the concentrations of heavy REE and yttrium in primitive arc andesites are interpreted as having been raised by reaction of eclogite melt with mantle peridotite at moderate melt/rock ratios (Kelemen, 1995; Kelemen et al., 1993, 2003b). Modeling shows that this process can produce a very close match to most high-Mg# andesite compositions (e.g., Kelemen et al., 2003b; figures 21d and 21e). In this interpretation, primitive arc basalts incorporate a finite but smaller amount of an eclogite melt component (e.g., Kelemen et al., 2003b; figure 21f).

As far as we know, there are few if any petrological or geochemical arguments that can be used to rule out this hypothesis. In fact, excluding heavy REEs and yttrium, the incompatible trace-element abundances in the ‘subduction component’ (McCullough and Gamble, 1991) inferred from inversion of major and trace elements in Marianas back-arc lavas (Stolper and Newman, 1992), an array of western Pacific arc lavas focused on the Vanuatu arc (Eiler et al., 2000), and primitive lavas from Shasta volcano in the southern Cascades (Grove et al., 2001) closely resemble traceelement concentrations experimental and predicted partial melts of eclogite (Kelemen, 1995; Kelemen et al., 1993, 2003b; Rapp et al., 1999), and of erupted high-Mg# andesites. One inverse model that is consistent with all available major-element, trace-element, and isotopic constraints (Eiler et al., 2000, p. 247) involves reaction between mantle peridotite and a silicate melt derived from subducting eclogite, with 30 wt% H_2O (appropriate for fluid saturation at 3–5 GPa; Dixon and Stolper, 1995; Dixon et al., 1995; Kawamoto and Holloway, 1997; Mysen and Wheeler, 2000).

Nevertheless, this hypothesis has been unpopular since the 1980s, because geodynamic models, incorporating either constant mantle viscosity or a rigid upper plate of prescribed thickness, predicted that solidus temperatures could not be reached in basalt or sediment at the top of the subducting

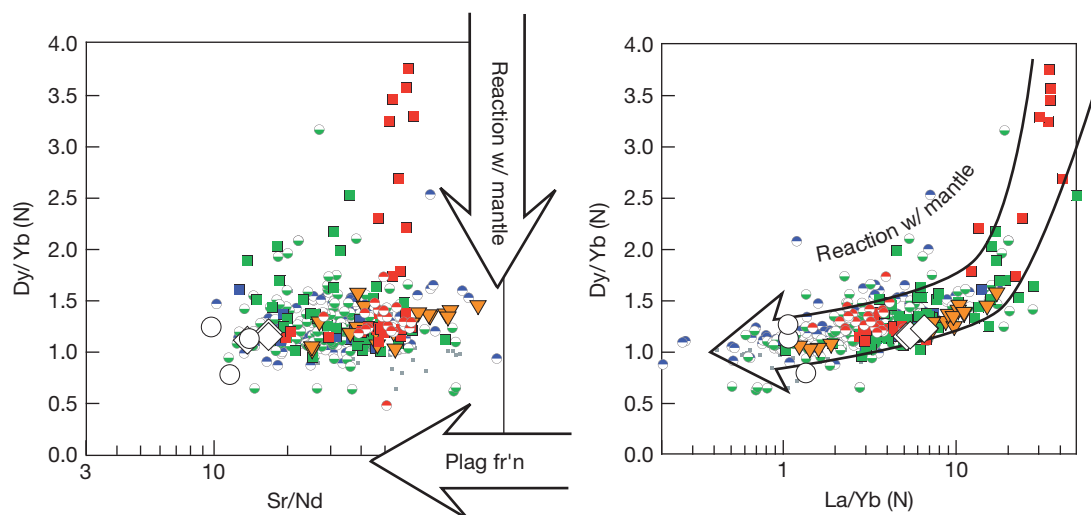


Figure 8 Relationship among Sr/Nd, La/Yb, and Dy/Yb for primitive arc lavas. High Dy/Yb is probably indicative of an important role for residual garnet in the genesis of some lavas. Not all lavas with very high La/Yb and Sr/Nd have high Dy/Yb. Thus, it may be unwise to use La/Yb and high Sr as indications that a given igneous rock is derived from a source with abundant, residual garnet. Arrows labeled 'reaction with mantle' show results for trace-element models of reaction of a partial melt of MORB in eclogite facies with upper mantle peridotite (Kelemen et al., 2003b). Arrow marked 'plag fr'n' emphasizes that because Sr is much more compatible than Nd in plagioclase, crystal fractionation of plagioclase or crystal assemblages with cotectic proportions of plagioclase lead to decreasing Sr/Nd. Data and symbols as for Figure 6. Sr/Nd on x-axis in left panel is not normalized, and is on a logarithmic scale.

plate, except under unusual circumstances (see reviews in Kelemen et al., 2003a; Peacock, 1996, 2003; Peacock et al., 1994). For example, Eiler et al. (2000, p. 247) discounted their successful model involving H₂O-rich silicate melt because "[the] successful melt-fluxed [model] ... require[s] ... temperatures ... that are ... not obviously compatible with ... thermal models ... (Peacock, 1996)."

Recently, as discussed in Section 4.21.3.3.4, subduction zone thermal models that incorporate thermally dependent viscosity and/or non-Newtonian viscosity in the mantle wedge predict temperatures higher than the fluid-saturated solidus near the top of the subducting plate beneath arcs at normal subduction rates and subducting plate ages (Kelemen et al., 2003a; van Keken et al., 2002). While this is an area of active research, it is no longer the case that thermal models 'rule out' partial melting of subducted material in eclogite facies.

(2) *Primary andesite magma from fluxed melting.* A more popular model for arc magma genesis is 'fluid-fluxed melting' (Section 4.21.3.2.1). An aqueous fluid derived from subducted basalt and sediment enriches the mantle source of arc magmas in 'mobile elements,' while simultaneously causing partial melting of that source (e.g., Abe et al., 1998; Eiler et al., 2000; Grove et al., 2001, 2003; Ozawa, 2001; Ozawa and Shimizu, 1995; Stolper and Newman, 1992; Vernieres et al., 1997). In this interpretation, high LILEs and light REEs are seen as the result of fluid enrichment, while low heavy REEs, titanium, and scandium are seen as the results of high degrees of melting. Again, high H₂O, K₂O, and Na₂O contents derived from the fluxing fluid may lead to relatively high SiO₂ melt in equilibrium with peridotite. Following this reasoning, primitive andesites could be the extreme products of fluxed melting (Grove et al., 2003).

A series of recent papers describes how this process can produce a very close match to high-Mg# andesites from the

Mt. Shasta volcano in the southern Cascades (Grove et al., 2001, 2003). However, as in previous inversions based on a variety of arc lavas (Eiler et al., 2000; Stolper and Newman, 1992), the required fluids have dissolved light REEs and thorium contents larger than predicted from experimental fluid/rock partitioning studies (Ayers et al., 1997; Brenan et al., 1996, 1995a,b; Kogiso et al., 1997; Stalder et al., 1998; Tatsumi and Kogiso, 1997). If the fluxing agent in flux melting were a silicate melt rather than an aqueous fluid, predicted REE and LILE contents would be much higher, potentially resolving this discrepancy. We return to this point in Section 4.21.3.3.1. From this perspective, 'melt-fluxed melting' can be considered more or less identical to (1).

(3) *Mixing of primary basalt and granitic lower crustal melts.* Although there are significant fluid mechanical barriers to such a process (e.g., Campbell and Turner, 1985), many chemical features of high-Mg# andesites could be explained as the result of mixing of primitive arc basalt with evolved, silica-rich melt with high LILEs and light REEs, and low heavy REEs, titanium, and scandium.

In the western Aleutians, high-Mg# andesites have abundant zoned phenocrysts that probably do reflect magma mixing processes. However, the most light REE-enriched, heavy REE-depleted magmas have the highest Mg# (Kelemen et al., 2003b; Yogodzinski and Kelemen, 1998), which is inconsistent with the hypothesis of mixing primitive basalt with enriched granitic melt outlined in the previous paragraph (Kelemen et al., 2003b; tables 18 and 19). Instead, mixing apparently combined primitive light REE-enriched andesites with more evolved, less enriched andesites.

With the exception of the western Aleutian arc, primitive and high-Mg# andesites (excluding boninites) are rare in intra-oceanic arcs (Figure 4). High-Mg# andesites are most common in continental arcs, where interaction between basalt and

preexisting crust might be important. Primitive andesites have been reported from the Cascades (Baker et al., 1994; Grove et al., 2001, 2003; Hughes and Taylor, 1986), Baja California (Rogers et al., 1985), southeast Costa Rica and western Panama (de Boer et al., 1988, 1995; Defant et al., 1991a,b, 1992), Ecuador (Beate et al., 2001; Bourdon et al., 2002; Monzier et al., 1997), Argentina (Kay and Kay, 1991, 1993), southern Chile (Sigmarsson et al., 2002, 1998; Stern and Kilian, 1996), the Philippines (Defant et al., 1989; Maury et al., 1992; Schiano et al., 1995), Papua New Guinea (Arculus et al., 1983), SW Japan (Shimoda et al., 1998; Tatsumi, 1982, 2001a,b; Tatsumi and Ishizaka, 1981, 1982), and Kamchatka (Kepzhinskis et al., 1997).

In all these localities, other than the Aleutians, most high-Mg# andesites have elevated $^{208}\text{Pb}/^{204}\text{Pb}$, compared to MORB (Figure 9). Thus, lead-isotope data suggest the presence of a component derived either from recycling of lead from subducting sediment, or from crustal interaction of primitive basalts with older continental crust and continentally derived sediment. Given the fact that so many primitive andesites are in 'continental' arcs, crustal interaction processes must be considered. This said, primitive andesites and basalts have overlapping $^{87}\text{Sr}/^{86}\text{Sr}$ and $^{143}\text{Nd}/^{144}\text{Nd}$, which restricts the range of crustal sources that could be involved in mixing or assimilation to create primitive andesites from basalts.

Lower crustal anatexis in arcs such as the Andes (e.g., Babeyko et al., 2002), which have thick crust and probably garnet at the base of the crust, might be expected to yield appropriate mixing end-members. Indeed, our compilation includes dacitic to rhyolitic lavas from the Andes with high Dy/Yb (Bourdon et al., 2000; Kay and Kay, 1994; Matteini et al., 2002). Mixtures of these compositions with primitive basalt have most of the major and trace-element characteristics of high-Mg# andesites (e.g., Figure 10). Thus, in this chapter, we reexamine the hypothesis that primitive andesites are produced by crustal mixing or assimilation using global data, rather than data from just the Aleutians. This reexamination could be extended to the western Aleutians as well; perhaps,

small proportions of high SiO_2 , small-degree melts of garnet granulite in arc lower crust are commonly produced but rarely erupted. Could such mixing explain the composition of primitive andesites in general?

Key data to address this question come from ratios of trace elements that are fractionated differently by partial melting of eclogite compared to garnet granulite. For example, because strontium is compatible in plagioclase, strontium is more incompatible than neodymium in melting of plagioclase-free eclogite, whereas strontium is more compatible than neodymium in partial melting of lower crustal granulite with substantial plagioclase. Because temperatures at the base of the crust in active arcs are high ($>800^\circ\text{C}$) and crustal thickness rarely exceeds 60 km, eclogite facies assemblages will not form in arc lower crust. However, formation of garnet granulites is possible where crustal thickness exceeds 25–30 km (e.g., Jull and Kelemen, 2001). Although garnet formation might be inhibited by slow kinetics in H_2O -poor lower crustal cumulates, observations from the Talkeetna and Kohistan arc crustal sections show that garnet did form at pressures where it was thermodynamically stable (Section 4.21.4). While some garnet in the Talkeetna lower crustal section is entirely metamorphic in origin, other samples include residual or cumulate igneous garnet (Section 4.21.4.3). As noted above, our arc lava compilation includes high Dy/Yb, evolved lavas from the Andes, which are probably partial melts of garnet granulite. However, while these lavas are appropriate in other ways as mixing end-members to produce high-Mg# andesites, they have low Sr/Nd (Figure 10). Therefore, these evolved Andean lavas could not mix with primitive arc basalt to produce high-Mg# andesites, which have higher Sr/Nd (Figure 10), and it is unlikely that any other lower crustal melts would be appropriate.

In many ways, the process of 'assimilation,' or melt/rock reaction, is comparable to magma mixing. Reaction between hot, primitive basalt and granitic wall rock, in particular, shares many characteristics with mixing of primitive basalt and a granitic partial melt of wall rock. For example, both processes tend to produce high, nearly constant compatible-element

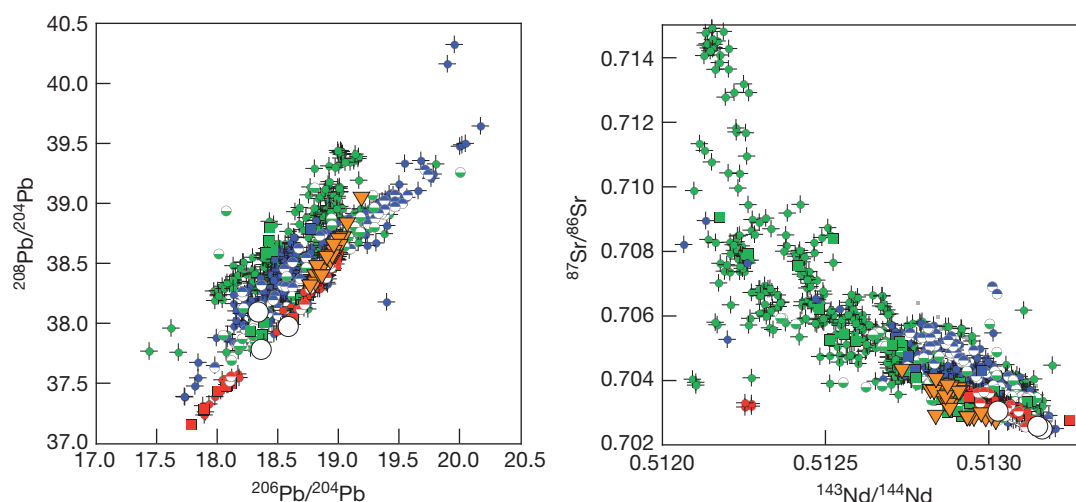


Figure 9 Pb, Sr, and Nd isotopes in primitive lavas from our arc compilation. In general, primitive andesites do not have distinctive isotopic characteristics, compared to primitive basalts. Primitive andesites from the western Aleutians have the most depleted values in our data compilation. Data and symbols as for Figures 1 and 6.

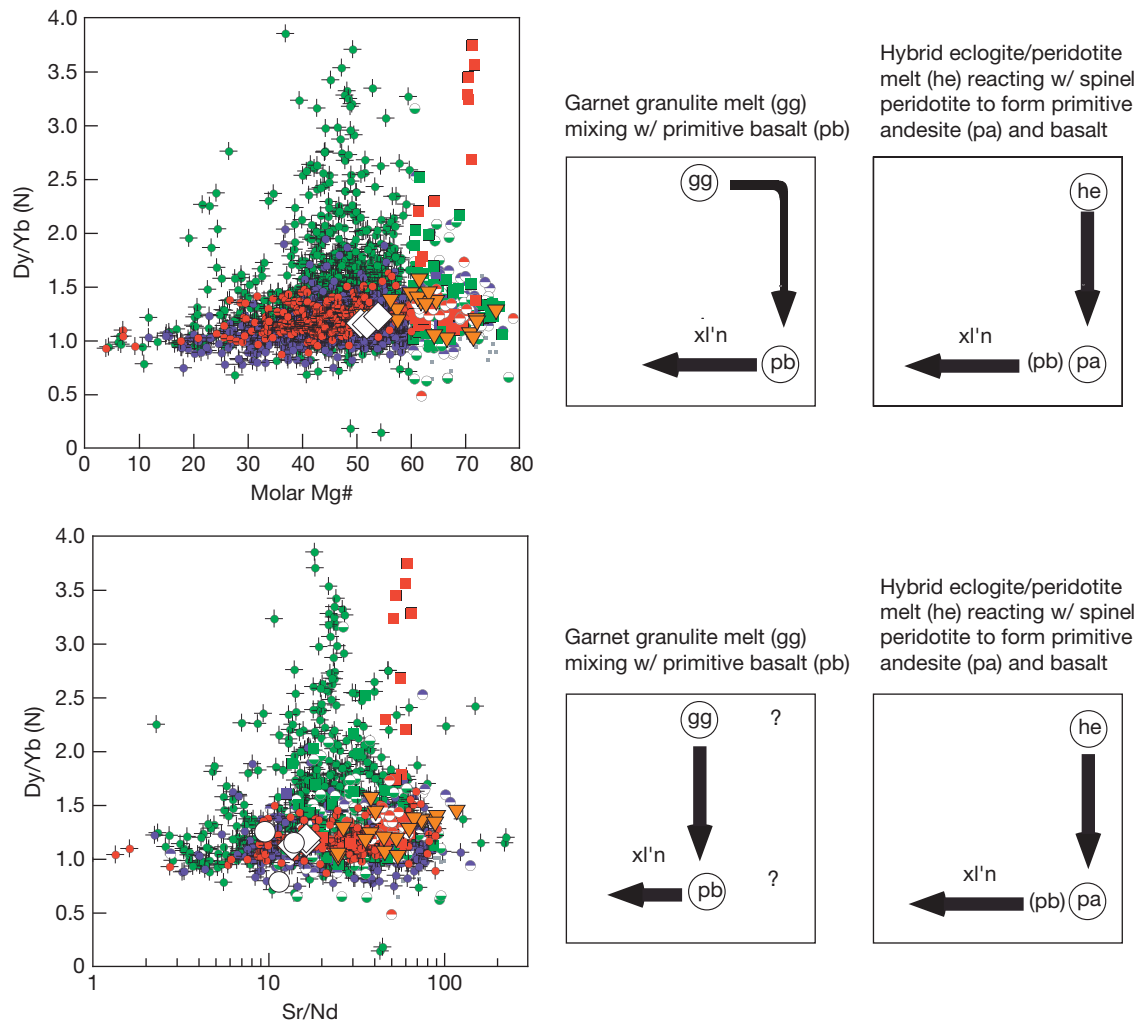


Figure 10 Relationship between Mg#, Dy/Yb, and Sr/Nd in arc lavas from our compilation. Partial melts of subducted, eclogite facies MORB have high Dy/Yb and Sr/Nd (e.g., Gill, 1974, 1978; Kay, 1978; Kelemen et al., 1993, 2003b; Rapp et al., 1999; Yogodzinski and Kelemen, 1998). When these melts react with overlying mantle, the hybrid liquid acquires a high Mg# (Kay, 1978; Kelemen et al., 1993, 2003b; Rapp et al., 1999; Yogodzinski and Kelemen, 1998). Western Aleutian primitive andesites may form in this way. Continued reaction increases heavy REE and Y contents to values in equilibrium with depleted mantle peridotite as melt/rock ratios decrease to ~ 0.1 or less (Kelemen et al., 1993, 2003b). High Sr/Nd, primitive andesites and even primitive basalts Dy/Yb ~ 1.5 may form in this way. Alternatively, primitive andesites could be mixtures of lower crustal melts and primitive basalt (e.g., Kay and Kay, 1994). Partial melts of lower crustal garnet granulites, as exemplified by some Andean andesite and dacites (Bourdon et al., 2000; Kay and Kay, 1994; Matteini et al., 2002), have high Dy/Yb at lower Mg# and Sr/Nd than Aleutian primitive andesites. Mixing with primitive basalt (e.g., average Marianas primitive basalt, Table 1) yields high Dy/Yb high-Mg# melts similar to Aleutian primitive andesites. However, such mixtures have low Sr/Nd, unlike Aleutian and other primitive andesites. Because Sr is more compatible than Nd in plagioclase, this result is likely to be general. Thus, while magma mixing may have played some role in the genesis of many or most arc lavas, mixing is an unlikely explanation for the genesis of primitive andesite compositions.

concentrations and ratios (magnesium, iron, nickel, Mg#) together with substantial enrichment in incompatible trace elements, over much of the range of mixing or reaction progress (compare, e.g., DePaolo, 1981; and Kelemen, 1986 with O'Hara and Mathews, 1981).

In specific cases, the outcome of melt/rock reaction may be quite distinct from magma mixing. Selective dissolution of plagioclase in hydrous, plagioclase-undersaturated melt could enrich resulting liquids in Sr/Nd, potentially producing trends distinct from the mixing trends in Figure 10. However, note that selective dissolution of plagioclase alone might create a telltale anomaly with high Eu/Sm, and would not explain other characteristics of high-Mg# andesites, including

heavy REE, titanium, scandium, and vanadium depletion. Instead, selective dissolution of plagioclase would have to be coupled with crystallization of garnet to explain high-Mg# andesite genesis via crustal melt/rock reaction. In view of the fact that garnet is not saturated in primitive arc melts at pressures of $\sim 1\text{--}1.5$ GPa (e.g., Müntener et al., 2001), we view this as unlikely. Furthermore, on a global basis, high Sr/Nd is negatively correlated with $^{87}\text{Sr}/^{86}\text{Sr}$, ruling out assimilation of continental granitoids, or sediments derived from continental crust.

In summary, primitive andesites are probably derived from primary andesite magmas, produced by processes below the base of igneous arc crust, which are different from primary

magmas of primitive arc basalts. Mixing of primitive basalt and evolved partial melts of lower crustal garnet granulite probably cannot produce end-member high-Mg# andesite lava compositions. Similarly, lower crustal assimilation probably cannot produce typical high-Mg# andesites. Instead, we conclude that most primitive andesites are probably produced via process (1) described above, by reaction of small-degree partial melts of subducted, eclogite-facies sediment and/or basalt with the overlying mantle wedge. In our view, process (2), melting of the mantle fluxed by an enriched 'fluid' component derived from subducted sediment and/or basalt, is only viable if the fluxing 'fluid' is, in fact, a melt or a supercritical fluid with partitioning behavior similar to melt/rock partitioning. Thus, viable versions of process (2) are the same as process (1).

Primary magmas parental to primitive andesites may also be parental to calc-alkaline, evolved arc magmas. It is evident that fractionation of olivine, pyroxene, and/or plagioclase from a primitive andesite melt leads to higher SiO_2 and alkali contents, at a given degree of crystallization, compared to fractionation of the same phases from primitive basalt (Figure 11). The key here is that olivine + pyroxene cumulates, and olivine + pyroxene + plagioclase cumulates have $\sim 50\%$ SiO_2 as determined by mineral stoichiometry and cotectic proportions. Crystallizing these solid assemblages from a basalt with $\sim 50\%$ SiO_2 does not change the SiO_2 content of the resulting liquid, whereas removing the same cumulates from an andesite with 55 or even 60 wt% SiO_2 leads to an increase in SiO_2 in the derivative liquid. (Note that the variation in Figure 11, taken out of context, might also be attributed to fractionation from a common parental magma with $\text{Mg\#} \sim 0.8$; however, trace-element and isotope variation precludes this possibility.) The high SiO_2 and – probably – H_2O contents of primitive andesites may make them difficult to erupt. As they reach the midcrust, become saturated in H_2O , and degas, their viscosity must rise abruptly, leading to slower melt transport and enhanced rates

of crystallization. For these reasons, primitive andesites may be more common among melts entering the base of the igneous crust than among erupted lavas.

It is not clear to what extent this analysis can be extended to high-Mg# andesite compositions typical of plutonic rocks in calc-alkaline batholiths. Some Aleutian and Cascades plutonic rocks are high Sr/Nd, high-Mg# andesites that cannot be produced via crustal mixing, but high Sr/Nd in these rocks could arise via incorporation of cumulate plagioclase. Many calc-alkaline plutonic rocks have relatively low Sr/Nd, and could be mixtures of lower crustal melts and primitive basalt. Because plagioclase crystallization leads to decreasing Sr/Nd with decreasing Mg#, most calc-alkaline plutonic rocks could also be derived via crystal fractionation from primitive andesite. Therefore, the Sr/Nd discriminant between lower crustal melts (low Sr/Nd) and eclogite melts (high Sr/Nd) is only useful for lavas that retain high Dy/Yb. Unfortunately, this means that Sr/Nd cannot be used to determine the extent to which the high-Mg# andesite composition of continental crust is due to crystal fractionation from a primitive andesite parent, versus the extent to which it is due to mixing of primitive basalt and lower crustal melts.

Why are primitive andesites rare? In Sections 4.21.3.2.5 and 4.21.3.3, we argue that a component derived from partial melting of subducting sediment and/or basalt is included in most arc magmas. This is consistent with a substantial body of work calling upon partial melts of subducting sediment to explain trace-element enrichments in arc basalts, but inconsistent with the theory that primitive andesites with 'adakite' trace-element signatures (Section 4.21.3.2.4), which apparently include tens of percent eclogite melt (Kelemen et al., 2003b), are only found in arcs with unusually hot subduction zones – due to subduction of young oceanic crust, very slow convergence rates allowing substantial time for conductive heating, and/or discontinuous 'tears' that enhance mantle

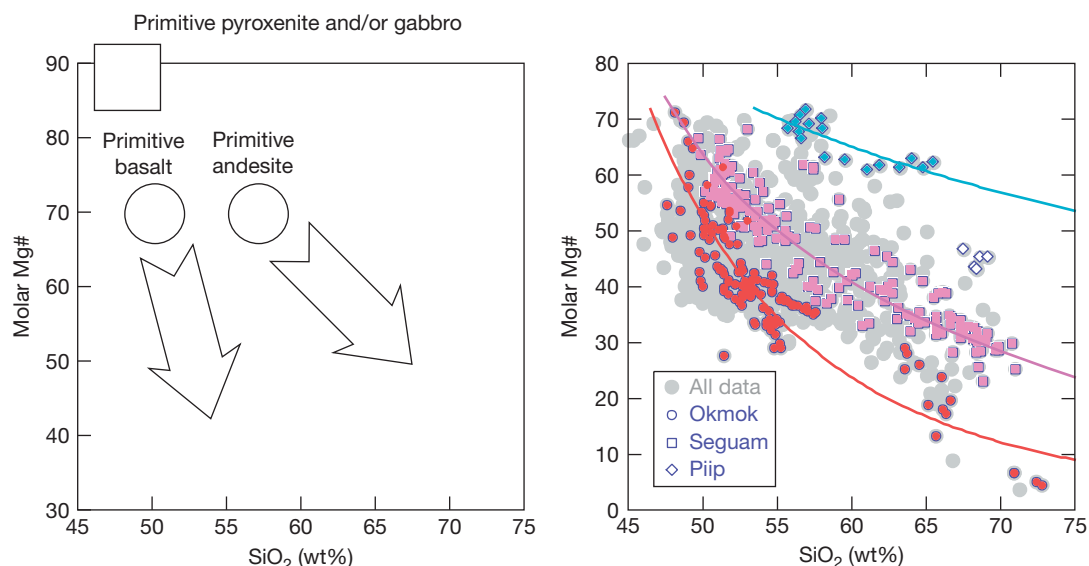


Figure 11 On the left, a schematic illustration showing how fractionation of primitive pyroxenite or gabbro from primitive basalt leads to decreasing Mg# at nearly constant SiO_2 , while fractionation of the same crystal assemblages from primitive andesite leads to increasing SiO_2 . On the right, data from the oceanic Aleutian arc (compiled by Kelemen et al., 2003b) show how variation between lava series from different volcanoes might arise as a result of this effect. Sources of data for Seguam, Okmok, and Piip volcanoes are given in the caption for Figure 2. Filled symbols for each volcano were used in power law curve fits. Open symbols were omitted.

convection in the subducting plate and allow conductive heating from the side, as well as the top and bottom (e.g., de Boer et al., 1991, 1988; Defant and Drummond, 1990; Yogodzinski et al., 1995, 2001, 1994).

If partial melts of subducted material are ubiquitous in arcs, why do they form large proportions of arc magma in a few places, and very small proportions (a few percent, e.g., Class et al., 2000) in most arcs? Following Kelemen et al. (2003b), we offer the following tentative explanation. Arcs that have primitive andesites are similar in having slow convergence rates, and it may be true that many are situated above 'tears' in the subducting plate. Most (except the Aleutians) are in regions of young plate subduction. Thus, the subduction zone may be unusually hot, and may yield a larger proportion of partial melt. However, it is hard to imagine that this can account for a factor-of-ten difference in the proportion of subduction zone melt in arc lavas. Instead, other factors may be involved. Slow convergence leads to slow convection in the mantle wedge, enhancing the amount of conductive cooling. This could be very important, because of positive feedback: increased viscosity due to cooling could slow wedge convection still further. Thus, we suggest that primitive andesites are found in areas in which the subducting plate is relatively hot, producing more partial melt, and the overlying wedge is relatively cold, producing less partial melt. In contrast, in normal arcs, abundant melts derived from the mantle wedge overwhelm the subduction zone melt signature, except for distinctive isotope ratios and thorium contents carried in partial melts of sediment.

In addition, as outlined in Sections 4.21.3.1.3 and 4.21.3.1.4, primitive andesites may contain more H₂O than primitive basalts (e.g., Grove et al., 2003). If so, they will become H₂O saturated and degas at mid-crustal depths. As a result of degassing, these magmas will undergo rapid crystal fractionation, so that only evolved andesites and dacites reach the surface. Also, as a result of degassing together with their relatively high SiO₂ contents, primitive andesites will become very viscous in the mid-crust, and this may inhibit their eruption.

4.21.3.3 Trace Elements, Isotopes, and Source Components in Primitive Magmas

4.21.3.3.1 Incompatible trace-element enrichment

Lava compositions from arcs worldwide share many characteristics that are, in turn, very distinct from those of MORBs. These distinctions have been known for decades, and we cannot hope to provide a comprehensive review of the entire literature on this topic. However, we wish to use our data compilation to quantify the differences between arc and MORB lavas. Thus, cesium, rubidium, radium, barium, thorium, uranium, and potassium are enriched in most arc lavas relative to MORB, together with light REEs, potassium, lead, and strontium (Figure 12). Moderately incompatible elements (middle- to heavy-REE and titanium) are generally depleted relative to MORB (Figure 6). These characteristics are present in both oceanic and continental arcs. Globally, these characteristics are observed even in the most primitive lavas, and some of the most enriched lavas in our data set are western Aleutian primitive andesites with low ⁸⁷Sr/⁸⁶Sr and lead (Yogodzinski et al., 1995) isotope ratios (Kelemen et al., 2003b, 1994). Thus,

it seems likely that the enrichments do not arise mainly as a result of crustal processes, and instead are present in melts entering the base of arc crust, and have a sub-Moho origin, at least in part.

On the basis of a similar reasoning, a host of studies in the 1980s and 1990s were designed to decipher the subcrustal source of enriched incompatible trace-element contents in arc magmas. Possible sources of enrichment, relative to the MORB mantle source, include (1) aqueous fluids derived by dehydration of subducting metabasalt, (2) aqueous fluids derived by dehydration of subducting metasediment, (3) aqueous fluids derived by dehydration of partially serpentinized mantle peridotite, (4) hydrous partial melts of subducting basalt, (5) hydrous partial melts of subducting sediment, and (6) the presence of 'enriched mantle' similar to the various mantle source components inferred for ocean island basalt. These could act upon, or mix with (7) fertile mantle peridotite similar to the MORB source, or (8) mantle peridotite depleted by melt extraction beneath a mid-ocean ridge and/or a back arc basin. Given the relatively poorly known (and probably variable) compositions of these various components, their poorly known (and variable) proportions in a given primary arc magma, and the poorly known processes through which different components might interact with additional trace-element fractionation, there may be numerous combinations of these components which could account for the composition of a given primary magma. As a result, most authors have tried to simplify the geochemical interpretation of arc petrogenesis by concentrating on just a few of these components, whose interaction might account for much of the trace-element variability in arc basalts.

(1) *Three main components? Using trace-element ratios.* Studies that call upon three principal components in arc basalt petrogenesis have been particularly influential: (1) aqueous fluids derived from metabasalt, (2) partial melts of subducting sediment, and (3) MORB source mantle (e.g., Class et al., 2000; Ellam and Hawkesworth, 1988a; Elliott, 2003; Elliott et al., 1997; Hawkesworth et al., 1997; Johnson and Plank, 1999; Miller et al., 1994; Plank and Langmuir, 1993, 1998; Turner et al., 2003, 2000a,c). These studies generally rely on analyses of both primitive and evolved basalts, and so they use incompatible trace-element ratios in an attempt to remove the effects of crystal fractionation. In these studies, one component, with relatively low Ba/La and Th/La, and MORB-like isotope ratios is interpreted as the preexisting mantle source, prior to fluid and sediment melt enrichment.

Also in these studies, enrichments in 'fluid mobile' elements relative to light REE (e.g., high U/Th, Ra/Th, Ba/La, Pb/Ce, and Sr/Nd), are attributed to an aqueous fluid component. In some arcs and in Elliott's worldwide compilation of ICP-MS data on arc basalts, this component has isotopic characteristics similar to hydrothermally altered MORB (e.g., ⁸⁷Sr/⁸⁶Sr ~ 0.7035, ¹⁴³Nd/¹⁴⁴Nd ~ 0.5132; ²⁰⁸Pb/²⁰⁴Pb down of 38).

High boron concentrations and high boron and oxygen-isotope ratios in the aqueous fluid component relative to the MORB source are attributed to hydrothermal alteration in the fluid source (Bebout et al., 1993, 1999; Domanik et al., 1993; Eiler et al., 2000; Ishikawa and Nakamura, 1994; Leeman, 1987, 1996; Ryan and Langmuir, 1992; Ryan et al., 1989; You et al., 1993, 1995). Our data compilation includes few

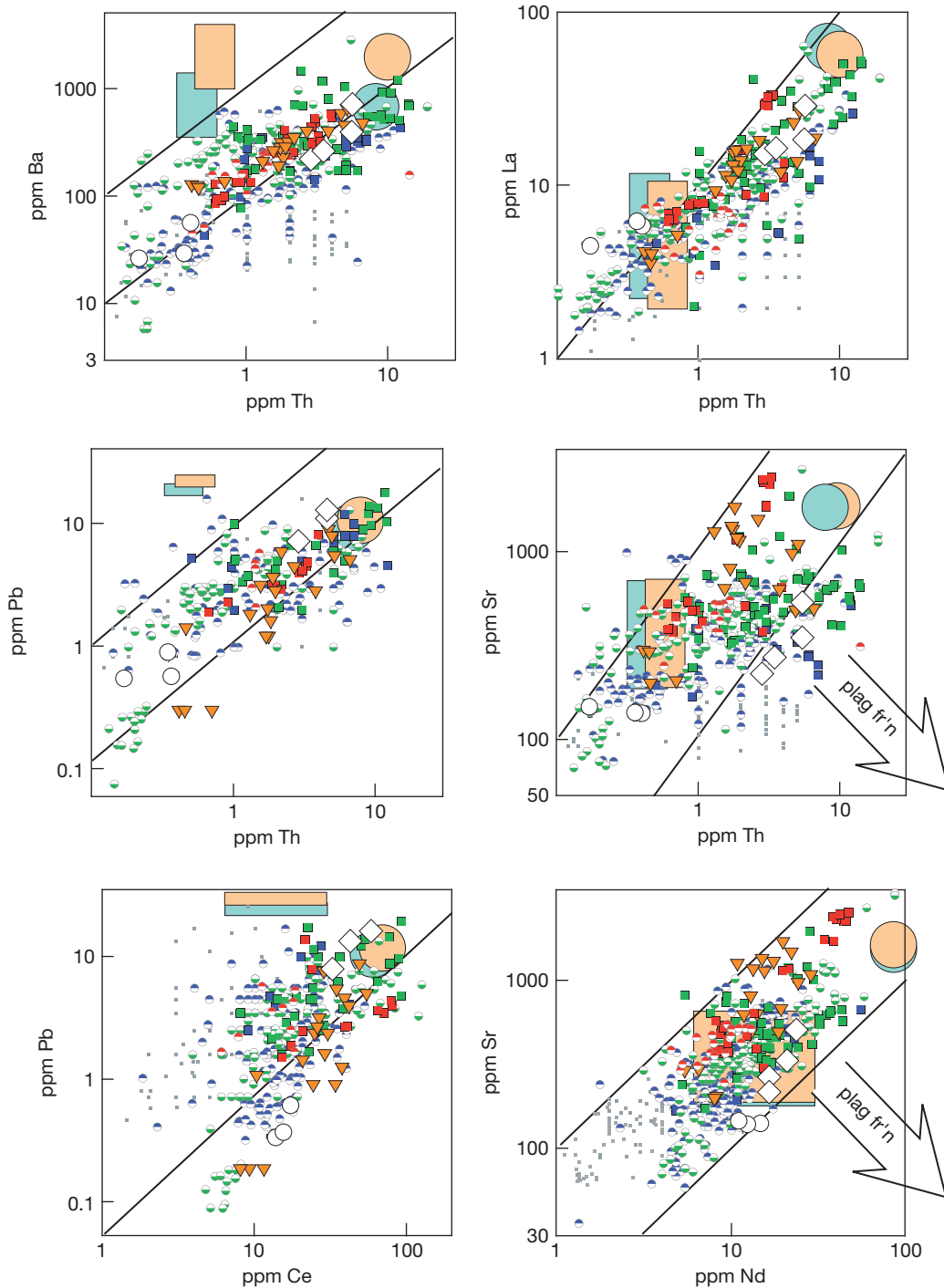


Figure 12 Trace-element concentrations, in ppm, for primitive lavas in our compilation. In general, primitive arc lavas are enriched in Th, Ba, La, Pb, Ce, Sr, and Nd, compared to average MORB. (Concentrations of these elements in primitive MORB are even lower than the average values.) This is somewhat at odds with theories invoking separate enrichment processes involving aqueous fluids for Ba, Pb, and Sr, and partial melts of subducting sediment for Th, La, Ce, and Nd. Diagonal lines illustrate constant trace-element ratios. The overall trends of the compiled data do not diverge dramatically from constant ratios of these elements (diagonal lines). If anything, ‘fluid-mobile’ Ba, Pb, and Sr show less variation and less enrichment relative to MORB than ‘immobile’ Th and La. Since all these elements are highly incompatible during melting of eclogite facies sediment and basalt, and in peridotite/melt equilibria, similar enrichment of all of them is a natural consequence of melting and melt transport. Conversely, because Th, La, Ce, and Nd are less soluble in aqueous fluids than Ba, Pb, and Sr, dehydration and aqueous fluid transport should fractionate these elements. Large symbols show estimated compositions of fluid (rectangles) and melt (circles) in equilibrium with eclogite for Marianas (blue) and Aleutians (yellow) at 2 wt% fluid or melt extracted (Table 2b). The size of the rectangle reflects different partition coefficients used in the estimate. Nd concentration is not calculated and is assumed to be the same as Ce concentration (not shown in Table 2). Arrow outline labeled ‘plag fr’n’ in diagrams involving Sr reminds readers that even small amounts of plagioclase crystallization will lead to decreasing Sr together with increasing concentrations of Th and Nd. Symbols as in Figures 1 and 6.

data on boron and concentration, or on boron and oxygen isotopes, and so we have not attempted to re-visit these topics.

In contrast, enrichments in ‘fluid immobile’ Th relative to light REE (e.g., Th/La) and enrichments of light/middle REE (e.g., La/Sm) are attributed to a partial melt of subducted material. This component is thought to be a sediment melt because in some arcs it has isotopic characteristics similar to subducting sediment (e.g., $^{87}\text{Sr}/^{86}\text{Sr}$ up to 0.706; $^{143}\text{Nd}/^{144}\text{Nd}$ down to 0.5127; $^{208}\text{Pb}/^{204}\text{Pb} \sim 39.0$) and because thorium enrichments at a given $^{143}\text{Nd}/^{144}\text{Nd}$ are larger than can be accounted for by simple mixing of mantle peridotite and sediment. The fact that basalt mainly contributes aqueous fluid whereas the sediment-rich component is mainly transported in melt might be attributed to the steep thermal gradient at the top of a subducting plate, in which only the topmost layers are heated above their fluid-saturated solidus, giving rise to the aphorism “sediments melt, basalts dehydrate.”

The role of subducted sediment is particularly well documented for selected high-quality data on arc basalts in which the high Th/La component has Th/La identical to that in the subducting sediment column (Plank, 2003). Very efficient recycling of subducted thorium, together with subducted ^{10}Be (present only in surficial sediments), has also been taken as evidence for transport of sediment-derived thorium and beryllium in a partial melt, rather than an aqueous fluid (e.g., Johnson and Plank, 1999; Kelemen et al., 1995a); but apparently in disagreement with Ryan and Chauvel (see Chapter 3.13) and Schmidt and Poli (see Chapter 4.19).

(2) *Two main components? Using trace-element abundance.* In our data compilation, there are many primitive lavas whose trace-element abundance is minimally affected by crystal fractionation, so we decided to dispense with the use of ratios such as Ba/La and Th/La. We did this because many arc lavas are enriched in both light REEs (the denominator) and barium, thorium, lead, and strontium (the numerator) in commonly used trace-element ratios. Thus, for example, a lava with 1 ppm lanthanum, Ba/La of 100, and Th/La of 0.1 has less lanthanum, barium, and thorium than a lava with 50 ppm lanthanum, Ba/La of 20, and Th/La of 0.3. Thus, in Figures 12 and 13, we plot incompatible trace-element abundances in primitive lavas. These data present a somewhat different picture from the three-component hypothesis outlined in Section 4.21.3.3.1.

In Figure 13, one can see that oceanic lavas with high Ba/La generally have lower $^{87}\text{Sr}/^{86}\text{Sr}$ than lavas with high Th/La, and that in most oceanic arcs, lavas with high Ba/La have low Th/La and lavas with high Th/La have low Ba/La, as outlined in Section 4.21.3.3.1. However, almost all data for the oceanic Aleutian arc have low $^{87}\text{Sr}/^{86}\text{Sr}$ (<0.7035) despite a wide range of Ba/La and Th/La, and the Aleutians show strong positive correlation between Ba/La and Th/La. Figure 13 also shows that most oceanic arc lavas show positively correlated barium, thorium, lanthanum, and $^{87}\text{Sr}/^{86}\text{Sr}$, while oceanic Aleutian arc lavas and continental arc lavas show wide variation in barium, thorium, and lanthanum, which is not correlated with $^{87}\text{Sr}/^{86}\text{Sr}$ or, for example, $^{208}\text{Pb}/^{204}\text{Pb}$. Thus, for example, enrichments in thorium can occur in primitive arc lavas without incorporation of radiogenic strontium and lead, (and unradiogenic neodymium) from subducted sediments (Kelemen et al., 2003b).

High thorium in primitive arc magmas with MORB-like lead, neodymium, and strontium-isotope ratios, such as in primitive andesites from the western Aleutians, is probably ‘not’ attributable to incorporation of a sedimentary thorium component, yet it has very similar thorium enrichment (though lower Th/La) compared with magmas that ‘are’ thought to incorporate thorium derived from subducted sediment. However, experimental studies of eclogite/aqueous fluid and peridotite/aqueous fluid partitioning show that thorium is not very soluble (Ayers et al., 1997; Brenan et al., 1996, 1995a,b; Johnson and Plank, 1999; Kogiso et al., 1997; Stalder et al., 1998; Tatsumi and Kogiso, 1997). In contrast, thorium is strongly enriched in small-degree melts of basalt or sediment (e.g., Johnson and Plank, 1999; Rapp et al., 1999; Ryerson and Watson, 1987). For this reason, we attribute thorium enrichment in arc magmas generally to incorporation of thorium in a partial melt of eclogite facies, subducted basalt ‘and/or’ sediment (e.g., Kelemen et al., 1993, 2003b). We return to this topic in Section 4.21.3.3.1.

Somewhat to our surprise, over the past few years several investigators have found that small-degree partial melts of eclogite may also have some characteristics normally attributed to an aqueous fluid component in arc magmas, such as high Ba/La, Pb/Ce, and Sr/Nd (e.g., Kelemen et al., 2003b; Rapp et al., 1999; Tatsumi, 2000). Thus, it may be difficult to distinguish between partial melts of eclogite and an aqueous fluid component using these trace-element ratios. Although we do not doubt that, for instance, barium, lead, and strontium ‘can’ be fluid-mobile, fluid enrichment of the arc magma source may not be the dominant control on barium, lead, and strontium enrichment in arc magmas in our compilation. Correlation of barium, lead, and strontium with thorium suggests that either ‘fluid’ and ‘melt’ components generally combine in similar proportions worldwide, or that some process can produce both barium and thorium enrichment simultaneously. This observation and its interpretation are very similar to observations and interpretation of ^{10}Be versus B/Be systematics (e.g., Morris et al., 1990).

Most primitive arc lavas have elevated barium, thorium, lanthanum, lead, cesium, strontium, ‘and’ neodymium, compared to MORBs. Because all these components are incompatible during melting of eclogite or peridotite, while they are fractionated from each other by fluid/rock partitioning, it may be that the difference between arc lavas and MORBs is primarily due to incorporation of a partial melt of subducted, eclogite facies sediment and/or basalt into the arc magma source. Where sediments are present, high sediment thorium and lead concentrations together with distinctive sediment isotope ratios are likely to impart a sedimentary signature to melts of subducted material. Where sediments are absent, Th/La and Pb/Ce are likely to be somewhat lower, and isotope ratios in subduction zone melts are likely to be closer to those in the MORB source.

We do not mean to imply that dehydration reactions in subducting material do not evolve aqueous fluid. However, much of that fluid may escape into the fore-arc region. And, certainly, scatter in Figure 12 – with logarithmic axes – is indicative of a wide range of Ba/Th, Pb/Ce, and Sr/Nd. These variations may result from additional enrichment of barium, lead, and strontium (and boron) relative to thorium and light

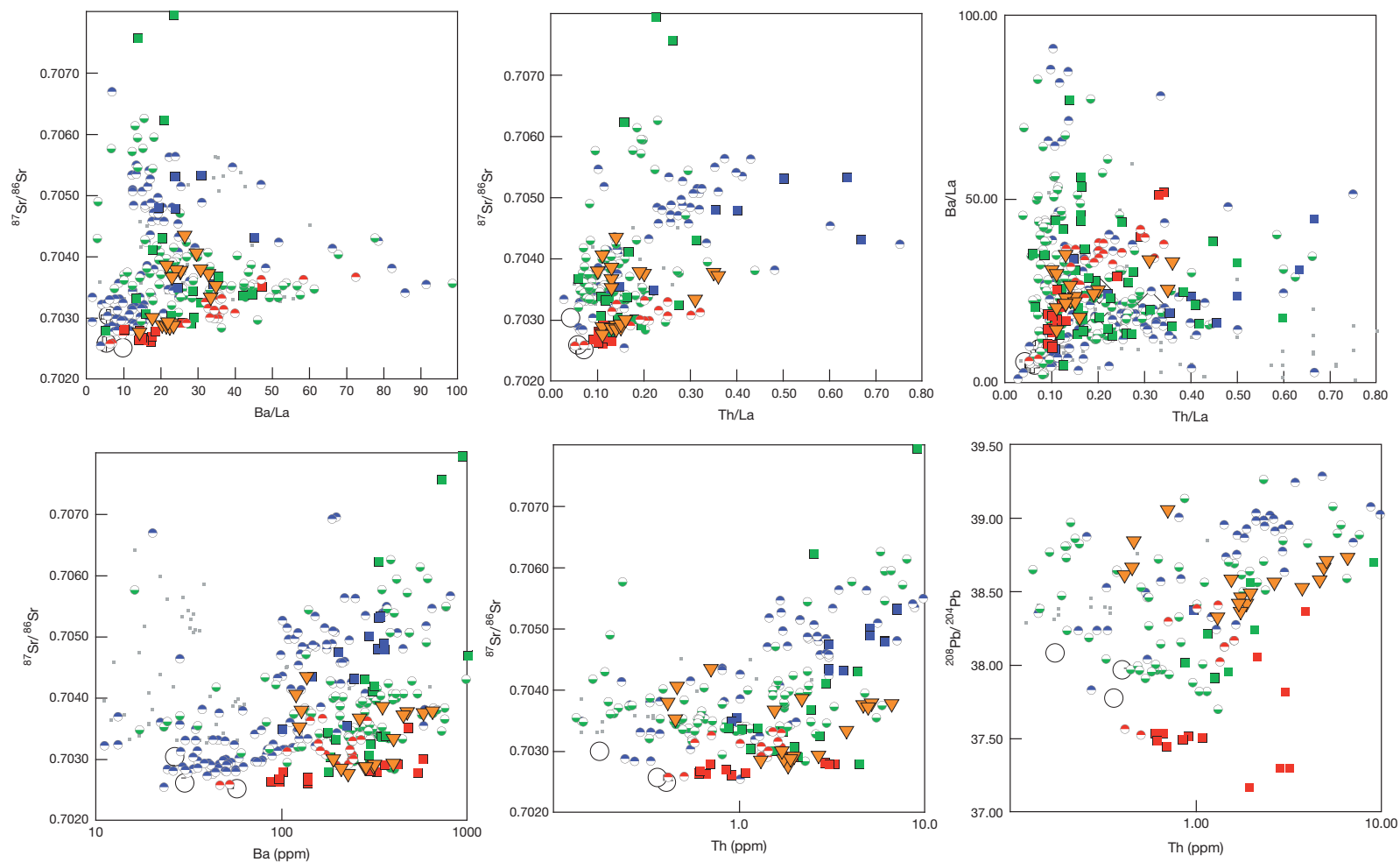


Figure 13 Trace-element concentrations in ppm, trace-element ratios, and isotope ratios for primitive arc lavas in our compilation. A high Ba/La, low Th/La component has $^{87}\text{Sr}/^{86}\text{Sr} \sim 0.704$, while a distinct low Ba/La, high Th/La component in most oceanic arcs has $^{87}\text{Sr}/^{86}\text{Sr} \sim 0.706$. However, continental arcs, the oceanic Aleutian arc, and some other primitive arc lavas have relatively high Ba/La and Th/La. For most oceanic arcs, Ba and Th concentration in primitive lavas are correlated (Figure 12) and both are correlated with $^{87}\text{Sr}/^{86}\text{Sr}$. With very few exceptions, primitive andesites from the oceanic Aleutian arc and from continental arcs show lower $^{87}\text{Sr}/^{86}\text{Sr}$ and $^{208}\text{Pb}/^{204}\text{Pb}$, at a given Ba or Th concentration, compared to lavas from other oceanic arcs at the same Ba or Th concentration. Symbols as in Figures 1 and 6.

REE in some arcs due to an aqueous fluid component, as described in [Section 4.21.3.3.1](#).

(3) *Melt and fluid compositions and arc mass balance.* As already mentioned, it is particularly important to consider enrichments in lanthanum and thorium, since these are relatively insoluble in aqueous fluids under subduction-zone conditions (Ayers et al., 1997; Brenan et al., 1996, 1995a,b; Johnson and Plank, 1999; Kogiso et al., 1997; Stalder et al., 1998; Tatsumi and Kogiso, 1997). Given probable values for arc magma flux, average arc lava concentrations of these elements, assumptions about are lower crustal composition, experimentally measured solubilities for these elements in aqueous fluids, estimates of the subducting flux of H₂O, and assumptions about the mantle source of arc magmas, it has often been concluded that aqueous fluids derived from subducting material cannot explain the magmatic flux of lanthanum and thorium in arcs (e.g., Elliott, 2003; Elliott et al., 1997; Hawkesworth et al., 1997; Johnson and Plank, 1999; Kelemen et al., 1993, 2003b; Plank, 2003; Plank and Langmuir, 1988, 1993, 1998). If true, this is crucial because it requires that almost *all* arcs require enrichment of the mantle source in lanthanum and thorium ‘via some mechanism other’ than aqueous fluid transport from subducting material.

Because this is so crucial, we offer our own flux calculations in [Table 2](#). These calculations support previous work on the subject. Using experimental eclogite/fluid distribution coefficients, 2–5% fluid equilibrating with the entire section of subducted oceanic crust+sediments beneath an arc (see, e.g., [Chapter 4.19](#)) could carry the entire excess magmatic flux (primitive arc basalt – primitive MORB) of barium, lead, and strontium. Some experimental data have lanthanum solubilities in subduction fluids just high enough to account for the excess magmatic lanthanum flux in arcs. However, our results are consistent with previous calculations showing that aqueous fluid transport cannot account for the excess magmatic thorium flux. Further, our simple calculations support the idea that aqueous fluid transport should result in large fractionations of barium from thorium, lead from cesium, and strontium from neodymium. Thus, calculated fluid compositions lie at high Ba/Th, Pb/Ce, and Sr/Nd compared to barium, thorium, lead, strontium, and light REE-enriched primitive arc lavas ([Figure 12](#)). In contrast, transport in 2–5% melt of basalt+sediment in eclogite facies can account for excess magmatic flux of barium, thorium, lanthanum, lead, and strontium, and this mechanism will produce relatively small fractionations between these different elements. As a result, calculated melt compositions plot at the enriched end of the trend from MORB to barium, thorium, lead, strontium, and light REE-enriched primitive arc lavas ([Figure 12](#)).

(4) *Fluids, melts, or goo above the solvus?* The suggestion that aqueous fluids might play a minor role in arc magma genesis is apparently at odds with interpretations of data on oxygen isotopes versus trace-element enrichment in several arcs (Eiler et al., 2000). These data were inferred to indicate that enrichment in arcs is via an aqueous fluid, with a relatively high O/Ti ratio, rather than a silicate liquid with a much lower O/Ti ratio. However, the Eiler et al. result applies mainly to their relatively large data set for the Vanuatu arc, and depends on the composition of depleted boninite magmas, and questionable assumptions about mantle source composition (e.g., initial Cr/

(Cr + Al) = 0.1). Further, although they did make a successful model involving melt transport rather than fluid transport, Eiler et al. (2000) discounted the result because it was apparently at odds with thermal models that rule out melting of subducting material. In their successful melt transport model, the melt has 30 wt% H₂O, within the range 25–50 wt% H₂O inferred for aqueous fluid saturated melts at 3–5 GPa (Dixon and Stolper, 1995; Dixon et al., 1995; Kawamoto and Holloway, 1997; Mysen and Wheeler, 2000).

The suggestion that aqueous fluids may not play a key role in subduction zone petrogenesis may seem at first to be at odds with the decades-old inference that addition of H₂O to the mantle wedge is one of the key causes of mantle melting and arc magmatism. However, this is certainly not what we wish to propose. Instead, as elegantly shown in calculations by Eiler et al. (2000), the effect of adding H₂O to peridotite is very similar whether the added H₂O is in an aqueous fluid or dissolved in silicate melt. Thus, assuming that the effect of other possible fluxes such as K₂O is second order, if 10% fluid-fluxed melting requires addition of ~1 wt% fluid with ~90 wt% H₂O, then 10% melt-fluxed melting might require addition of ~3 wt% melt with 30 wt% H₂O, or ~wt% melt with 45 wt% H₂O.

About 30–50 wt% H₂O in a silicate melt corresponds to molar H/Si ~3–6, which raises the question, is a fluid-saturated melt at 3–5 GPa more like an anhydrous melt or an aqueous fluid? It is possible that the H₂O-rich phase generated via dehydration reactions in subducting plates at 3–5 GPa might form at conditions where there is no longer a solvus separating distinct melt and fluid phases (Bureau and Keppler, 1999; Keppler, 1996). In this interpretation, the differences in experimentally constrained partitioning behavior at subduction zone pressures, for example, between fluid/eclogite (Ayers et al., 1997; Brenan et al., 1996, 1995a,b; Johnson and Plank, 1999; Kogiso et al., 1997; Stalder et al., 1998; Tatsumi and Kogiso, 1997) and melt/eclogite (Rapp et al., 1999), might arise as a result of the H₂O/silicate ratio in a given experimental bulk composition, rather the existence of distinct melt and fluid phases. Alternatively, the traditional interpretation, in which distinct fluid and melt phases can be present in H₂O-eclogite at, for example, 3–5 GPa and 700–900 °C, may well be correct.

The presence or absence of a solvus between melt and fluid in equilibrium with eclogite at high pressure and moderate temperature is likely to be controversial for several years to come. Meanwhile, the message from our flux calculations ([Table 2](#)) and calculated fluid versus melt compositions ([Figure 12](#)) remains clear: it is easiest to understand the range of trace-element enrichment in arc lavas, relative to MORBs, if transport of barium, thorium, lead, strontium, and light REEs from subducted sediment and basalt is mainly in a phase whose partitioning characteristics are similar to those measured for relatively H₂O-poor ‘melt’/rock, and different from those measured for relatively H₂O-rich ‘fluid’/rock.

4.21.3.3.2 Tantalum and niobium depletion

Tantalum and niobium in arc magmas are depleted relative to REEs, so that Nb/La and Ta/La are lower than in the primitive mantle and in MORBs. Depletion of primitive arc magmas in

Table 2a Arc inputs and outputs assuming 5 wt% H₂O or 5 wt% melt extracted

		<i>Aleutians</i>	<i>Marianas</i>	<i>Izu-Bonin</i>	<i>Kermadec</i>	<i>Tonga</i>	<i>Ref. D</i>
Age	My	55	45	45	30	24	
Thickness arc crust	km	20	20	20	18	12	
Material subducted	10 ⁶ kg km ⁻¹ year ⁻¹	1321	592	896	1154	1564	
Magmatic flux	10 ⁶ kg km ⁻¹ year ⁻¹	115	140	140	150	113	
Magmatic flux	km ³ km ⁻¹ year ⁻¹	38	47	47	50	38	
Excess La	kg km ⁻¹ year ⁻¹	292	155	95	503	569	
Excess Th	kg km ⁻¹ year ⁻¹	117	31	209	166	67	
Excess Ba	kg km ⁻¹ year ⁻¹	20 809	7224	5023	19 823	29 367	
Excess Sr	kg km ⁻¹ year ⁻¹	38 016	16 601	12 361	29 106	38 075	
Excess Pb	kg km ⁻¹ year ⁻¹	396	83	542	416	619	
La flux in fluid	kg km ⁻¹ year ⁻¹	133	67	106	131	171	1
La flux in fluid	kg km ⁻¹ year ⁻¹	679	345	541	673	876	2
Th flux in fluid	kg km ⁻¹ year ⁻¹	27	10	16	22	23	1
Th flux in fluid	kg km ⁻¹ year ⁻¹	52	20	31	42	44	3
Ba flux in fluid	kg km ⁻¹ year ⁻¹	99 692	15 605	22 725	37 121	37 576	3
Ba flux in fluid	kg km ⁻¹ year ⁻¹	47 136	7378	10 745	17 551	17 766	2
Sr flux in fluid	kg km ⁻¹ year ⁻¹	11 827	5215	7738	10 152	13 616	1
Sr flux in fluid	kg km ⁻¹ year ⁻¹	33 566	14 800	21 963	28 813	38 646	3
Sr flux in fluid	kg km ⁻¹ year ⁻¹	37 606	16 581	24 606	32 281	43 297	2
Pb flux in fluid	kg km ⁻¹ year ⁻¹	861	323	547	1175	1399	1
Pb flux in fluid	kg km ⁻¹ year ⁻¹	957	360	609	1307	1556	3
La flux in melt	kg km ⁻¹ year ⁻¹	2689	1364	2143	2662	3465	4
Th flux in melt	kg km ⁻¹ year ⁻¹	356	134	209	287	300	4
Ba flux in melt	kg km ⁻¹ year ⁻¹	72 557	11 358	16 540	27 017	27 348	4
Sr flux in melt	kg km ⁻¹ year ⁻¹	79 353	34 988	51 922	68 117	91 363	4
Pb flux in melt	kg km ⁻¹ year ⁻¹	573	215	364	782	931	4

Note: Arc ages from [Jarrard \(1986\)](#), except Aleutians, which is from [Scholl et al. \(1987\)](#). Material subducted is calculated assuming 7-km thick subducting oceanic crust with densities of 3.0 g cm⁻³, sediment thicknesses and densities from [Plank and Langmuir \(1998\)](#); subduction rates from [England et al. \(2003\)](#). Magmatic flux is calculated using arc crust thickness from [Holbrook et al. \(1999\)](#) (Aleutians), [Suyehiro et al. \(1996\)](#) (Izu-Bonin) and [Plank and Langmuir \(1988\)](#) (Marianas, Kermadec and Tonga), subtracting 6 km preexisting oceanic crust, and assuming a 150-km arc width. Excesses of selected trace elements are calculated subtracting abundances in N-MORB ([Hofmann, 1988](#)) from average abundances in primitive arc basalt (Table 1). Trace-element fluxes in fluid and melt are calculated assuming modal batch melting (5% in [Table 2a](#), 2% in [Table 2b](#)). Because estimates of partition coefficients (*D*s) between eclogite and fluid are highly variable, more than one value was used for each element. References for the values used are listed in the column labeled *Ref. D*. Partition coefficients are from (1) [Ayers \(1998\)](#), (2) [Stalder et al. \(1998\)](#), (3) [Brenan et al. \(1995b\)](#), and (4) [Kelemen et al. \(2003b\)](#). Average composition for Izu Bonin primitive basalt is not included in Table 1 (too few analyses) and is (in ppm) La = 4.57, Th = 1.68, Ba = 49.75, Sr = 201.49, Pb = 4.36.

Table 2b Arc inputs and outputs assuming 2 wt% H₂O or 2 wt% melt extracted

		<i>Aleutians</i>	<i>Marianas</i>	<i>Izu-Bonin</i>	<i>Kermadec</i>	<i>Tonga</i>	<i>Ref. D</i>
La flux in fluid	kg km ⁻¹ year ⁻¹	52	26	42	52	67	1
La flux in fluid	kg km ⁻¹ year ⁻¹	284	144	226	281	366	2
Th flux in fluid	kg km ⁻¹ year ⁻¹	11	4	6	9	9	1
Th flux in fluid	kg km ⁻¹ year ⁻¹	22	8	13	17	18	3
Ba flux in fluid	kg km ⁻¹ year ⁻¹	99 012	15 499	22 570	36 868	37 320	3
Ba flux in fluid	kg km ⁻¹ year ⁻¹	25.678	4019	5853	9561	9679	2
Sr flux in fluid	kg km ⁻¹ year ⁻¹	4811	2121	3148	4130	5539	1
Sr flux in fluid	kg km ⁻¹ year ⁻¹	15 009	6618	9820	12 883	17 280	3
Sr flux in fluid	kg km ⁻¹ year ⁻¹	17 131	7553	11 209	14 705	19 723	2
Pb flux in fluid	kg km ⁻¹ year ⁻¹	621	233	395	848	1010	1
Pb flux in fluid	kg km ⁻¹ year ⁻¹	764	287	486	1044	1243	3
La flux in melt	kg km ⁻¹ year ⁻¹	1466	744	1168	1451	1889	4
Th flux in melt	kg km ⁻¹ year ⁻¹	264	99	155	212	223	4
Ba flux in melt	kg km ⁻¹ year ⁻¹	50 570	7916	11 528	18 830	19 061	4
Sr flux in melt	kg km ⁻¹ year ⁻¹	44 852	19 776	29 347	38 501	51 640	4
Pb flux in melt	kg km ⁻¹ year ⁻¹	321	121	204	438	522	4

Data sources and calculations as in [Table 2a](#). Concentration ranges in fluids and concentrations in melts shown in [Figure 12](#), are calculated as flux divided by water/melt mass.

tantalum and niobium relative to lanthanum and thorium (Figure 14) is ubiquitous (a few niobium-enriched lavas – e.g., Kepezhinskas et al., 1997 – form a distinct anomaly, which will not be discussed in this chapter). For this reason, and because thorium, tantalum, and niobium are relatively immobile in low-temperature alteration of basalts, low Nb/Th and Ta/Th have been used as discriminants between arc magmas and both ocean island basalts and MORBs, to constrain the provenance of lavas where tectonic accretion has obscured their original setting (e.g., Pearce, 1982; Pearce and Peate, 1995).

While tantalum and niobium are relatively depleted, compared to other incompatible elements, many primitive arc magmas have higher tantalum and niobium concentrations than MORB (Figure 14). This is particularly true of primitive continental arc lavas, both basalts and andesites. Oceanic arc lavas tend to have tantalum and niobium concentrations as low as or lower than MORBs, and elevated lanthanum concentrations compared to MORBs.

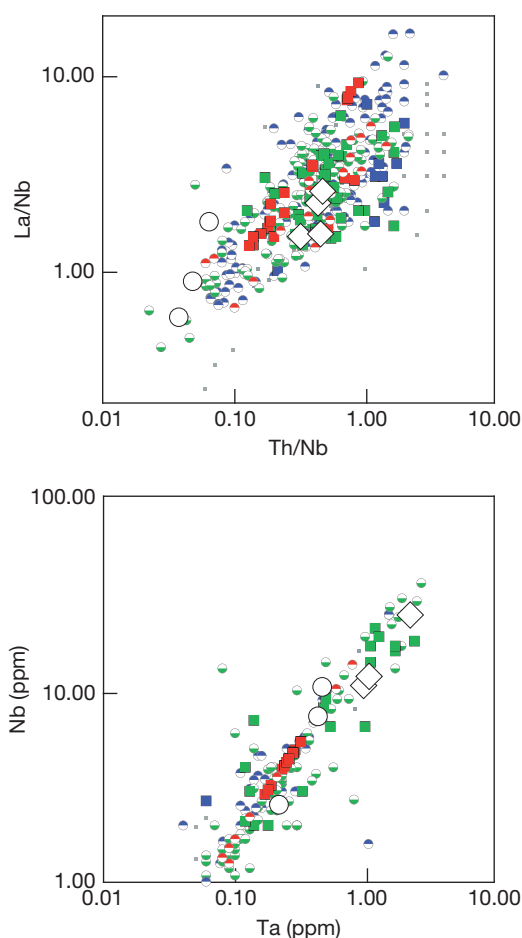


Figure 14 Relative depletion of Nb relative to Th and La in primitive arc lavas compared to MORB. For samples without Nb analyses (mostly, Aleutian data), we estimated $\text{Nb} \sim 17 \cdot \text{Ta}$. Primitive andesites have among the highest Th/Nb and La/Nb in the compiled data. Nb, Ta, and La concentrations are all higher than MORB in some continental arc lavas; in most oceanic arc lavas, including Aleutian primitive andesites, Nb and Ta concentrations are similar to or less than in MORB, while La is enriched compared to MORB. Symbols as in Figures 1 and 6.

Depletion of tantalum and niobium relative to other incompatible elements in arc lavas has been ascribed to many processes (review in Kelemen et al., 1993) including (1) crystal fractionation of Fe–Ti oxides in the crust, (2) fractionation of titanium-rich hydrous silicates such as phlogopite or hornblende in the mantle or crust, (3) extensive chromatographic interaction between migrating melt and depleted peridotite, (4) the presence of phases such as rutile or sphene in the mantle wedge (Bodinier et al., 1996), (5) relative immobility of tantalum and niobium relative to REE and other elements in aqueous fluids derived from subducting material, (6) inherited, low Ta/Th and Nb/Th from subducted sediment (Plank, 2003), and (7) the presence of residual rutile during partial melting of subducted material.

Primitive basalts have not been affected by extensive FeTi oxide fractionation in the crust, and they have magmatic temperatures too high for amphibole or biotite crystallization, ruling out (1) and (2) in the previous paragraph. Chromatographic fractionation of niobium and tantalum from thorium and lanthanum requires melt/rock ratios $\sim 10^{-3}$, and thus – given estimated arc fluxes – requires that parental arc magmas react with the entire mass of the mantle wedge during ascent (Kelemen et al., 1993), so (3) seems unlikely. Consistently low Nb/La and Nb/Th is observed in arc magmas, even in primitive basalts that are hot and far from rutile saturation at mantle pressures (Kelemen et al., 2003b), eliminating (5) for most arc basalts. Finally, as noted above, lanthanum and thorium enrichment in arc magmas probably occurs via addition of a melt from subducting sediment or basalt in eclogite facies, and not via aqueous fluid metasomatism, so high La/Nb and Th/Ta does not arise as a result of fluid/rock fractionation (6). In some arc lavas, it appears that niobium, tantalum, and lanthanum concentrations are equally enriched, compared to MORBs, and thus low Nb/La and Ta/La in these may be due to transport of all these elements in a melt of subducted continental sediment without residual rutile (Johnson and Plank, 1999). If so, however, this raises the question of how low Nb/La and Ta/La originally formed in the continents. Suites without a strong signature of recycled sediment (many oceanic arc lavas and, particularly, primitive Aleutian andesites) generally show lanthanum enrichment without niobium and tantalum enrichment, relative to MORBs.

For these reasons, if a single explanation for niobium and tantalum depletion in primitive arc lavas is to be sought, we prefer hypothesis (7), fractionation of niobium and tantalum from other highly incompatible elements via partial melting of subducting eclogite facies basalt or sediment with residual rutile (Elliott et al., 1997; Kelemen et al., 1993; Ryerson and Watson, 1987; Turner et al., 1997). If this inference is correct, it follows that nearly all arc magmas include a component derived from partial melting subducted material in eclogite facies, with residual rutile.

4.21.3.3.3 U-series isotopes

There have been numerous recent papers and reviews on U/Th, U/Pa, and Ra/Th isotopic disequilibrium in arc lavas (Bourdon et al., 1999, 2000; Clark et al., 1998; George et al., 2003; Gill and Condomines, 1992; Gill and Williams, 1990; Newman et al., 1984, 1986; Reagan and Gill, 1989; Reagan et al., 1994; Regelous et al., 1997; Sigmarsson et al., 2002,

1990, 1998; Thomas et al., 2002; Turner et al., 2003, 2000a–c, 2001, 1997; Turner and Foden, 2001). This is a complicated topic, and we cannot provide sufficient background information to make it accessible to a nonspecialist. However, because these data have bearing on other topics covered in this chapter, we summarize our understanding of recent work in this section. An explanation of the basic principles governing U-series fractionation and isotopic evolution is given by Spiegelman and Elliott (see [Chapter 4.15](#)).

Several recent papers have emphasized the presence of substantial ^{226}Ra excess (over parent ^{230}Th) in arc lavas. In the Marianas and Tonga arcs, ^{226}Ra excess correlates with Ba/La, Ba/Th, and Sr/Th (George et al., 2003; Sigmarsson et al., 2002; Turner et al., 2003, 2000a–c, 2001; Turner and Foden, 2001). As a result, ^{226}Ra excess is linked in these papers to the transport of a fluid component from subducted material to arc volcanoes in less than a few thousand years.

The argument that ^{226}Ra excess is generated by deep, subduction-zone processes is particularly compelling for lavas from southern Chile, in which $^{10}\text{Be}/^9\text{Be}$ correlates with ^{226}Ra excess, suggesting that a component derived from young, subducted sediment may reach arc volcanoes in 1000 or 2000 years (Sigmarsson et al., 2002). In contrast, a data set on beryllium- and uranium-series isotopes from the Aleutian arc does not show correlation of ^{226}Ra excess and $^{10}\text{Be}/^9\text{Be}$ (George et al., 2003). Unfortunately, Sigmarsson et al. (2002) do not report sufficient geochemical data to evaluate whether Ba/La is high in lavas with high ^{226}Ra excess as in other data sets, and/or whether Th/La and Th/Ba are high as in the proposed sediment melt component ([Section 4.21.3.3.1](#)), which might transport ^{10}Be . If the high ^{226}Ra component in the southern Andes has high barium and thorium, we would propose that radium, barium, thorium, and beryllium are all carried in a partial melt of subducted sediment or basalt, not in an aqueous fluid.

Transport of fluid and/or melt from the subduction zone directly beneath an arc to the surface in approximately one half-life of ^{226}Ra requires transport rates of order $\sim 100\text{ m year}^{-1}$, and this cannot be sustained during diffuse porous flow of melt through peridotite at porosities $< \sim 0.03$. Instead, melt flow must be focused into high porosity conduits or cracks (Sigmarsson et al., 2002; Turner et al., 2001). It has been claimed that velocities $\sim 100\text{ m year}^{-1}$ require flow of melt in fractures rather than via porous flow (e.g., Sigmarsson et al., 2002). However, simple calculations show that if melt/fluid viscosity is $\sim 2\text{ Pa s}$, density contrast between mantle and fluid/melt is $\sim 500\text{ kg m}^{-3}$ and mantle grain size is between 4 and 10 mm; the velocity of buoyancy-driven porous flow of melt through mantle peridotite will exceed 100 m year^{-1} at porosities of 0.09–0.035 (Kelemen et al., 1997a). Estimates of porous flow velocity depend on uncertain parameterizations of mantle permeability, poorly constrained grain size in the mantle wedge, and so on. Nonetheless, it is apparent that even if all ^{226}Ra excess arises from dehydration and/or partial melting in subduction zones at a depth of $\sim 100\text{ km}$, and ^{226}Ra excess data require transport in less than one half-life of ^{226}Ra (1600 year), this result cannot be used to discriminate between transport in fractures versus focused flow in high-porosity conduits.

In addition, while the currently accepted interpretation may well be correct, the present understanding of U-series data in arcs is reminiscent of early work on ^{226}Ra excess in MORB, in which it was suggested that ^{226}Ra excess forms during the initial stages of decompression melting, $\sim 100\text{ km}$ below the seafloor, and is transported to ridge lavas in less than a few thousand years (e.g., McKenzie, 1985; Richardson and McKenzie, 1994). Currently available data on young MORB show a negative correlation between ^{226}Ra excess and ^{230}Th excess (e.g., Sims et al., 2002). Because ^{230}Th excess is probably formed by melting or melt/rock reaction involving garnet peridotite (e.g., McKenzie, 1985; Spiegelman and Elliot, 1992), garnet pyroxenite (e.g., Hirschmann and Stolper, 1996; Lundstrom et al., 1995), or fertile, high-pressure clinopyroxene (e.g., Turner et al., 2000b; Wood et al., 1999), the negative correlation between ^{230}Th and ^{226}Ra excesses may be indicative of a role for shallow-level processes in the generation of ^{226}Ra excess (e.g., melt/rock reaction in the shallow mantle, interaction with lower crustal plagioclase (Jull et al., 2002; Lundstrom, 2000; Lundstrom et al., 2000, 1995, 1999; Saal et al., 2002; Spiegelman and Elliot, 1992; Van Orman et al., 2002). As a result, ^{226}Ra excess may not be a reliable indicator of melt transport velocities in the mantle beneath mid-ocean ridges (see [Chapter 4.15](#)).

Arc lavas, like MORB, also show a negative correlation between ^{226}Ra excess and ^{230}Th excess (or $1/^{238}\text{U}$ excess), allowing for some ^{226}Ra decay (George et al., 2003; Reagan et al., 1994; Sigmarsson et al., 2002; Turner et al., 2003, 2000a,c, 2001) ([Figure 15](#)). Since the generation of ^{230}Th excess probably involves garnet and/or fertile clinopyroxene at pressures of 2 GPa or more, we anticipate the evolution of theories in which ^{230}Th excess forms deep, while shallow processes play a role in generating ^{238}U and ^{226}Ra excess in arc lavas, as well as in MORB. However, because radium, thorium, and uranium concentrations are higher in most arc lavas than in MORB, shallow-level processes capable of generating ^{238}U and ^{226}Ra excess in arcs may differ from those beneath mid-ocean ridges. Thus, reaction between ascending melt and anhydrous mantle peridotite may not be capable of generating large ^{226}Ra and ^{238}U excesses in primitive arc lavas (Thomas et al., 2002), and assimilation of young plagioclase may also be an unlikely explanation for ^{226}Ra excess in arc lavas (e.g., George et al., 2003). However, steady-state diffusive gradients involving radium- and barium-rich minerals such as phlogopite or biotite could produce ^{226}Ra excess correlated with high Ba/La in melts interacting with the upper mantle or lower arc crust (Feineman and DePaolo, 2002). In this interpretation, relatively high Sr/Th in Marianas and Tonga lavas with high ^{226}Ra excess (Turner et al., 2003) might be due to interaction with both biotite and plagioclase. Because radium and barium are geochemically similar to each other, and very different from thorium and lanthanum, there may be other processes that result in enrichment of radium and barium relative to thorium and lanthanum. From this perspective, not all lavas with high Ba/La and Ba/Th necessarily record selective enrichment of barium via aqueous fluid metasomatism in the mantle source.

If ^{226}Ra excess were 'always' the result of relatively shallow processes, then correlation of high $^{10}\text{Be}/^9\text{Be}$ with high ^{226}Ra excess in southern Chilean lavas would imply a shallow source

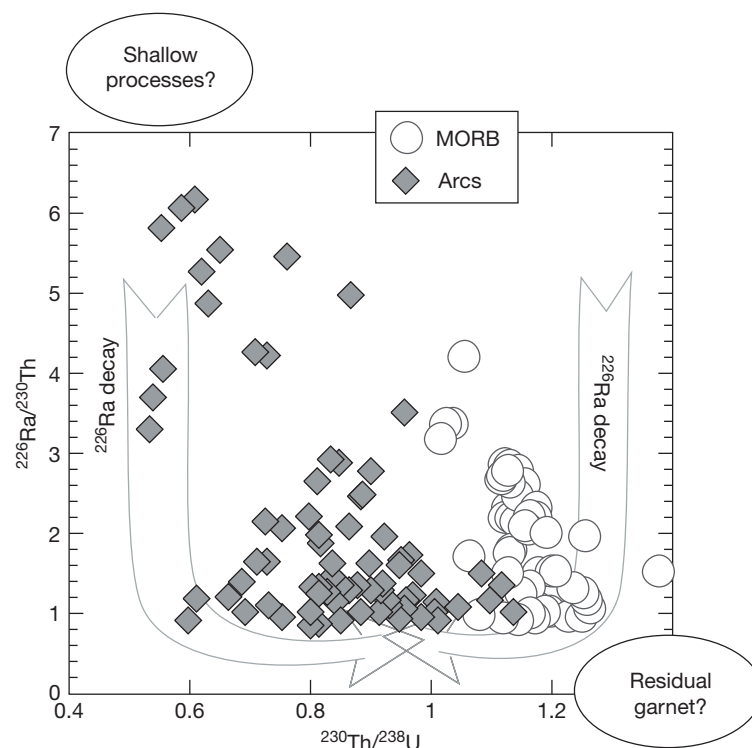


Figure 15 ^{226}Ra excess versus ^{230}Th excess in MORB and arc magmas. MORB data compiled by Sims et al. (2002). Arc data compiled by Turner et al. (2003). ^{226}Ra decay may explain very low ^{226}Ra excess in some lavas. However, the highest ^{226}Ra excess at any given $^{230}\text{Th}/^{238}\text{U}$ shows a negative correlation with ^{230}Th excess. In the MORB data, ^{230}Th excess may arise at depths of 2–3 GPa, via U/Th exchange between melt and garnet, or melt and high-pressure fertile clinopyroxene compositions. Lavas with high ^{226}Ra excess do not show this high-pressure signature, and so many hypotheses call upon shallow melt/mantle interaction, or even lower crustal processes, to explain the genesis of ^{226}Ra excess. Similar theories have been advanced to explain the arc data. See text for discussion and references.

for ^{10}Be enrichment as well. Some of the Chilean samples analyzed for ^{226}Ra (Sigmarsson et al., 2002) are evolved (Stern and Kilian, 1996), and not enough data are presented to determine whether any of the other Chilean samples are primitive or not. While excess ^{226}Ra and ^{10}Be may be transported from subduction zone depths in some arcs, it may also be worthwhile to reevaluate the extent to which some evolved magmas interact with meteoric water, or assimilate alteration products that have high ^{226}Ra excess and high $^{10}\text{Be}/^9\text{Be}$.

It is not yet clear whether high-thorium primitive lavas worldwide have high ^{230}Th excess or not. ^{230}Th excess has been observed in a few arc lavas, notably primitive andesites from Mt. Shasta in the southern Cascades (Newman et al., 1986), and high-Mg# andesites from the Austral Andes in southernmost Chile (Sigmarsson et al., 2002). This is consistent with the hypothesis that primitive andesites contain a substantial proportion of partial melt from a source rich in residual garnet, such as subducting, eclogite facies sediment, and/or basalt (Section 4.21.3.2.5).

Substantial ^{230}Th excess is also observed in some primitive basalts from Central America (Thomas et al., 2002). If primitive basalts do not include a substantial eclogite melt component, then the ^{230}Th excess in Central American basalts might reflect melting or melt/rock reaction in the presence of garnet in the mantle wedge. (Another alternative is that ^{230}Th excess arises as a result of melting, or melt/rock reaction, in the presence of fertile high-pressure clinopyroxene; Turner et al.,

2000b; Wood et al., 1999.) Two factors favor a potentially large role for garnet in the mantle wedge, compared to the melting region beneath mid-ocean ridges. First, relatively high H_2O fugacity in the mantle beneath most arcs lowers mantle solidus temperatures at a given pressure. Because of the positive pressure/temperature slope of reactions such as pyroxene + spinel = olivine + garnet, lower solidus temperature lowers the minimum depth at which garnet can be stable on the arc mantle solidus (e.g., Gaetani and Grove, 1998). Second, theoretical considerations suggest that both porous and/or fracture transport of melt in the mantle wedge to the base of arc crust might be diagonal, beginning at depths of 150 km or more beneath the back arc region (Davies, 1999; Spiegelman and McKenzie, 1987). Thus, the maximum pressure of mantle melting beneath an arc may not be constrained by the depth to the subduction zone directly beneath the arc. Because the maximum pressure of melting might be as large or larger beneath arcs, and the minimum pressure of garnet stability on the mantle solidus is probably lower beneath arcs, the interval in which garnet could react with arc melts is probably larger beneath arcs compared to ridges. We will return to this point in Section 4.21.3.3.4.

More generally, arc lavas show ^{238}U excess, usually interpreted to be indicative of high U/Th solubility in aqueous fluids derived from subducting material. ^{226}Ra excess is correlated with ^{238}U excess in most data sets on historically erupted lavas. Thus, if ^{226}Ra excess is formed at great depth, it is likely (though not required; see Thomas et al., 2002) that ^{238}U excess

is also formed at depth. Conversely, shallow processes that fractionate thorium from radium could also fractionate thorium from uranium.

4.21.3.3.4 Geodynamic considerations

Theory and observation were in conflict, and theory seemed to get the better of it.

Fenner (1937, p. 166)

Since the 1980s, most geochemists and petrologists working on arcs have considered partial melting of subducted material to be relatively unusual, and absent beneath most modern arcs. This is based on three main lines of reasoning.

First, very few arc lavas show strong heavy REE/middle REE depletion, but such depletion is predicted and observed in melts of eclogite or garnet amphibolite (e.g., Gill, 1974, 1978; Kelemen et al., 2003b; Rapp et al., 1999). In addition, partial melts of subducted material are likely to be granitic (e.g., Johnson and Plank, 1999; Nichols et al., 1994; Rapp et al., 1999; Rapp and Watson, 1995), and close to H₂O saturation at 3 GPa or more, with ~25–50 wt% H₂O (Dixon and Stolper, 1995; Dixon et al., 1995; Kawamoto and Holloway, 1997; Mysen and Wheeler, 2000). In these ways, no arc magma resembles a fluid-saturated melt of sediment or basalt in eclogite facies.

Second, because many dehydration reactions in the subducting plate may be complete by 2 GPa, it is not evident that free fluid will be available to facilitate fluid-saturated melting (e.g., Davies and Stevenson, 1992; Peacock et al., 1994; Rapp and Watson, 1995).

Third, thermal models for arcs published between 1980 and 2002 uniformly indicate that the top of the subducting plate in 'normal' subduction zones (convergence rate >0.03 m year⁻¹, subducting oceanic crust older than 20 Ma) does not reach temperatures above the fluid-saturated solidus for metabasalt or metasediment (see reviews in Kelemen et al., 2003a; Peacock, 1996, 2003; Peacock et al., 1994).

Recently, all three of these lines of reasoning have been challenged.

First, modeling of reaction between heavy REE-depleted melts of eclogite facies basalt or sediment and mantle peridotite shows that heavy REE abundances rise to levels in equilibrium with spinel peridotite at melt/rock ratios <~0.1, while the light REEs and other highly incompatible elements are almost unaffected (Kelemen et al., 1993, 2003b). Thus, primitive arc lavas with flat, middle to heavy REE patterns at low abundance, and light REE enrichment, could be formed by reaction between a partial melt of subducted material and the overlying mantle wedge. In addition, anatexis, H₂O-rich melts of subducting sediment or basalt will both decompress and heat up as they rise into the overlying mantle. This 'super-adiabatic' ascent may enhance melt/rock reaction, leading to a net increase in the liquid mass (Grove et al., 2001, 2003; Kelemen, 1986, 1990, 1995; Kelemen et al., 1993, 2003b). Thus, major elements in hybrid melts may be primarily derived from the mantle wedge, while highly incompatible trace elements may reflect the original, eclogite facies residue.

Note that the conclusion of the previous paragraph seems to be somewhat at odds with Section 4.21.3.3.3, in which it was proposed that ²²⁶Ra and ²³⁸U excesses might arise via some shallow process. If this were so, then presumably other incompatible-element concentrations would also be affected by this shallow process. However, based on data from Newman et al. (1984) and Sigmarsson et al. (2002), we anticipate that primitive andesites with a substantial eclogite melt component will have ²³⁰Th excess and little or no ²²⁶Ra excess.

Second, it is now apparent that continuous dehydration reactions involving hydrous phases in metasediment and upper oceanic crust with higher pressure stability than glaucophane plus extensive solid solution, such as lawsonite, chloritoid, phengite, and zoisite, provide a small but nearly continuous source of fluid from shallow depths to those exceeding ~250 km (review in Chapter 4.19). In addition, hydrous phases such as serpentine and talc in the uppermost mantle of the subducting plate have an extensive stability field extending to high pressure, and will continue to dehydrate due to conductive heating of the cold interior of the subducting plate to depths up to ~200 km (review in Chapter 4.19). Finally, aqueous fluid may not be wetting in eclogite facies assemblages with abundant clinopyroxene. H₂O-rich fluid in clinopyroxenite does not become interconnected until fluid fractions exceeding 7 vol% (Watson and Lupulescu, 1993). Thus, some of the H₂O evolved by dehydration reactions may remain within the metamorphic protolith until melting increases the permeability and permits H₂O dissolved in the melt to escape the subducting slab by porous flow (Kelemen et al., 2003b), or until enough low-density interconnected aqueous fluid is present to fracture the overlying rock due to fluid overpressure (Davies, 1999). Thus, although some of the processes described in this paragraph are highly speculative, it is likely that through some combination of these processes, aqueous fluid is present to flux melting of subducting material at depths shallower than ~200–300 km.

Third, computational and theoretical advances have made it possible for thermal models to incorporate temperature-dependent viscosity, and/or non-Newtonian viscosity, in the mantle wedge (Conder et al., 2002; Furukawa, 1993b; Furukawa and Tatsumi, 1999; Kelemen et al., 2003a; Kincaid and Sacks, 1997; Rowland and Davies, 1999; van Keken et al., 2002). This has several important effects, among them eliminating the necessity for prescribing the thickness of a rigid upper plate (Kelemen et al., 2003a). When the lithosphere in the upper plate is allowed to 'find its own thickness,' this results in upwelling of the mantle to shallow depths near the wedge corner, so that asthenospheric potential temperatures extend to depths as shallow as 40 km beneath the arc. We think that these models are preferable to previous isoviscous models because they provide a much closer match to the high metamorphic temperatures recorded in exposures of arc Moho and lower crust (Kelemen et al., 2003a) and to calculated arc melt/mantle equilibration conditions (~1300 °C at 1.2–1.5 GPa; Bartels et al., 1991; Draper and Johnston, 1992; Elkins Tanton et al., 2001; Sisson and Bronto, 1998; Tatsumi et al., 1983). They also provide an explanation for the anomalously slow seismic structure observed in the uppermost mantle beneath arcs

(e.g., Zhao et al., 1992, 1997), for the high heat flow in arcs (Blackwell et al., 1982; Furukawa, 1993b), and for the sharp gradient in the transition to very low heat flow in fore arcs (Kelemen et al., 2003a).

The most recent of these models predict temperatures in the wedge and the top of the slab that are significantly higher compared to isoviscous models. Predicted temperatures are higher than the fluid-saturated solidus for both basalt and sediment (Johnson and Plank, 1999; Lambert and Wyllie, 1972; Nichols et al., 1994; Schmidt and Poli, 1998; Stern and Wyllie, 1973) near the top of the subducting plate directly beneath arcs at normal subduction rates and subducting plate ages (Kelemen et al., 2003a; van Keken et al., 2002). It would be premature to conclude that the tops of most subducting plates cross the fluid-saturated solidus directly beneath arcs, because this is an area of ongoing research. Also, it is not clear that subducting metasediment and/or metabasalt are fluid-saturated at these depths. And, even if fluids are present, natural rocks might evolve fluids with H_2O activities lower, and melting temperatures higher, than in most melting experiments (Becker et al., 1999, 2000; Johnson and Plank, 1999). Nonetheless, it is clear that thermal models should no longer be invoked to 'rule out' partial melting of subducted material in eclogite facies.

Our community has been focused for a long time on very simple pictures of subduction. While this is expedient for maintaining sanity, it is intriguing to speculate briefly on the possibility of solid material transfer across the Benioff zone (Figure 16). Several decades ago, geochemists suggested that physical mixing of a few percent sediment with peridotite in the mantle wedge beneath arcs could account for many geochemical features of arc lavas (Armstrong, 1981; Kay, 1980). Indeed, by analogy with predicted gravitational instability of dense lower crust (e.g., Arndt and Goldstein, 1989; DeBari and Sleep, 1991; Ducea and Saleeby, 1996; Herzberg et al., 1983; Kay and Kay, 1988, 1991, 1993, 1985; Turcotte, 1989), subducting sediment may 'delaminate' and rise into the overlying mantle wedge. Subducting sediment in eclogite facies is likely to be substantially less dense than the overlying mantle. Thus, viscous density instabilities will arise provided subducting sediment layers have thicknesses of 100 m to 1 km, once the overlying mantle viscosity becomes less than some critical value. For example, our calculations (Jull and Kelemen, 2001) suggest that for density contrasts of $50\text{--}150\text{ kg m}^{-3}$ and background strain rates $\sim 10^{-14}$, a 1-km-thick layer of subducting sediment would form unstable diapirs and rise into the overlying mantle at $\sim 750^\circ\text{C}$. This process will lead to mechanical mixing of sediment and mantle peridotite. In addition, rising, heating diapirs of sediment would certainly undergo partial melting in the mantle wedge.

In another mechanism of solid transfer across the Benioff zone, imbrication of the subduction thrust at shallow depth, or downward migration of the subduction shear zone at greater depth, may transfer material from the top of the downgoing plate into the hanging wall, reducing its convergence velocity and allowing more time for conductive heating (Figure 16).

'Subduction erosion' may transfer relatively hot, middle to lower crust from the fore-arc (metasediment, etc.) or the arc (garnet granulite, and pyroxenite) to the top of the subducting plate (Clift and MacLeod, 1999; Ranero and von Huene, 2000; Vannucchi et al., 2001; von Huene and Scholl, 1991, 1993)

(Figure 16). Because this material has a low melting point compared to the mantle but is already hot compared to the top of the subducting oceanic crustal section, conductive heating will take it above its fluid-saturated solidus in a relatively short time, while fluid may be supplied from the underlying subducting plate. Similarly, although it is not 'subduction,' delamination of dense crustal cumulates could lead to transformation of gabbroic rocks into eclogites, followed by heating, and partial melting (Gromet and Silver, 1987; Kay and Kay, 1993), as descending diapirs become entrained in the ductile flow of the mantle wedge (Figure 16).

Another important consideration is that partial melts of subducted material do not necessarily rise vertically through the mantle wedge from the subduction zone to the base of arc crust. One might expect initial trajectories to trend diagonally upward, away from the trench, due to the sum of buoyancy-induced upwelling and diagonal downward solid flow in the mantle wedge. Higher in the wedge, theoretical considerations suggest that both porous flow and fracture transport of melt would be diagonally upward, toward the trench (Davies, 1999; Spiegelman and McKenzie, 1987). This diagonal, trenchward upwelling would be enhanced if solid flow in the upper part of the mantle wedge is also diagonally upward toward the trench, as is predicted from models incorporating a temperature-dependent mantle viscosity (Conder et al., 2002; Furukawa, 1993b; Furukawa and Tatsumi, 1999; Kelemen et al., 2003a; Kincaid and Sacks, 1997; Rowland and Davies, 1999; van Keken et al., 2002). As a result, it may be a mistake to concentrate solely on whether subducted material exceeds its fluid-saturated solidus directly beneath an arc. Instead, if subducted material crosses the solidus at 150 or even 250 km, the resulting melt might be transported diagonally to the base of arc crust.

In summary, for a variety of reasons, it is unwarranted to use geodynamical models to rule out partial melting of eclogite facies sediment, basalt, or lower crustal gabbro beneath arcs. Meanwhile, we believe that geochemical data on primitive arc lavas are best understood if a partial melt of subducted sediment and/or basalt (and/or gabbro) is the primary medium for transport of incompatible trace elements into the mantle wedge.

4.21.4 Arc Lower Crust

Ever clearer became the danger of restricting attention to the 'observed facts'. Direct observations are usually restricted to ... a two-dimensional field. ... Three dimensional it must be, in any case, even at the cost of one's peace of mind—even at the cost of risking the quagmire of speculation about the invisible and intangible. There is, indeed, no other way. By declining Nature's own invitation to think intensively about her third dimension, petrologists have 'lost motion' and have held back the healthy progress of their science. What petrology needs is controlled speculation about the depths of the Earth.

Reginald A. Daly,
Igneous Rocks and the Depths of the Earth
(Daly, 1933)

To reason without data is nothing but delusion.

Arthur Holmes,
The Age of the Earth
(Holmes, 1937, p. 152)

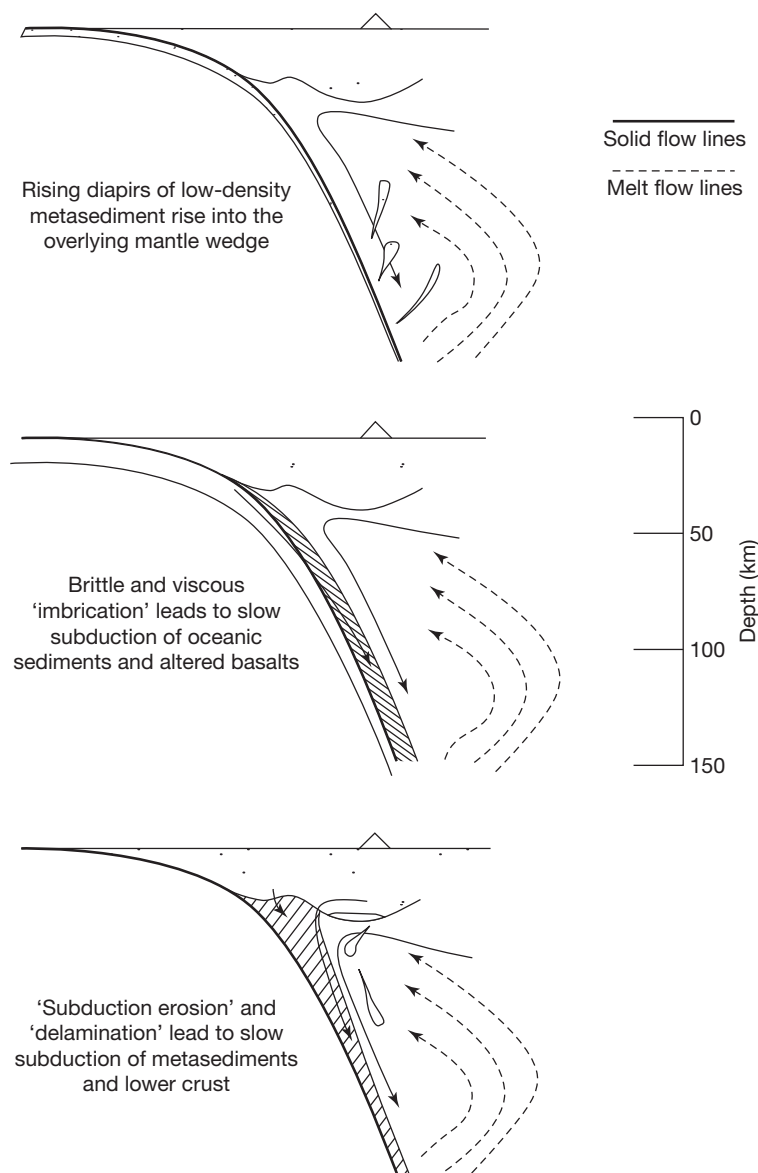


Figure 16 Schematic illustration of mechanisms for transfer of sediments, volcanics, and/or lower crustal gabbros into the mantle wedge from the subducting plate and the base of arc crust. The thick black line indicates the position of the 'subduction zone'; below this line, material subducts at the convergence velocity. Above this line, material is carried downward more slowly. Any process leading to slow transport of low-melting point metasediment, metabasalt, or metagabbro into the mantle wedge would lead to partial melting of this material beneath an arc.

4.21.4.1 Talkeetna Arc Section

Although there are outcrops of middle to lower crustal plutonic rocks with arc provenance in many places (e.g., DeBari, 1994; DeBari et al., 1999; Pickett and Saleeby, 1993, 1994), in this part of the chapter we will concentrate on data from the Talkeetna (south-central Alaska) and Kohistan (Pakistan Himalaya) arc crustal sections (e.g., Bard, 1983; Barker and Grantz, 1982; Burns, 1985; Coward et al., 1982; DeBari and Coleman, 1989; DeBari and Sleep, 1991; Jan, 1977; Miller and Christensen, 1994; Plafker et al., 1989; Tahirkheli, 1979). Both regions preserve tectonically dissected but relatively complete sections, from volcanics and sediments at the top to residual mantle peridotites near the base. Metamorphic

equilibria at the Moho in both sections record conditions of $\sim 1000^\circ\text{C}$ and 1–1.2 GPa. In addition, high P/T metamorphism, with pressure perhaps as high as 1.8 GPa, may be recorded by the Jijal complex, along the Main Mantle thrust at the base of the Kohistan section (Anczkiewicz and Vance, 2000; Ringuette et al., 1999; Yamamoto, 1993) and by late veins in the Kamila amphibolites (Jan and Karim, 1995); this is probably related to continental collision and exhumation of high P rocks along the Indian–Asian suture zone (Gough et al., 2001; Treloar, 1995; Treloar et al., 2001). Because we are most familiar with the Talkeetna section, we will emphasize data from our recent studies there, with supporting data from the Kohistan section.

The Talkeetna section represents an arc fragment, ranging in age from ~200 to ~175 Ma that was accreted along the North American margin and is now exposed in south central Alaska and along the Alaska Peninsula (Barker and Grantz, 1982; Detterman and Hartsock, 1966; Grantz et al., 1963; Martin et al., 1915; Millholland et al., 1987; Newberry et al., 1986; Nokleberg et al., 1994; Palfy et al., 1999; Plafker et al., 1989; Rioux et al., 2002b, 2001b; Roeske et al., 1989). The general geology and petrology of the Talkeetna section has been summarized by Burns (1983, 1985), Burns et al. (1991), DeBari (1990), DeBari and Coleman (1989), DeBari and Sleep (1991), Newberry et al. (1986), Nokleberg et al. (1994), Pavlis (1983), Plafker et al. (1989), and Winkler et al. (1981). It is bounded to the north, along a contact of uncertain nature, by the accreted Wrangellia terrane. To the south, the Talkeetna arc section is juxtaposed along the Border Ranges Fault with accretionary wedge melanges, the Liberty Creek, McHugh, and Valdez complexes. This major fault has been a thrust and a right lateral strike-slip fault. Although the Border Ranges Fault is near vertical at present, a flat-lying klippe of gabbroic rocks, almost certainly derived from the Talkeetna section, overlies the McHugh complex in the Chugach Mountains north of Valdez. This is called the Klanelneechina klippe.

Preliminary data suggest no inheritance in 200–180 Ma zircons from Talkeetna plutonic rocks (Rioux et al., 2001a, 2002a). The small contrast between neodymium isotopes in Talkeetna gabbros with neodymium isotopes for Jurassic MORB resembles the small neodymium isotope difference between Marianas arc lavas and present-day MORB (Greene et al., 2003). Small bodies of metaquartzite and marble intruded by Talkeetna plutonic rocks contain little or no zircon, and are interpreted as pelagic sediments (J. Amato, personal communication, 2003), while amphibolite rafts have andesitic compositions and the trace-element signatures of arc magmas (e.g., high La/Nb and Th/Nb; Kelemen, Hanghøj, and Greene, unpublished data). Thus, recent work is consistent with the hypothesis that the entire Talkeetna arc section is composed of Late Triassic to Middle Jurassic rocks that formed in an intra-oceanic arc.

After reconnaissance mapping and sampling (Barker et al., 1994; Barker and Grantz, 1982; Newberry et al., 1986), the volcanic section of the Talkeetna arc has received relatively little study until now. Our preliminary data agree with earlier estimates that the volcanics are 5–7 km thick. High-Mg# basalts are relatively common, though 11 of our 87 samples are high-Mg# andesites. More evolved lavas range from mainly tholeiitic andesites through tholeiitic and calc-alkaline dacites, to calc-alkaline rhyodacites and rhyolites. The volcanics are underlain and intruded by felsic to gabbroic plutons.

Excellent descriptions of the petrology and major-element composition of the Talkeetna lower crust (e.g., Burns, 1985; DeBari and Coleman, 1989; DeBari and Sleep, 1991) and our recent work (Greene et al., 2003) show that much of the section is composed of compositionally monotonous gabbro-norites. Some, but not all, include abundant magnetite. Prismatic hornblende of obvious igneous origin is rare, though most samples have hornblende rims – probably of deuteric origin – around prismatic pyroxene crystals. Olivine

is extremely rare, even at the base of the crustal section. Both Talkeetna and Kohistan lower crustal gabbroic rocks have very high aluminum contents, compared to gabbroic rocks from ophiolites and to the average composition of continental lower crustal xenoliths (Rudnick and Presper, 1990). Because they have such high aluminum, these rocks can form more than 30% garnet at garnet granulite facies conditions, and are thus denser than mantle peridotite at the same pressure and temperature (Jull and Kelemen, 2001).

DeBari and Coleman (1989), building on previous mapping by Burns, Newberry, Plafker, Coleman and others, concentrated much of their work in the Tonsina area, where several small mountains preserve a laterally continuous Moho section, with relatively mafic gabbro-norites overlying a thin but regionally continuous horizon of mafic garnet granulite (orthogneiss), overlying ~500 m of pyroxenite (mostly clinopyroxene-rich websterite), in turn overlying residual mantle harzburgite with ~10% dunite (Figure 17). The harzburgite, in turn, is bounded by the Border Ranges Fault to the south. It is important to emphasize that gabbro-norites, garnet granulites, pyroxenites, and harzburgites show ‘conformable’ high-temperature contacts that extend across intermittent outcrop for several kilometers. In this area, garnet granulites record conditions of ~1000 °C and 1 GPa (DeBari and Coleman, 1989; Kelemen et al., 2003a), indicating that at the time of garnet growth, the crustal thickness was probably ~30 km. Previous studies (Burns, 1985; DeBari and Coleman, 1989; DeBari and Sleep, 1991) and our recent work (Greene et al., 2003) have found that Talkeetna gabbro-norites and lavas form a cogenetic, igneous differentiation sequence.

4.21.4.1.1 Geochemical data from the Talkeetna section

We turn now to new geochemical data on the Talkeetna section (averages in Table 3). As in pilot data from Barker et al. (1994), REE patterns in all but two lavas are relatively flat, just slightly more light REE-enriched than MORB (Figure 18). Extended trace-element ‘spidergrams’ show the distinctive characteristics of arc magmas, such as high Th/Nb, La/Nb, Ba/La, Pb/Ce, and Sr/Nd. Many lavas, particularly the ones with the highest abundance of incompatible trace elements, show low Eu/Sm, consistent with plagioclase fractionation, and low Ti/Dy, which is probably due, at least in part, to magnetite fractionation. Many of these lavas are pervasively altered. Nonetheless, the parallelism of most trace-element patterns suggests that few of the geochemical characteristics summarized here have been substantially modified by alteration. Felsic plutonic rocks, primarily calc-alkaline tonalites, have spidergram patterns similar to the lavas.

The gabbroic rocks, mostly gabbro-norites, have spidergram patterns that are remarkably similar to the lavas in many ways, with high Th/Nb, La/Nb, Ba/La, Pb/Ce, and Sr/Nd (Figure 19). While DeBari and Coleman (1989) emphasized the presence of a few gabbroic samples with REE patterns reminiscent of MORB, suggesting that they might represent older oceanic crust into which the Talkeetna arc was emplaced, the extended trace-element patterns of all our gabbroic samples show arc-like signatures. For example, Talkeetna gabbro-norites have average Th/Nb of 0.4, substantially

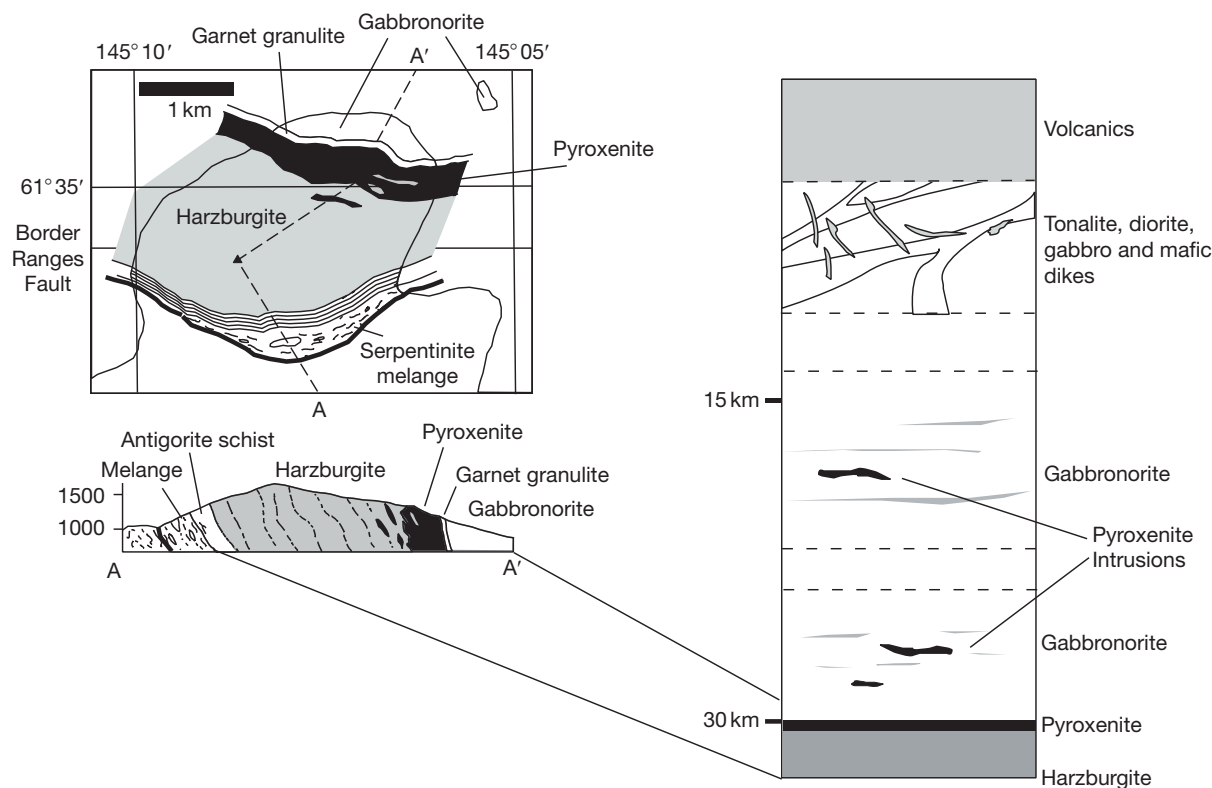


Figure 17 Schematic cross section of the accreted Jurassic Talkeetna arc in south-central Alaska based on new data and compilations by [Greene et al. \(2003\)](#), together with a geologic map and cross section of the Moho exposure at Bernard Mountain, in the Tonsina region of the Talkeetna arc section, simplified from [DeBari and Coleman \(1989\)](#).

higher than in gabbroic rocks in the Oman ophiolite (averaging 0.1 in our unpublished data) and lower oceanic crust (averaging 0.05; [Hart et al., 1999](#)).

High Ti/Dy in many gabbro-norite samples is indicative of the presence of cumulate magnetite, which fractionates titanium from dysprosium during igneous crystallization, and high Eu/Sm reflects plagioclase accumulation. Similarly, high Pb/Ce and Sr/Nd in the gabbroic rocks may arise in part from lead and strontium enrichments in parental melts, and in part from the presence of cumulate plagioclase. To constrain which additional characteristics of the Talkeetna gabbro-norites are inherited from trace-element features in parental, arc magmas, and characteristics of which reflect igneous fractionation, we divide the average Talkeetna gabbro-norite composition by the average lava composition to yield a highly approximate bulk crystal/liquid distribution coefficient pattern ([Figure 20](#)). This shows that despite complementary lead and strontium enrichments in the lavas, high Pb/Ce and Sr/Nd in the gabbroic rocks also reflect the presence of cumulate plagioclase. In addition, note that thorium and uranium are more incompatible than rubidium, barium, and potassium in plagioclase.

Spidergrams for mafic garnet granulites from the Tonsina area show no evidence for the presence of cumulate igneous garnet, which would be reflected in high heavy REE/middle REE ratios ([Figure 21](#)). Instead, they are very similar to typical Talkeetna gabbro-norites. Thus, following [DeBari and](#)

[Coleman \(1989\)](#), we believe that the garnets in this area are entirely of metamorphic origin. In contrast, gabbro-norite, two-pyroxene quartz diorite, and tonalite in garnet granulite facies from the Klanelneechina klippe, which record $\sim 700^\circ\text{C}$ and 0.7 GPa, do show evidence for the presence of cumulate igneous garnet ([Figure 22](#)). These rocks have all evolved compositions (wholerock $\text{Mg\#} < 50$). They could be cumulates from evolved melts crystallizing in the lower crust, and/or restites produced via partial melting of high-temperature lower crust.

Trace-element contents of pyroxenites from the Tonsina area are shown in [Figure 23](#). Although data on the most depleted of these may be very imprecise, they show high Pb/Ce and Sr/Nd, and generally low niobium and tantalum relative to potassium, lanthanum, and thorium. All these characteristics are probably inherited from equilibrium with primitive arc magmas. [Müntener et al. \(2001\)](#) emphasized the strikingly low Al_2O_3 contents (16.5 wt%, averaging 3.4 wt% in our data) in many Talkeetna and Kohistan pyroxenites, despite their high pressures of crystallization. These low Al_2O_3 contents were not produced in experiments on hydrous, fluid-undersaturated arc basalt at 1.2 GPa, but were reproduced in experiments on primitive arc andesite under the same conditions. However, preliminary traceelement and neodymium-isotope data on Talkeetna pyroxenites suggest that they equilibrated with parental melts similar to the tholeiitic basalts that formed the overlying gabbroic and volcanic sections of the arc.

Table 3 New geochemical data on the Talkeetna section. Compiled geochemical data for the Talkeetna arc section, updated in 2013, is available as a supplement to this chapter. Please note the text and figures in this chapter were last updated in 2003.

	<i>Tonsina pyroxenite</i>	<i>N</i>	<i>Std. error</i>	<i>Talkeetna gabbro-norite</i>	<i>N</i>	<i>Std. error</i>	<i>Tonsina garnet granulite</i>	<i>N</i>	<i>Std. error</i>	<i>Klanelneechina garnet diorite and tonalite</i>	<i>N</i>	<i>Std. error</i>	<i>Intermediate to felsic plutons</i>	<i>N</i>	<i>Std. error</i>	<i>Lavas, tuffs and volcano- clastic</i>	<i>N</i>	<i>Std. error</i>
<i>Normalized oxides (wt%)</i>																		
SiO ₂	49.95	17	0.296	47.86	95	0.047	46.55	6	1.234	51.60	7	0.880	68.54	28	0.210	59.64	114	0.069
TiO ₂	0.07	17	0.003	0.66	95	0.004	0.79	6	0.122	0.89	7	0.086	0.50	28	0.011	0.86	114	0.003
Al ₂ O ₃	3.42	17	0.126	19.00	95	0.030	18.66	6	0.153	18.92	7	0.352	15.19	28	0.057	16.53	114	0.017
FeO*	8.31	17	0.229	9.94	95	0.035	10.04	6	0.722	10.30	7	0.248	4.06	28	0.092	7.78	114	0.026
MnO	0.17	17	0.002	0.18	95	0.001	0.19	6	0.014	0.21	7	0.005	0.11	28	0.003	0.19	114	0.001
MgO	27.95	17	0.343	7.78	95	0.027	7.86	6	0.486	4.89	7	0.187	1.67	28	0.035	3.57	114	0.017
CaO	9.88	17	0.355	12.53	95	0.025	14.58	6	0.903	10.41	7	0.275	4.66	28	0.063	6.30	114	0.033
Na ₂ O	0.22	17	0.006	1.82	95	0.009	1.08	6	0.081	2.51	7	0.111	4.38	28	0.025	3.82	114	0.011
K ₂ O	0.02	17	0.001	0.16	95	0.002	0.18	6	0.067	0.13	7	0.033	0.76	28	0.019	1.03	114	0.007
P ₂ O ₅	0.01	17	0.000	0.08	95	0.001	0.07	6	0.019	0.14	7	0.013	0.13	28	0.003	0.18	114	0.001
Mg#	86	17	0.2	58	95	0.1	58	6	2.8	45	7	0.6	43	28	0.4	43	114	0.1
<i>XRF data (ppm)</i>																		
Ni	516	17	15	42	31	1	41	6	3	11	7	3	4.8	13	0.2	17.2	86	0.3
Cr	3239	17	105	167	31	4	188	6	21	55	7	10	6.3	13	0.4	45.2	86	0.7
Sc	31.5	17	1.0	39.5	31	0.5	52	6	2	38.7	7	1.4	21.4	13	0.9	29.3	86	0.1
V	106	17	4	250	31	5	295	6	30	242	7	11	94	13	7	168.0	86	1.2
Ba	15.5	17	0.5	75	31	3	55	6	13	36	7	3	519	13	17	409	86	5
Rb	1.1	17	0.1	2.0	31	0.1	3.2	6	1.4	0.7	7	0.2	17.8	13	0.7	15.2	86	0.2
Sr	18.4	17	1.5	303	31	2	225	6	9	277	7	4	235	13	5	249	86	2
Zr	6.2	17	0.2	17.4	31	0.5	18	6	3	45	7	11	112	13	4	92.0	86	0.6
Y	2.8	17	0.1	9.8	31	0.2	16	6	2	17	7	2	31	13	1	28.8	86	0.1
Nb	1.8	17	0.0	1.9	31	0.0	1.9	6	0.2	3.6	7	0.4	4.2	13	0.2	4.2	86	0.0
Ga	4.2	17	0.1	15.7	31	0.1	16.2	6	0.6	17.9	7	0.4	15.3	13	0.2	16.5	86	0.0
Cu	43.9	17	2.9	88	31	2	152	6	27	34	7	2	25	13	4	45.1	86	0.5
Zn	43.4	17	1.8	55.8	31	0.7	60	6	8	85	7	2	48	13	2	96.6	86	0.9

Pb	0.6	17	0.1	1.6	31	0.1	2.3	6	0.5	0.4	7	0.2	3.0	13	0.1	3.3	86	0.0
La	6.6	17	0.4	5.6	31	0.2	9.7	6	2.2	5.3	7	0.8	10.1	13	0.9	9.8	86	0.1
Ce	2.9	17	0.4	8.3	31	0.2	11.3	6	2.5	14	7	2	24.4	13	0.9	23.3	86	0.1
Th	1.2	17	0.1	1.3	31	0.0	1.2	6	0.2	1.0	7	0.2	2.0	13	0.1	1.6	86	0.0
<i>ICP-MS data (ppm)</i>																		
La	0.192	16	0.019	1.153	31	0.040	1.565	6	0.377	2.985	7	0.611	7.815	13	0.331	7.490	42	0.103
Ce	0.417	16	0.040	2.901	31	0.095	3.734	6	0.769	7.616	7	1.475	17.358	13	0.714	16.825	42	0.219
Pr	0.059	16	0.005	0.466	31	0.014	0.605	6	0.103	1.161	7	0.197	2.387	13	0.096	2.360	42	0.028
Nd	0.328	16	0.025	2.625	31	0.076	3.594	6	0.552	6.133	7	0.911	11.506	13	0.450	11.573	42	0.127
Sm	0.149	16	0.009	1.020	31	0.027	1.519	6	0.209	2.140	7	0.258	3.650	13	0.148	3.702	42	0.037
Eu	0.063	16	0.003	0.474	31	0.008	0.654	6	0.070	0.941	7	0.077	0.966	13	0.024	1.095	42	0.007
Gd	0.244	16	0.013	1.350	31	0.033	2.160	6	0.282	2.667	7	0.274	4.264	13	0.174	4.260	42	0.041
Tb	0.049	16	0.002	0.253	31	0.006	0.410	6	0.052	0.484	7	0.046	0.777	13	0.033	0.776	42	0.008
Dy	0.362	16	0.017	1.701	31	0.041	2.793	6	0.356	3.167	7	0.281	5.092	13	0.220	5.083	42	0.050
Ho	0.081	16	0.004	0.367	31	0.009	0.616	6	0.080	0.673	7	0.055	1.110	13	0.048	1.097	42	0.011
Er	0.236	16	0.011	1.020	31	0.025	1.716	6	0.232	1.861	7	0.146	3.174	13	0.138	3.094	42	0.032
Tm	0.034	16	0.001	0.150	31	0.004	0.243	6	0.033	0.273	7	0.021	0.481	13	0.021	0.462	42	0.005
Yb	0.219	16	0.009	0.941	31	0.024	1.500	6	0.212	1.714	7	0.124	3.104	13	0.134	2.951	42	0.032
Lu	0.035	16	0.001	0.151	31	0.004	0.232	6	0.033	0.271	7	0.019	0.510	13	0.021	0.473	42	0.005
Ba	4.254	16	0.357	65	31	3	43	6	13	27	7	4	516	13	18	434	42	10
Th	0.024	16	0.002	0.071	31	0.004	0.152	6	0.043	0.097	7	0.037	1.716	13	0.101	1.268	42	0.023
Nb	0.096	16	0.011	0.399	31	0.019	0.749	6	0.190	1.882	7	0.468	2.407	13	0.131	2.407	42	0.040
Y	2.030	16	0.095	9.472	31	0.240	15.728	6	2.143	17.415	7	1.450	30.467	13	1.356	29.107	42	0.303
Hf	0.052	16	0.004	0.385	31	0.014	0.463	6	0.100	0.978	7	0.247	3.381	13	0.143	2.610	42	0.038
Ta	0.012	16	0.001	0.028	31	0.001	0.050	6	0.012	0.116	7	0.036	0.174	13	0.009	0.147	42	0.003
U	0.008	16	0.000	0.043	31	0.003	0.064	6	0.022	0.048	7	0.016	0.877	13	0.044	0.669	42	0.012
Pb	0.456	16	0.038	1.212	31	0.031	1.525	6	0.373	0.649	7	0.038	3.331	13	0.085	4.260	42	0.083
Rb	0.271	16	0.010	1.744	31	0.131	3.617	6	1.472	0.633	7	0.199	16.850	13	0.702	13.732	42	0.313
Cs	0.256	16	0.022	0.469	31	0.017	0.607	6	0.166	0.202	7	0.025	1.301	13	0.064	0.932	42	0.046
Sr	13.0	16	1.4	300	31	2	229	6	10	285	7	4	228	13	4	248	42	4
Sc	35.4	16	1.1	43.7	31	0.5	57	6	2	45	7	1	20.4	13	1.0	26.9	42	0.3
Zr	1.49	16	0.13	10.7	31	0.5	13	6	4	37	7	11	108	13	4	84.3	42	1.3

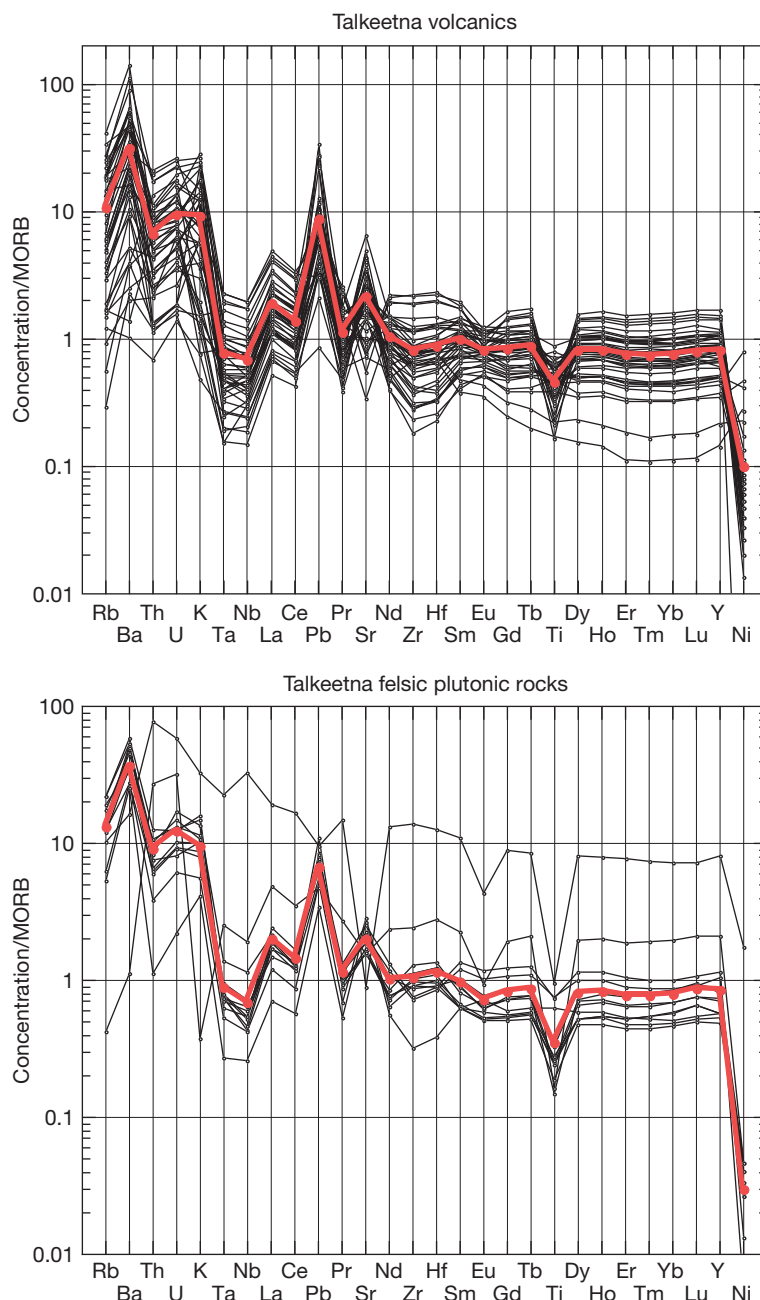


Figure 18 Extended trace-element diagrams (hereafter, spidergrams) for volcanics and felsic plutonic rocks from the Talkeetna arc section, south central Alaska. Concentrations are normalized to N-MORB (Hofmann, 1988). Thick red lines are average values from Table 3. Talkeetna lavas, and plutonic rocks interpreted as liquid compositions, are only slightly enriched in light REE compared to MORB, but show depletion of Nb and Ta, and enrichment of Pb and Sr, typical for arc lavas worldwide. Their trace-element contents are similar to, for example, lavas from the modern Tonga arc. Data from Greene et al. (2003) and our unpublished work (see supplementary material).

4.21.4.1.2 Composition, fractionation, and primary melts in the Talkeetna section

DeBari and Sleep (1991) estimated the bulk composition of the Talkeetna arc crust in the Tonsina area by adding compositions of different samples in proportions determined by their abundance in outcrop. They then added olivine, to calculate a primary magma composition for the Talkeetna arc in equilibrium with mantle olivine with an Mg# of 90. This approach

requires several assumptions. For example, the structural thickness of the Tonsina section cannot be more than ~15 km, whereas the garnet granulites at the base of the section record an original thickness of ~30 km. Thus, DeBari and Sleep assumed that tectonic thinning was homogeneously distributed over the entire section. Also, DeBari and Sleep assumed that outcrop exposures provided a representative estimate of the proportions of different rock types. This could be questioned.

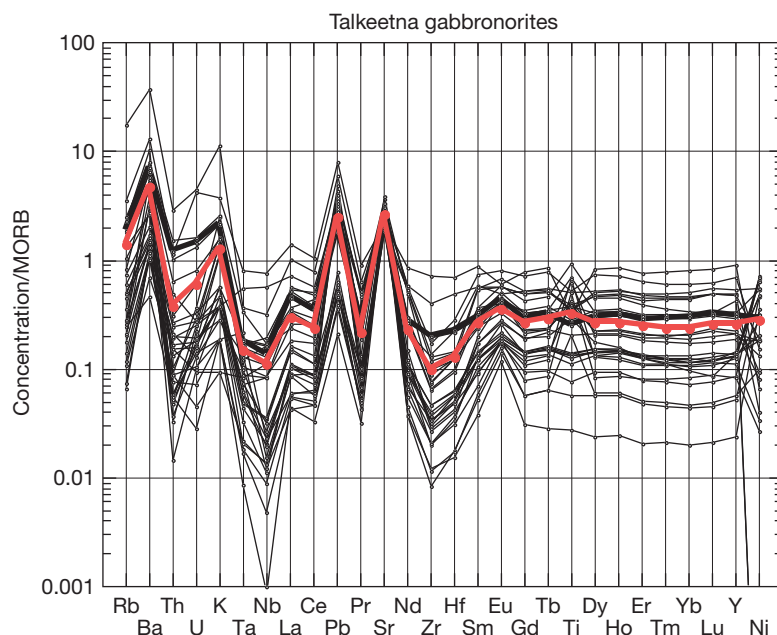


Figure 19 MORB-normalized spidergrams for lower crustal gabbronorites in the Talkeetna arc section, south-central Alaska. The thick red line is average from [Table 3](#). In these cumulate gabbros, some of the Nb and Ta depletion, and Pb and Sr enrichment is inherited from parental arc magmas, but the pattern is modified by high Ti (and probably Nb and Ta) in cumulate magnetite and high Pb and Sr in cumulate plagioclase. Data from [Greene et al. \(2003\)](#) and our unpublished work (see supplementary material).

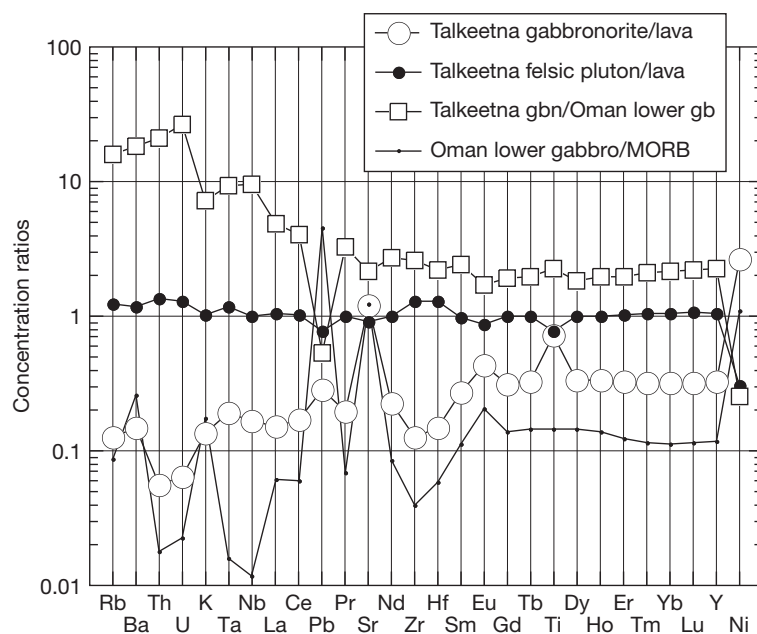


Figure 20 Spidergrams showing ratios of trace-element concentration in Talkeetna arc gabbronorites/lavas (approximating bulk crystal/liquid distribution coefficients), Talkeetna felsic plutons/lavas, Talkeetna gabbronorite (gbn)/lower crustal gabbros from the Oman ophiolite, and Oman lower crustal gabbros/MORB. The gabbronorite/lava 'distribution coefficients' show the effects of cumulate plagioclase (high Pb/Ce, Sr/Nd, and Eu/Gd, and high Rb, Ba, and K relative to Th and U) and magnetite (high Ti/Dy and very slightly high Ta and Nb/La). Talkeetna intermediate to felsic plutons have trace-element contents virtually identical to those in lavas, supporting the idea that the plutons represent melt compositions. Talkeetna gabbronorites are richer in REE and other incompatible elements, except Pb, than Oman lower crustal gabbros. Higher Pb in Oman versus Talkeetna lower crust probably reflects the influence of sulfide/sulfate equilibria during igneous crystallization. Oman cumulate gabbros show very depleted, smooth REE patterns extending to low Nb, Ta, U, and Th. This depleted pattern is interrupted by marked enrichments in Eu, Sr, Pb, K, Ba, and Rb, all of which reflect the presence of cumulate plagioclase. Talkeetna data from [Greene et al. \(2003\)](#) and our unpublished work (see supplementary material). Oman data are samples from the Khafifah crustal section, Wadi Tayin massif, analyzed by ICP-MS at the Université de Montpellier by Marguerite Godard, from [Garrido et al. \(2001\)](#) and our unpublished work.

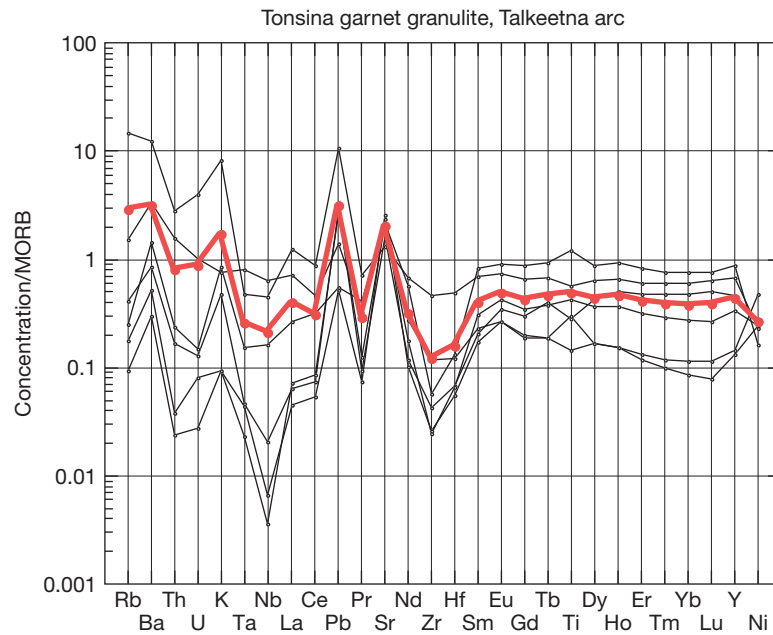


Figure 21 MORB-normalized spidergrams for mafic garnet granulites from the Tonsina area, at the base of the Talkeetna arc section at ~1 GPa, 1000 °C (DeBari and Coleman, 1989; Kelemen et al., 2003a). The thick red line is average from Table 3. These orthogneisses formed via metamorphic recrystallization of protoliths with major- and trace-element contents identical to gabbro-norites from higher in the Talkeetna section. Garnet in these rocks is metamorphic, as previously proposed (DeBari and Coleman, 1989). Data from our unpublished work (see supplementary material).

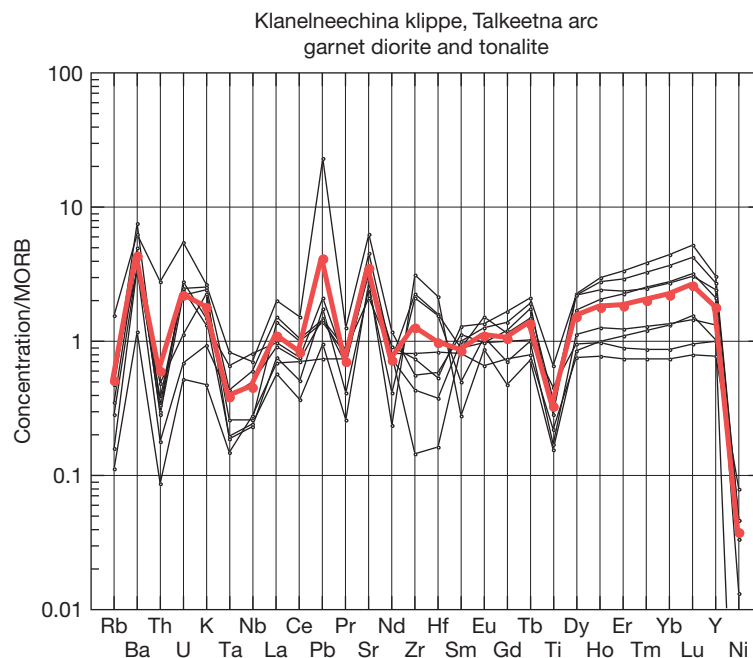


Figure 22 MORB-normalized spidergrams for garnet diorites and tonalites from the Klanelneechina klippe, recording lower crustal depths (~0.7 GPa, 700 °C; Kelemen et al., 2003a) from the Talkeetna arc section. The thick red line is average from Table 3. These evolved rocks ($Mg\# < 50$) all include cumulate, igneous garnet, as indicated by their high heavy REE contents. They probably record partial melting of older arc lithologies under lower crustal conditions. Data from our unpublished work (see supplementary material).

Upsection from the Moho level exposures, outcrop exposures in the Tonsina area are poor due to subducted topography and the presence of a major, Tertiary sedimentary basin to the NE. However, our new data on the composition of the most

primitive Talkeetna lavas, high-alumina basalts with $Mg\# \sim 60$, are very similar to the bulk composition of the crust derived by DeBari and Sleep on the basis of observed rock compositions and proportions.

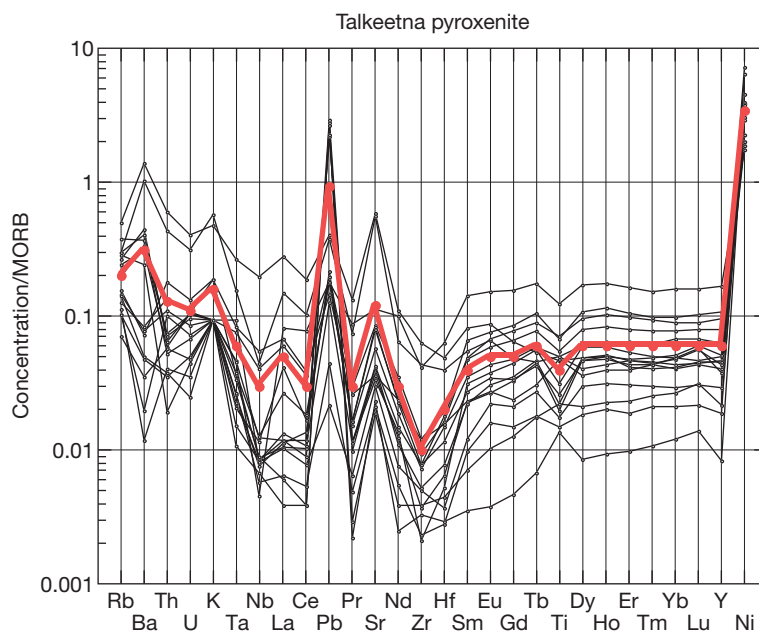


Figure 23 MORB-normalized spidergrams for pyroxenites from the Tonsina area, at the base of the Talkeetna arc section. The thick red line is average from [Table 3](#). Trace-element concentrations in these rocks are low, and data for, for example, U and Th may be very imprecise. Nonetheless, it is apparent that the pyroxenites inherited high Pb/Ce and Sr/Nd, and low Nb and Ta relative to K, Th, and U, from parental arc magmas. Data from our unpublished work (see supplementary material).

In addition, DeBari and Sleep assumed that the entire crust could be derived from a single, parental magma composition. Many arcs have isotopically and compositionally heterogeneous primitive magmas. However, our preliminary analyses show remarkable homogeneity in initial $^{143}\text{Nd}/^{144}\text{Nd}$ ratios ([Greene et al., 2003](#)). Also, with two exceptions, the lavas show nearly parallel spidergram patterns ([Figure 18](#)). In all these respects, our new data are consistent with the first-order assumption that most of the Talkeetna arc section was derived from a single type of primitive magma. Thus, the bold first-order approach of [DeBari and Sleep \(1991\)](#) has been largely vindicated by more extensive data.

To better constrain the possible proportions of different igneous rock types prior to tectonic thinning, we recently completed least-squares modeling of crystal fractionation, using observed compositions and proportions of minerals in Talkeetna gabbro-norites to reproduce the liquid line of descent from the most primitive Talkeetna high-alumina basalts to average Talkeetna andesites and basaltic andesites ([Greene et al., 2003](#)). A striking result is that this modeling requires extensive crystallization of high-Mg# clinopyroxene, which is, in fact, very rare in the Talkeetna gabbro-norites. Modeling predicts that ~20–30% of the gabbroic lower crust should have clinopyroxene $\text{Mg}\# > 85$. In contrast, [Figure 24](#) illustrates that none of our gabbroic samples have such high-clinopyroxene $\text{Mg}\#$.

In addition, most primitive Talkeetna lavas have $\text{Mg}\#$ that are too low for Fe/Mg exchange equilibrium with mantle olivine and pyroxene (incorporating reasonable assumptions about oxygen fugacity and $\text{Fe}^{2+}/\text{Fe}^{3+}$ in arcs). Following [Müntener et al. \(2001\)](#), we infer that many hydrous, primary arc magmas are in a reaction relationship with olivine, forming by reactions such as orthopyroxene + clinopyroxene + spinel = olivine + melt. Such melts are in equilibrium with olivine, but will not crystallize

olivine upon isobaric cooling, and instead will crystallize websterites (two pyroxene pyroxenites). This is consistent with the observation that cumulate dunites (olivine $\text{Mg}\# < 90$) are absent and olivine pyroxenites are rare in the Talkeetna section. Thus, to constrain the composition of a primary magma in equilibrium with mantle peridotite, we performed pyroxenite addition calculations, using the observed phase proportions in Talkeetna pyroxenites. Approximately 20–30% crystallization of pyroxenites from a primary melt in Fe/Mg equilibrium with mantle peridotite was required to produce the most primitive Talkeetna basalts ([Greene et al., 2003](#)). In other words, this modeling predicts that ~20–30% of the arc section should be composed of pyroxenite.

4.21.4.2 Missing Primitive Cumulates: Due to Delamination

The great volume of andesite . . . in the orogenic belts is often taken up as a serious objection against the idea of its derivation from basalt magma by fractionation.

Kuno (1968, p. 165)

The large proportions of pyroxenite and primitive gabbro-norite predicted by fractionation modeling of primitive arc magmas contrast dramatically with the observed proportion of primitive gabbro-norites and pyroxenites in the Tonsina area. We have found no gabbro-norite or garnet granulite (and only a very small outcrop of plagioclase pyroxenite) with clinopyroxene $\text{Mg}\# > 85$. Moreover, the thickness of the pyroxenite layer between overlying gabbroic rocks and underlying residual mantle peridotites is $< \sim 500$ m.

The relationship between clinopyroxene $\text{Mg}\#$ and whole-rock $\text{Mg}\#$ in Talkeetna gabbro-norites ([Figure 24](#)), together

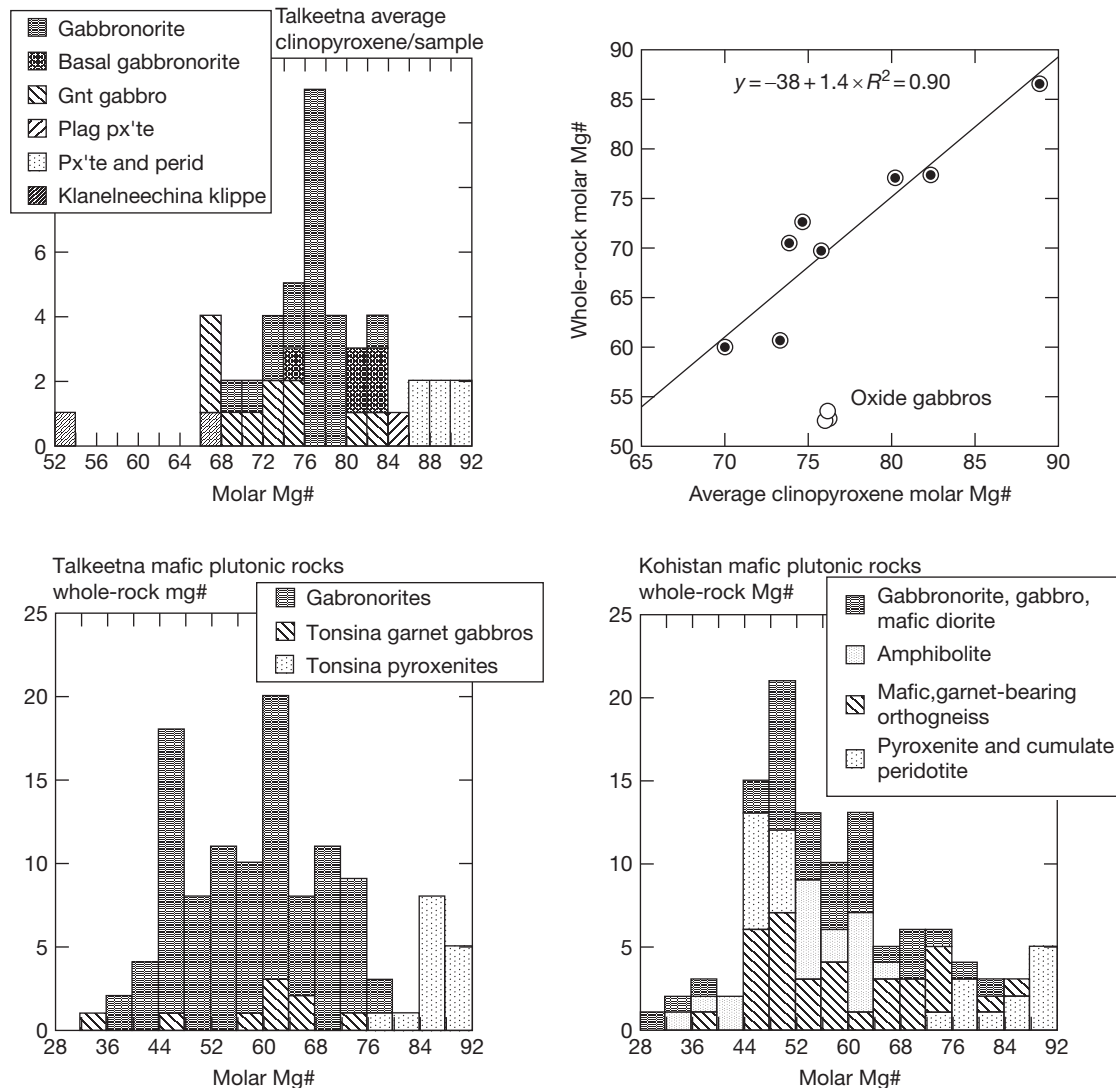


Figure 24 Histograms of clinopyroxene Mg# in mafic plutonic rocks from the Talkeetna arc section, whole-rock Mg# in mafic plutonic rocks from the Talkeetna arc section, and whole-rock Mg# in mafic plutonic rocks from the Kohistan arc section, NW Pakistan. Also shown is average clinopyroxene Mg# versus whole-rock Mg# for samples from the Talkeetna section. Assuming that the number of samples analyzed is representative of the proportion of different compositions present in the Talkeetna and Kohistan sections, these data show that no gabbroic rocks in the Talkeetna section have clinopyroxene Mg# >86 or whole-rock Mg# >80, and only 3 of 100 gabbroic rocks in the Kohistan section have whole-rock Mg# >80. Pyroxenites in the Tonsina area in the Talkeetna section, with clinopyroxene Mg# from 92 to 86 and whole-rock Mg# from 92 to 76, form a layer ~500 m thick between underlying residual peridotite and overlying garnet granulite and gabbronorite. Pyroxenites in the Kohistan section, with whole-rock Mg# from 92 to 72, mainly occur in a band a few kilometers thick between underlying residual mantle peridotites and overlying garnet granulite and gabbroic rocks in the Kohistan section. More evolved pyroxenites form volumetrically insignificant intrusions into gabbroic rocks in both sections. Crustal thickness in both sections is estimated to have been ~30 km, based on metamorphic equilibria (see text). Thus, pyroxenites and primitive gabbroic rocks with Mg# from 92 to 85 comprise a very small proportion of both the Talkeetna and Kohistan arc sections. These observed proportions are in striking contrast to estimates based on fractionation models and experimental data requiring ~30% crystallization of primitive cumulates with clinopyroxene Mg# between 92 and 85. Talkeetna data from [Greene et al. \(2003\)](#) and our unpublished work (see supplementary material). Kohistan whole-rock compositions from [George et al. \(1993\)](#), [Hanson \(1989\)](#), [Jan \(1988\)](#), [Jan and Howie \(1981\)](#), [Jan et al. \(1982\)](#), [Khan et al. \(1993, 1989\)](#), [Miller and Christensen \(1994\)](#), [Petterson et al. \(1991, 1993\)](#), [Petterson and Windley \(1985, 1992\)](#), [Shah and Shervais \(1999\)](#), [Sullivan et al. \(1993\)](#), [Treloar et al. \(1996\)](#), [Yamamoto and Yoshino \(1998\)](#), and [Yoshino and Satish-Kumar \(2001\)](#).

with our larger data set on whole-rock compositions confirms the observations based on clinopyroxene analyses. Modeling predicts that there should be a large proportion of gabbronorites and pyroxenites with whole-rock Mg# >80, but in fact there are very few. This observation is strikingly similar to compiled data on whole-rock Mg# in the Kohistan arc section,

in which there are no gabbroic rocks with Mg# >80, and pyroxenites with Mg# >80 are mainly found in a narrow band, <3 km thick, immediately above the Moho. There are small, ultramafic intrusions within the gabbroic lower crust in both the Talkeetna and Kohistan arc sections. However, they comprise <5% of the outcrop area. Also, at least in the

Talkeetna crustal section, these bodies generally have clinopyroxene Mg# < 85.

Thus, the proportions of igneous rocks calculated from modeling of the liquid line of descent in the lavas are strikingly different from those observed in the Talkeetna and Kohistan section. The bulk of the predicted primitive cumulates, with clinopyroxene Mg# between 92 and 85, are apparently missing. This result is both uncertain and important, and so we provide additional constraints on the modeling here. The crystal fractionation modeling of [Greene et al. \(2003\)](#) requires assumptions about the $\text{Fe}^{2+}/\text{Fe}^{3+}$ ratio, and about pyroxene/melt Fe/Mg equilibria, which are imprecise. For this reason, in [Figure 25](#), we present alternative methods for estimating the proportion of primitive cumulates that were produced by crystal fractionation in the Talkeetna arc section. The left-hand panel of [Figure 25](#), shows clinopyroxene Mg# in equilibrium with Talkeetna lavas versus ytterbium concentration in the same lavas. If ytterbium were a completely incompatible element quantitatively retained in melts during crystal fractionation, then a doubling of the ytterbium concentration would indicate 50% crystallization. In fact, ytterbium is only moderately incompatible, so doubling of ytterbium indicates more than 50% crystallization. It can be seen from these data that a decrease in clinopyroxene Mg# from 85 to 75 is accompanied by more than 50% crystallization. If this trend can be extrapolated to crystallization of more primitive melts, it suggests that the decrease in clinopyroxene Mg# from mantle values (~92) to typical Talkeetna gabbro norite values (<85) was produced by ~35% crystallization.

The right-hand panel in [Figure 25](#) illustrates results of experimental crystallization of pyroxenite and primitive gabbro norite from hydrous arc basalt and andesite at 1.2 GPa ([Müntener et al., 2001](#)). Again, these data indicate that ~30% crystallization is required for clinopyroxene Mg# to decrease from ~92 to ~85, consistent with the modeling of [Greene et al. \(2003\)](#). There is no evidence for extensive fractionation of olivine fractionation from primitive Talkeetna magmas. Dunites are present in the mantle section, but these are probably replacive melt conduits (see [Kelemen, 1990](#); [Kelemen et al., 1997a,b](#); and references therein). In any case, mantle dunites have olivine Mg# > 90, and thus it is apparent that they do not record extensive crystal fractionation. Nonetheless, in [Figure 25](#), we also illustrate a model for olivine fractionation alone. This yields a lower bound of ~15 wt% olivine crystallization required to decrease melt Mg# so that equilibrium clinopyroxene Mg# is decreased from 92 to 85. Finally, our results are similar to those of earlier least-squares fractionation models, which require 21% ([Conrad and Kay, 1984](#)) and 16–26% ([Gust and Perfit, 1987](#)) crystallization of ultramafic cumulates to produce high-aluminum basalt in island arcs.

There are at least four possible explanations for the discrepancy between the proportion of high-Mg# cumulates inferred from crystal fractionation modeling and that observed in the Talkeetna and Kohistan sections:

1. The exposed section is not representative of the original arc crustal section. In the Talkeetna area, outcrop is discontinuous due to numerous faults and subdued topography. It is evident that the present-day structural thickness of the section (~20 km from Moho to volcanics) cannot be as great as the thickness inferred on the basis of thermobarometry, ~30 km. However, the missing section is unlikely to be high-Mg# pyroxenites near the Moho, because the Tonsina area gabbro norites and garnet granulites with clinopyroxene Mg# < 85 are in high-temperature conformable contact with high-Mg# pyroxenites, which in turn are interfingered along high-temperature contacts with residual mantle peridotites. Thus, in this section, the original thickness of cumulates with clinopyroxene Mg# between 85 and 92 as exposed in continuous outcrop is only <500 m.
2. The missing Talkeetna arc high-Mg# plutonic rocks crystallized beneath the 'Moho' exposed in the Tonsina area. While arc mantle is rarely exposed, worldwide, it is apparent from dredging at mid-ocean ridges and from ophiolite studies that gabbroic and ultramafic intrusions can form lenses within the residual mantle beneath oceanic spreading ridges (e.g., [Cannat, 1996](#)). In the Tonsina area of the Talkeetna section, only 1–2 km of residual mantle is exposed. Thus, we cannot rule out the presence of high-Mg# pyroxenites emplaced as plutons or sills within mantle peridotites at greater depth.
3. Equilibrium crystallization of primitive magmas (as distinct from fractional crystallization) occurred until ~70–50% of the initial liquid remained. The remaining liquid was then efficiently extracted, leaving relatively pure gabbro norite cumulates with clinopyroxene Mg#s < 85. This might happen if, for example, dense, rising melts ponded near the Moho, underwent partial crystallization, and then less dense evolved melts were extracted to form the overlying crust. Calculated densities for Talkeetna average gabbro norite at pressures from 0.1 to 0.8 GPa are ~3000 kg m⁻³ ([Jull and Kelemen, 2001](#)). Calculated densities for the primary and primitive melts for the Talkeetna section ([Greene et al., 2003](#)) are ~2800 kg m⁻³ on an anhydrous basis, and would be less if – as we surmise – they contained several weight percent H₂O. Thus, primitive Talkeetna melts would have been buoyant with respect to the igneous crust and the Moho would not have been a zone of neutral buoyancy.

Alternatively, melts may have ponded at depths beneath a permeability barrier, in a transition from porous flow to flow in melt-induced fractures, as proposed for the base of the crust at mid-ocean ridges based on observations in the Oman ophiolite ([Kelemen and Aharonov, 1998](#); [Kelemen et al., 1997b](#); [Korenaga and Kelemen, 1997](#)) and geophysical data from the East Pacific Rise ([Crawford and Webb, 2002](#); [Crawford et al., 1999](#); [Dunn and Toomey, 1997](#)). However, the idea that primary Talkeetna magmas underwent 30–50% equilibrium crystallization to form gabbro norites with clinopyroxene Mg#s < 85 is not consistent with the presence of plagioclase-free pyroxenites with pyroxene Mg#s from 92 to 85, nor with experimentally determined phase equilibria for hydrous, primitive arc magmas that indicate a substantial interval for plagioclase-free, pyroxenite crystallization.

4. Gravitational instability of dense cumulates overlying less dense upper mantle peridotites may have induced viscous 'delamination' at the base of the crust. This is consistent with the observation that the Mg# 'gap' occurs near the Moho, and the few rocks with clinopyroxene Mg# from

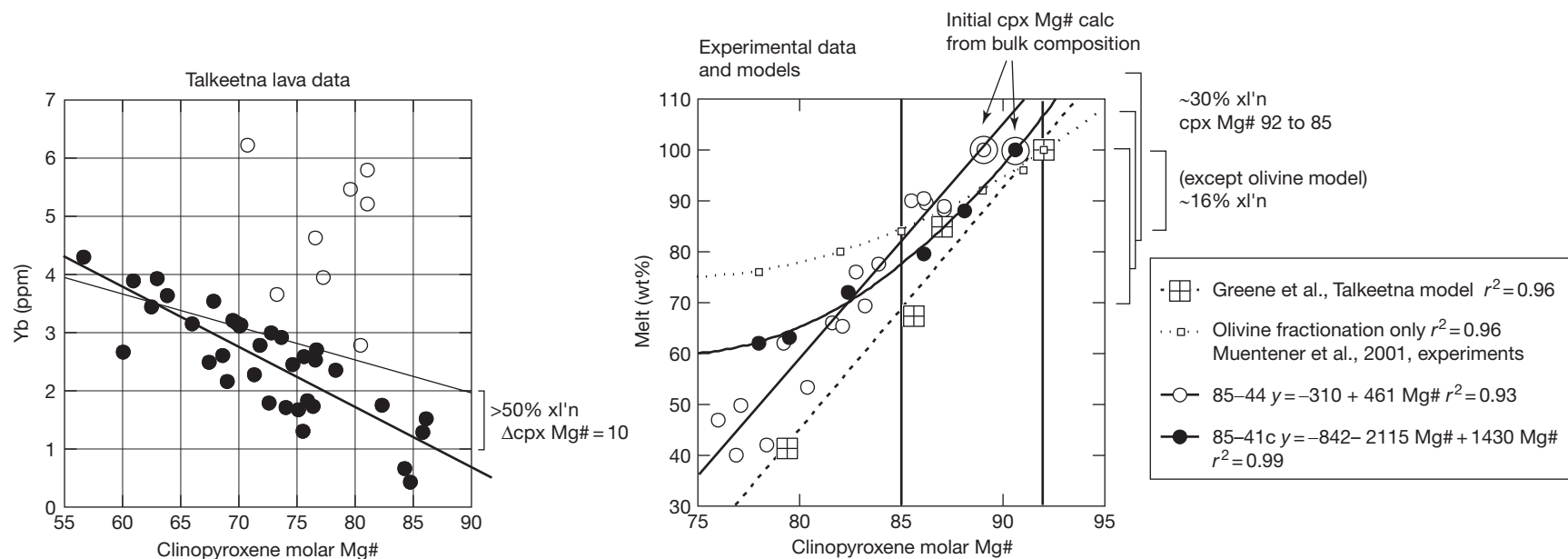


Figure 25 Estimates of melt fraction versus clinopyroxene Mg# from a variety of different methods. On the left, Talkeetna arc lava data are used to establish an empirical relationship between measured Yb concentration, and calculated clinopyroxene Mg# based on a clinopyroxene/melt Fe/Mg Kd of 0.23 (Sisson and Grove, 1993a). If Yb were a perfectly incompatible element, entirely retained in the melt, doubling of the Yb concentration would reflect 50% crystallization. Since Yb is not perfectly incompatible, doubling of Yb indicates more than 50% crystallization. Thus, a change in clinopyroxene Mg# from ~85 to ~75 is associated with more than 50% crystallization (filled symbols used in linear fit; open symbols omitted from fit). On the right, experimental and model results are used to constrain similar relationships. Data on experimental crystallization of hydrous primitive arc basalt (85–44) and primitive arc andesite (85–41c) at 1.2 GPa (Müntener et al., 2001) yield two empirical relationships between melt fraction and clinopyroxene Mg#, in which a change in clinopyroxene Mg# from 92 to 85 required ~30% crystallization. Least squares modeling of the Talkeetna liquid line of descent, based on Talkeetna lava, pyroxenite, and gabbroic compositions, provides a similar result (Greene et al., 2003). Olivine is rare in Talkeetna pyroxenite and gabbroic rocks. Olivine in dunites and residual mantle harzburgites underlying the pyroxenites in the Tonsina area has Mg# ~90 (in equilibrium with clinopyroxene Mg# ~92), so it does not record substantial crystal fractionation. Nonetheless, the right-hand panel in this figure also shows an olivine-only fractionation calculation, using an estimated Talkeetna primary melt (Greene et al., 2003), in terms of equivalent clinopyroxene Mg# versus melt fraction. This model provides a minimum bound of ~15% crystallization to shift clinopyroxene Mg# from 92 to 85.

90 to 85 are pyroxenites. As pointed out by Arndt and Goldstein (1989), and quantified by Jull and Kelemen (2001) and Müntener et al. (2001), pyroxenites are generally denser than uppermantle peridotites, because olivine and pyroxene densities are very similar at similar Mg#, but igneous pyroxenites have lower Mg# than residual peridotites. Furthermore, the density contrast between ultramafic cumulates and mantle peridotites is sufficient to drive viscous 'delamination' of a pyroxenite layer 1–2 km thick in ~ 10 Ma at $\sim 750^\circ\text{C}$ and $\sim 10^5$ years at $\sim 1000^\circ\text{C}$ (stress-dependent non-Newtonian olivine rheology at a background strain rate of 10^{-14} s^{-1} ; see Jull and Kelemen, 2001 for details and other estimates).

Although all four hypotheses outlined above remain possible, for the reasons outlined in the previous paragraphs we favor the fourth hypothesis, in which pyroxenites foundered into the underlying mantle as a result of density instabilities. Even if some of pyroxenites were emplaced into residual mantle beneath the Moho, the high temperature of sub-arc mantle and the high strain inferred from Talkeetna peridotite ductile deformation fabrics combined with the short instability times calculated by Jull and Kelemen (2001) suggest that any significant thickness of pyroxenite near the base of the crust or within the mantle would have been viscously removed during the duration of arc magmatism.

Garnet granulites with the composition of Talkeetna gabbro-norites would also be denser than the underlying mantle (Jull and Kelemen, 2001). We suggest that it is no coincidence that the 'Mg# gap' coincides with the garnet-in isograd at the base of the Talkeetna gabbroic section. Thus, along with the missing pyroxenites, we infer that garnet granulites may also have been removed from the base of the Talkeetna arc section via density instabilities. In this view, the narrow horizons of pyroxenite and garnet granulite along the Moho in the Talkeetna section are a small remnant of a much larger mass of primitive cumulates, most of which were removed by delamination.

4.21.4.3 Garnet Diorites and Tonalites: Igneous Garnet in the Lower Crust

In the Klanelneechina klippe, which was thrust south of the Talkeetna arc section over younger accretionary complexes, we found that most rocks are pyroxene quartz diorites to tonalites (bulk Mg# <50, plagioclase anorthite content <50 mol%), and include some garnet-bearing assemblages. Metamorphic equilibria in garnet + pyroxene bearing rocks record ~ 7 GPa, 700°C (Kelemen et al., 2003a). While these rocks will be discussed elsewhere in detail, they are pertinent to the question of continental genesis, and so we illustrate their trace-element contents in Figure 22. While their LILE, HFSE, and light REE patterns vary widely, these samples consistently show heavy REE enrichment, and low Ti/Dy. These characteristics are probably indicative of the presence of cumulate or residual, igneous garnet. Felsic melts extracted from these rocks were garnet-saturated at a depth of ~ 20 km in the Talkeetna arc crust. They were light REE-enriched, heavy REE-depleted, high SiO_2 , low Mg# melts that could have mixed with primitive melts to produce high-Mg# andesite compositions.

4.21.5 Implications for Continental Genesis

4.21.5.1 Role of Lower Crustal Delamination in Continental Genesis

The similarity of trace-element patterns in arc magmas and continental crust has led to the inference that most continental crust is derived from igneous, arc crust. We know of three potentially viable explanations for the generation of andesitic continental crust with an Mg# of ~ 0.5 via processes involving arc crust:

1. Crystal fractionation from, or partial melting of, a primitive arc basalt composition at high f_{O_2} and high $f_{\text{H}_2\text{O}}$, forming high-Mg# andesite melt and corresponding low- SiO_2 cumulates, followed by delamination of the resulting solid residue.
2. Magma mixing or simply juxtaposition of primitive arc basalt and evolved granitic rocks, together with delamination of the solid residue left after granite generation.
3. Crystal fractionation from, or partial melting of, a primitive arc andesite composition, followed by delamination of the corresponding cumulates.

In (1)–(3), delamination would be unnecessary if primitive cumulates or residues of lower crustal melting were ultramafic, and remained below the seismic Moho. However, the absence of pyroxenite layers ~ 10 km in thickness in the Talkeetna and Kohistan arc sections suggests that large proportions of ultramafic, igneous rocks are not present at the base of arc crust.

Thus, all three explanations for the genesis of continental crust require delamination of garnet granulite, eclogite, and/or pyroxenite. Moreover, recent dynamical calculations support the hypothesis that delamination is possible – even likely – where Moho temperatures exceed $\sim 750^\circ\text{C}$, crustal thicknesses reach 30 km or more, and ultramafic cumulates are present (Jull and Kelemen, 2001). The base of arc crust fulfills all these criteria. Finally, our data on the Talkeetna arc section, and more limited data on the Kohistan arc section, support the hypothesis that substantial proportions of pyroxenite, and perhaps also garnet granulite, were removed by viscous delamination from the base of the arc crust.

If delamination of dense lower crustal rocks has been essential to continental genesis, and the delaminated rocks constitute ~ 20 – 40% of the mass of the continents, one might expect to see evidence for this component in magmas derived from the convecting mantle. However, continental crust comprises only $\sim 0.5\%$ of the silicate Earth, so that – even if it represents 40% of the original crustal mass – recycled lower crust might comprise a very small fraction of the convecting mantle.

Tatsumi (2000) argued that recycled pyroxenite or cumulate gabbro, added to the convecting mantle via delamination from the base of arc crust, has produced the EM I isotopic end-member observed in some ocean island basalts, because he inferred on the basis of modeling that this recycled material would have high Rb/Sr, U/Pb, and Th/Pb, and low Sm/Nd compared to bulk Earth and the primitive mantle. However, although the Tonsina pyroxenites have variable trace-element patterns, the average and median compositions have U/Pb and Th/Pb ratios less than in MORBs and primitive mantle, and average Sm/Nd and Lu/Hf greater than in MORBs and

primitive mantle. In general, one might expect delaminated Talkeetna pyroxenite to evolve isotope ratios similar to, or more depleted than, the MORB source. Such compositions could, in fact, be present in the source of the more depleted end-members of the MORB isotope spectrum.

If a delaminated lower crustal component included substantial amounts of garnet granulite with the composition of garnet granulites or gabbro-norites from the Tonsina region in the Talkeetna arc section, the trace-element ratios and abundances in this reservoir would be different from those in delaminated pyroxenite. However, it remains true that Rb/Sr, U/Pb, and Th/Pb in most of our garnet granulite and gabbro-norite samples are lower than in the MORB source, while Sm/Nd and Lu/Hf are higher than in the MORB source. Again, as a consequence, long-term isotopic evolution followed by melting of this component during upwelling in the convecting mantle, would yield a melt with isotope ratios similar to, or more depleted than, the MORB source. While incompatible trace-element concentrations in pyroxenite are really very low, trace-element concentrations in the garnet granulites and gabbro-norites are comparable to those in MORBs. Thus, given the large strontium and lead anomalies in the garnet granulites, removal of substantial amounts of garnet granulite from the base of continental crust would tend to decrease Pb/Ce and Sr/Nd in the remaining crust. This provides one possible explanation for the fact that Sr/Nd in continental crust is lower than in otherwise geochemically similar arc magmas, as also noted by Kemp and Hawkesworth (2003) and Rudnick (1995).

4.21.5.2 Additional Processes are Required

The process of delamination – if it occurred – apparently did not produce an andesitic bulk composition in the remaining Talkeetna arc crust. Instead, the Talkeetna arc section probably has a basaltic bulk composition (DeBari and Sleep, 1991; Greene et al., 2003) even after removal of dense, primitive cumulates. This inference is consistent with seismic data, and the composition of primitive arc basalts from the central Aleutian arc and the Izu–Bonin–Marianas arc system, all of which appear to have bulk crust compositions that are basaltic rather than andesitic (Fliedner and Klemperer, 1999; Holbrook et al., 1999; Kerr and Klemperer, 2002; Suyehiro et al., 1996). As noted above, some additional processes must be required to produce continental crust.

4.21.5.2.1 Andesitic arc crust at some times and places

Our favored hypothesis is that continental crust was mainly produced by fractionation of olivine and clinopyroxene from primitive andesite. Following many others (Defant and Kepezhinskis, 2001; Drummond and Defant, 1990; Martin, 1986, 1999; Rapp and Watson, 1995; Rapp et al., 1991), we believe that higher mantle temperatures in the Archean led to more common, larger degrees of partial melting of subducting eclogite facies basalt. Alternatively, or in addition, dense lower crustal rocks foundering into the hot upper mantle may have commonly undergone partial melting (Zegers and van Keken, 2001). Also, due to higher degrees of melting

at hot spots and beneath spreading ridges, more depleted peridotite was present in the upper mantle, including the mantle wedge above Archean subduction zones. Thus, interaction between eclogite melts and highly depleted mantle peridotite yielded primitive andesite (e.g., Kelemen et al., 1998; Rapp et al., 1999; Ringwood, 1974; Rudnick et al., 1994), but produced little additional basaltic melt. Delamination removed mostly ultramafic cumulates from the base of the crust. Intracrustal differentiation of an andesitic bulk composition formed a felsic upper crust and a residual mafic lower crust.

4.21.5.2.2 Arc thickening, intracrustal differentiation, and mixing

However, fractionation of primitive andesite is clearly just one of many possibilities for the genesis of continental crust with the composition of high-Mg# andesite. An alternative view is that intracrustal differentiation, perhaps involving residual garnet and/or magnetite, has converted basaltic arc crust into andesitic continental crust. One mechanism for this is suggested by intermediate to felsic, garnet ‘cumulates’ in the Talkeetna lower crust. These may have been derived from intermediate plutonic rocks and/or evolved volcanics that were gradually buried in the growing arc edifice (Figure 26, also see figure 9 in Kuno, 1968). Later, heating of the lower crust formed light REE-enriched, heavy REE-depleted melts that were extracted from these rocks. Mixing between primitive basalt and crustal melts with garnet-bearing residues could form high-Mg# andesite (although we see little, if any, evidence for such mixing among Talkeetna arc volcanics). Then, delamination of the residues of lower crustal melting could yield an andesitic bulk composition for the entire crust.

4.21.6 Conclusions

Arc magmas are dramatically different, on average, from MORBs. Together with boninites, primitive and high-Mg# andesites exemplify these differences. Unfortunately, primitive andesites are rare in intra-oceanic arcs, and so there is some possibility that they are produced by special intracrustal differentiation processes specific to continental arcs. However, there are primitive andesites in the oceanic Aleutian arc, and these lack any evidence for crustal assimilation, or even for recycling of components from subducted continental sediments. Aleutian primitive andesites and other primitive andesites with high Sr/Nd cannot be produced by the mixing of primitive arc basalts and lower crustal melts. In most respects, the Aleutian primitive andesites are similar to all other primitive andesites, indicating that these magmas can be derived from primary andesite melts.

Primary andesites are probably produced by interaction between mantle peridotite and a partial melt of eclogite facies, subducting sediment and/or basalt. Thermal modeling cannot be used to rule out partial melting of subducting material beneath arcs, as has previously been supposed. Some characteristics of all primitive arc magmas, such as enrichment in thorium and lanthanum, and large depletions of niobium and tantalum relative to thorium and lanthanum, are best explained by a similar process, in which thorium and

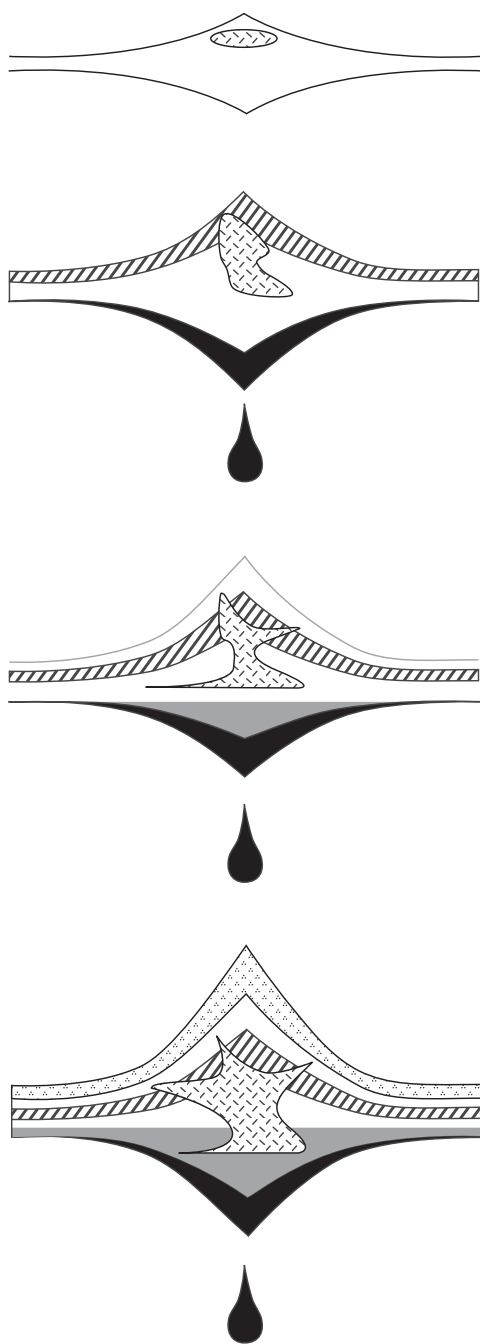


Figure 26 Schematic illustration of the process of progressive burial of early formed plutonic and volcanic rocks within a growing arc edifice (also see Kuno, 1968, figure 9). Pyroxenites near the base of the crust are always denser than the underlying mantle, and temperatures are high near the Moho, so that these ultramafic cumulates may delaminate repeatedly whenever their thickness exceeds some critical value (e.g., Jull and Kelemen, 2001). Increasing pressure forms abundant garnet in Al-rich, mafic, gabbroic rocks near the base of the section, and these too may delaminate. Intermediate to felsic plutonic rocks, and even volcanics, may be buried to lower crustal depths, where they undergo partial melting. Mixing of lower crustal melts with primitive basalt could produce high-Mg# andesite magmas. This last process, together with delamination, provides a possible explanation for the formation of andesitic continental crust from initially basaltic arc crust.

lanthanum are carried into the mantle wedge in a partial melt of subducting material in eclogite facies. Thus, the difference between primitive basalt and andesite may be largely determined by the relative proportions of mantle versus subduction zone melt components, together with a fluid component derived from relatively shallow dehydration of subducting materials.

Although we favor the notion that fractionation of olivine and/or pyroxene from primitive andesites has played a key role in the formation of continental crust, which has a high-Mg# andesite composition, this process alone is not sufficient to change the Mg# of the crust from a value of ~ 70 , typical for primary melts in equilibrium with mantle olivine, to the value of ~ 50 estimated for bulk continental crust. Instead, removal of the crystalline products of fractionation from the crust into the mantle is also required. In fact, all 'recipes' for continental crust probably require delamination. We show that the Talkeetna and Kohistan arc sections provide evidence for such a process, in the sense that they only contain a small proportion of the primitive lower crustal cumulates that must have originally formed. The remaining primitive cumulates, which are pyroxenites and garnet granulites, were denser than the underlying mantle during arc crustal formation, while overlying gabbroic rocks were less dense. Thus, the Mg# gap in both sections is observed only where rocks become denser than residual peridotite. Removal of pyroxenite and garnet granulite from the base of arc crust leaves the remaining crust with lower Sr/Nd and Pb/Ce than in primary arc magmas. Delaminated recycled primitive arc cumulates would evolve to isotope signatures as depleted as or more depleted than the MORB source.

Acknowledgments

We thank Sue DeBari for advice and support for Andrew Greene, Bärbel Sarbas for information from the GeoRoc database, Nate Hart for help with data entry, John Eiler for discussions, Tim Grove, Simon Turner, and Terry Plank for sharing preprints and sane advice, and Roberta Rudnick for forbearance during our long struggle to complete this chapter. Formal and informal reviews of a draft manuscript by Terry Plank, Steve Eggins, Simon Turner, Chris Hawkesworth, Bernard Bourdon, and Charlie Langmuir were both helpful and tolerant. We hope they find the finished product substantially improved. Research by Kelemen and Hanghoj for this chapter was supported in part by National Science Foundation Research Grants EAR-0125919, EAR0087706, EAR-9910899, and OCE-9819666, plus the Charles Francis Adams Senior Scientist Chair at Woods Hole Oceanographic Institution.

References

- Abe N, Arai S, and Yurimoto H (1998) Geochemical characteristics of the uppermost mantle beneath the Japan island arcs: Implications for upper mantle evolution. *Physics of the Earth and Planetary Interiors* 107: 233–248.
- Abratis M and Worner G (2001) Ridge collision, slabwindow formation, and the flux of Pacific asthenosphere into the Caribbean realm. *Geology* 29: 127–130.
- Anczkiewicz R and Vance D (2000) Isotopic constraints on the evolution of metamorphic conditions in the Jijal-Patan Complex and Kamila Belt of the Kohistan Arc, Pakistan Himalaya. In: *Tectonics of the Nanga Parbat Syntaxis and*

- the Western Himalaya, *Geological Society Special Publication*, vol. 170, pp. 321–331.
- Anderson AT (1974) Evidence for a picritic, volatile-rich magma beneath Mt. Shasta, California. *Journal of Petrology* 15: 243–267.
- Arculus RJ, Johnson RW, Chappell BW, McKee CO, and Sakai H (1983) Ophiolite-contaminated andesites, trachybasalts, and cognate inclusions of Mount Lamington, Papua New Guinea: Anhydrite-amphibole-bearing lavas and the 1951 cumulodome. *Journal of Volcanology and Geothermal Research* 18: 215–247.
- Armstrong RL (1981) Radiogenic isotopes: The case for crustal recycling on a near-steady-state no-continental-growth Earth. *Philosophical Transactions of the Royal Society Series A* 301: 443–472.
- Arndt NT and Goldstein SL (1989) An open boundary between lower continental crust and mantle: Its role in crust formation and crustal recycling. *Tectonophysics* 161: 201–212.
- Asimow P and Stolper E (1999) Steady-state mantle-melt interactions in one dimension. I: Equilibrium transport and melt focusing. *Journal of Petrology* 40: 475–494.
- Ayers J (1998) Trace element modeling of aqueous fluid: Peridotite interaction in the mantle wedge of subduction zones. *Contributions to Mineralogy and Petrology* 132: 390–404.
- Ayers JC, Dittmer SK, and Layne GD (1997) Partitioning of elements between peridotite and H₂O at 2.0–3.0 GPa and 900–1100 °C, and application to models of subduction zone processes. *Earth and Planetary Science Letters* 150: 381–398.
- Babeyko AY, Sobolev SV, Trumbull RB, Oncken O, and Lavie LL (2002) Numerical models of crustal scale convection and partial melting beneath the Altiplano-Puna plateau. *Earth and Planetary Science Letters* 199: 373–388.
- Baker DR and Eggler DH (1983) Fractionation paths of Atka (Aleutians) high-alumina basalts: Constraints from phase relations. *Journal of Volcanology and Geothermal Research* 18: 387–404.
- Baker DR and Eggler DH (1987) Compositions of anhydrous and hydrous melts coexisting with plagioclase, augite and olivine or low-Ca pyroxene form 1 atm to 8 kbar: Application to the Aleutian volcanic center of Atka. *American Mineralogist* 72: 12–28.
- Baker MB, Grove TL, and Price R (1994) Primitive basalts and andesites from the Mt. Shasta region N. California: Products of varying melt fraction and water content. *Contributions to Mineralogy and Petrology* 118: 111–129.
- Bard JP (1983) Metamorphism of an abducted island arc: Example of the Kohistan Sequence (Pakistan) in the Himalayan collided range. *Earth and Planetary Science Letters* 65(1): 133–144.
- Barker F, Aleinikoff JN, Box SE, et al. (1994) Some accreted volcanic rocks of Alaska and their elemental abundances. In: Plafker G and Berg HC (eds.) *The Geology of North America. The Geology of Alaska*, vol. G-1. Washington, DC: Geological Society of America.
- Barker F and Grantz A (1982) Talkeetna formation in the southeastern Talkeetna Mountains, southern Alaska: An early Jurassic andesitic intraoceanic island arc. *Geological Society of America Abstracts with Programs* 14: 147.
- Bartels KS, Kinzler RJ, and Grove TL (1991) High pressure phase relations of primitive high-alumina basalts from Medicine Lake volcano, northern California. *Contributions to Mineralogy and Petrology* 108: 253–270.
- Beate B, Monzier M, Spikings R, et al. (2001) Mio-Pliocene adakite generation related to flat subduction in southern Ecuador: The Quimsacocha volcanic centre. *Earth and Planetary Science Letters* 192: 561–570.
- Bebout GE, Ryan JG, and Leeman WP (1993) B–Be systematics in subduction-related metamorphic rocks: Characterization of the subducted component. *Geochimica et Cosmochimica Acta* 57: 2227–2237.
- Bebout GE, Ryan JG, Leeman WP, and Bebout AE (1999) Fractionation of trace elements by subduction-zone metamorphism—effect of convergent-margin thermal evolution. *Earth and Planetary Science Letters* 171: 63–81.
- Becker H, Jochum KP, and Carlson RW (1999) Constraints from high-pressure veins in eclogites on the composition of hydrous fluids in subduction zones. *Chemical Geology* 160: 291–308.
- Becker H, Jochum KP, and Carlson RW (2000) Trace element fractionation during dehydration of eclogites from high-pressure terranes and the implications for element fluxes in subduction zones. *Chemical Geology* 163: 65–99.
- Blackwell DD, Bowen RG, Hull DA, Riccio J, and Steele JL (1982) Heat flow, arc volcanism, and subduction in northern Oregon. *Journal of Geophysical Research* 87: 8735–8754.
- Blatter DL and Carmichael ISE (1998) Hornblende peridotite xenoliths from central Mexico reveal the highly oxidized nature of subarc upper mantle. *Geology* 26: 1035–1038.
- Bloomer SH and Hawkins JW (1987) Petrology and geochemistry of boninite series volcanic rocks from the Mariana trench. *Contributions to Mineralogy and Petrology* 97: 361–377.
- Bodinier JL, Merlet C, Bedini RM, Simien F, Remaidi M, and Garrido CJ (1996) Distribution of niobium, tantalum, and other highly incompatible trace elements in the lithospheric mantle: The spinel paradox. *Geochimica et Cosmochimica Acta* 60(3): 545–550.
- Bourdon B, Turner S, and Allegre C (1999) Melting dynamics beneath the Tonga–Kermadec island arc inferred from ²³¹Pa–²³⁵U systematics. *Science* 286: 2491–2493.
- Bourdon B, Woerner G, and Zindler A (2000) U-series evidence for crustal involvement and magma residence times in the petrogenesis of Paríacota Volcano, Chile. *Contributions to Mineralogy and Petrology* 139: 458–469.
- Bourdon E, Eissen JP, Monzier M, et al. (2002) Adakite-like lavas from Antisana Volcano (Ecuador): Evidence from slab melt metasomatism beneath the Andean northern volcanic zone. *Journal of Petrology* 192: 561–570.
- Bowen NL (1928) *The Evolution of the Igneous Rocks*. Princeton, NJ: Princeton University Press.
- Brandon AD and Draper DS (1996) Constraints on the origin of the oxidation state of mantle overlying subduction zones: An example from Simcoe, Washington, USA. *Geochimica et Cosmochimica Acta* 60: 1739–1749.
- Brenan JM, Shaw HF, and Ryerson RJ (1995a) Experimental evidence for the origin of lead enrichment in convergent margin magmas. *Nature* 378: 54–56.
- Brenan JM, Shaw HF, Ryerson RJ, and Phinney DL (1995b) Mineral-aqueous fluid partitioning of trace elements at 900 °C and 2.0 GPa: Constraints on trace element chemistry of mantle and deep crustal fluids. *Geochimica et Cosmochimica Acta* 59: 3331–3350.
- Brenan JM, Shaw HF, Ryerson FJ, and Phinney DL (1996) Erratum to “Experimental determination of trace-element partitioning between pargasite and a synthetic hydrous andesitic melt.” [Earth Planet. Sci. Lett. 135 (1995) 1–11] *Earth and Planetary Science Letters* 140: 287–288.
- Brophy JG (1987) The Cold Bay volcanic center, Aleutian volcanic arc. II: Implications for fractionation and mixing mechanisms in calc-alkaline andesite genesis. *Contributions to Mineralogy and Petrology* 97: 378–388.
- Brophy JG (1989) Basalt convection and plagioclase retention: A model for the generation of high-alumina arc basalt. *Journal of Geology* 97: 319–329.
- Brophy JG and Marsh BD (1986) On the origin of high alumina arc basalt and the mechanics of melt extraction. *Journal of Petrology* 27: 763–789.
- Bureau H and Keppler H (1999) Complete miscibility between silicate melts and hydrous fluids in the upper mantle: Experimental evidence and geochemical implications. *Earth and Planetary Science Letters* 165: 187–196.
- Burns LE (1983) *The Border Ranges Ultramafic and Mafic Complex: Plutonic Core of an Intraoceanic Island Arc*. PhD Thesis, Stanford University.
- Burns LE (1985) The border ranges ultramafic and mafic complex, south-central Alaska: Cumulate fractionates of island-arc volcanics. *Canadian Journal of Earth Sciences* 22: 1020–1038.
- Burns LE, Pessel GH, Little TA, et al. (1991) Geology of the northern Chugach Mountains, southcentral Alaska. *State of Alaska Division of Geological and Geophysical Surveys, Professional Report* 94: 1–63.
- Campbell IH and Turner JS (1985) Turbulent mixing between fluids with different viscosities. *Nature* 313: 39–42.
- Cannat M (1996) How thick is the magmatic crust at slow spreading oceanic ridges? *Journal of Geophysical Research* 101: 2847–2857.
- Carr MJ, Feigenson MD, and Bennett EA (1990) Incompatible element and isotopic evidence for tectonic control of source mixing and melt extraction along the Central American Arc. *Contributions to Mineralogy and Petrology* 105: 369–380.
- Carroll MR and Wyllie PJ (1989) Experimental phase relations in the system tonalite–peridotite–H₂O at 15 kb: Implications for assimilation and differentiation processes near the crust–mantle boundary. *Journal of Petrology* 30: 1351–1382.
- Chauvel C and Hemond C (2000) Melting of a complete section of recycled oceanic crust: Trace element and Pb isotopic evidence from Iceland. *Geochimica, Geophysics, Geosystems* 1: Paper number 1999GC000002.
- Christensen NI and Mooney WD (1995) Seismic velocity structure and composition of the continental crust: A global view. *Journal of Geophysical Research* 100: 9761–9788.
- Cigolini C, Kudo AM, Brookins DG, and Ward D (1992) The petrology of Poas Volcano lavas: Basalt–andesite relationship and their petrogenesis within the magmatic arc of Costa Rica. *Journal of Volcanology and Geothermal Research* 48: 367–384.
- Clark SK, Reagan MK, and Plank T (1998) Trace element and U-series systematics for 1963–1965 tephra from Irazu Volcano, Costa Rica: Implications for magma generation processes and transit times. *Geochimica et Cosmochimica Acta* 62: 2689–2699.
- Class C, Miller DL, Goldstein SL, and Langmuir CH (2000) Distinguishing melt and fluid components in Umnak Volcanics, Aleutian Arc. *Geochimica, Geophysics, Geosystems* 1(June 1): Paper number 1999GC000010.
- Clift PD and MacLeod CJ (1999) Slow rates of subduction erosion estimated from subsidence and tilting of the Tonga forearc. *Geology* 27: 411–414.
- Conder JA, Weins DA, and Morris J (2002) On the decompression melting structure at volcanic arcs and backarc spreading centers. *Geophysical Research Letters* 29(15): 4 pp.

- Conrad WK and Kay RW (1984) Ultramafic and mafic inclusions from Adak Island: Crystallization history, and implications for the nature of primary magmas and crustal evolution in the Aleutian Arc. *Journal of Petrology* 25: 88–125.
- Conrad WK, Kay SM, and Kay RW (1983) Magma mixing in the Aleutian arc: Evidence from cognate inclusions and composite xenoliths. *Journal of Volcanology and Geothermal Research* 18: 279–295.
- Coward MP, Jan MQ, Rex D, Tarney J, Thirlwall MF, and Windley BF (1982) Structural evolution of a crustal section in the western Himalaya. *Nature* 295(5844): 22–24.
- Crawford AJ (1989) *Boninites*, London: Unwin Hyman.
- Crawford AJ, Falloon TJ, and Eggins S (1987) The origin of island arc high-alumina basalts. *Contributions to Mineralogy and Petrology* 97: 417–430.
- Crawford WC and Webb SC (2002) Variations in the distribution of magma in the lower crust and at the Moho beneath the East Pacific Rise at 9 degrees–10 degrees N. *Earth and Planetary Science Letters* 203: 117–130.
- Crawford WC, Webb SC, and Hildebrand JA (1999) Constraints on melt in the lower crustal and Moho at the East Pacific Rise, 9 degrees 48'N, using seafloor compliance measurements. *Journal of Geophysical Research* 104: 2923–2939.
- Daly RA (1933) *Igneous Rocks and the Depths of the Earth*. New York: McGraw-Hill.
- Davidson JP (1996) Deciphering mantle and crustal signatures in subduction zone magmatism. In: Bebout GE, Scholl DW, Kirby SH, and Platt JP (eds.) *Subduction, Top to Bottom, Geophysical Monograph Series*, vol. 96, pp. 251–262.
- Davies JH (1999) The role of hydraulic fractures and intermediate-depth earthquakes in generating subduction zone magmatism. *Nature* 398: 142–145.
- Davies JH and Stevenson DJ (1992) Physical model of source region of subduction zone volcanics. *Journal of Geophysical Research* 97: 2037–2070.
- de Boer JZ, Defant MJ, Stewart RH, and Bellon H (1991) Evidence for active subduction below western Panama. *Geology* 19: 649–652.
- de Boer JZ, Defant MJ, Stewart RH, Restrepo JF, Clark LF, and Ramirez AH (1988) Quaternary calc-alkaline volcanism in western Panama: Regional variation and implication for the plate tectonic framework. *Journal of South American Earth Sciences* 1: 275–293.
- de Boer JZ, Drummond MS, Bordon MJ, Defant MJ, Bellon H, and Maury RC (1995) Cenozoic magmatic phases of the Costa Rican island arc (Cordillera de Talamanca). In: Mann P (ed.) *Geologic and Tectonic Development of the Caribbean Plate Boundary in Southern Central America, GSA Special Papers*, vol. 295, pp. 35–55. Boulder, CO: Geological Society of America.
- DeBari SM (1990) *Comparative Field and Petrogenetic Study of Arc Magmatism in the Lower Crust: Exposed Examples from a Continental Margin and an Intraoceanic Setting*. PhD Thesis, Stanford University.
- DeBari SM (1994) Petrogenesis of the Fiambalá gabbroic intrusion, northwestern Argentina, a deep crustal syntectonic pluton in a continental magmatic arc. *Journal of Petrology* 35: 679–713.
- DeBari SM, Anderson RG, and Mortensen JK (1999) Correlation among lower to upper crustal components in an island arc: The Jurassic Bonanza Arc, Vancouver Island, Canada. *Canadian Journal of Earth Sciences* 36: 1371–1413.
- DeBari SM and Coleman RG (1989) Examination of the deep levels of an island arc: Evidence from the Tonsina ultramafic-mafic assemblage, Tonsina, Alaska. *Journal of Geophysical Research* 94(B4): 4373–4391.
- DeBari SM and Sleep NH (1991) High-Mg, low-Al bulk composition of the Talkeetna island arc, Alaska: Implications for primary magmas and the nature of arc crust. *Geological Society of America Bulletin* 103: 37–47.
- Defant MJ, Clark LF, Stewart RH, et al. (1991a) Andesite and dacite genesis via contrasting processes: The geology and geochemistry of El Valle Volcano, Panama. *Contributions to Mineralogy and Petrology* 106: 309–324.
- Defant MJ and Drummond MS (1990) Derivation of some modern arc magmas by melting of young subducted lithosphere. *Nature* 347: 662–665.
- Defant MJ, Jackson TE, Drummond MS, et al. (1992) The geochemistry of young volcanism throughout western Panama and southeastern Costa Rica: An overview. *Journal of the Geological Society* 149: 569–579.
- Defant MJ, Jacques D, Maury RC, de Boer JZ, and Joron JL (1989) Geochemistry and tectonic setting of the Luzon arc, Philippines. *Geological Society of America Bulletin* 101: 663–672.
- Defant MJ and Kepezhinskis P (2001) Evidence suggests slab melting in arc magmas. *Eos, Transactions American Geophysical Union* 82: 65–69.
- Defant MJ, Richerson PM, de Boer JZ, et al. (1991b) Dacite genesis via both slab melting and differentiation: Petrogenesis of La Yeguada Volcanic Complex, Panama. *Journal of Petrology* 32: 1101–1142.
- DePaolo DJ (1981) Trace element and isotopic effects of combined wallrock assimilation and fractional crystallization. *Earth and Planetary Science Letters* 53: 189–202.
- Detterman R and Hartsock J (1966) Geology of the Iniskin-Tuxedni region, Alaska. *US Geological Survey Professional Paper* 512: 1–78.
- Dick HJB (1989) Abyssal peridotites, very slow spreading ridges and ocean ridge magmatism. *Geological Society Special Publication (Magmatism in the Ocean Basins)* 42: 71–105.
- Dixon J and Stolper E (1995) An experimental study of water and carbon dioxide solubilities in mid-ocean ridge basaltic liquids. II: Applications to degassing. *Journal of Petrology* 35: 1633–1646.
- Dixon J, Stolper E, and Holloway J (1995) An experimental study of water and carbon dioxide solubilities in mid ocean ridge basaltic liquids. I: Calibration and solubility models. *Journal of Petrology* 36: 1607–1631.
- Domanik KJ, Hervig RL, and Peacock SM (1993) Beryllium and boron in subduction zone minerals: An ion microprobe study. *Geochimica et Cosmochimica Acta* 57: 4997–5010.
- Draper DS and Johnston AD (1992) Anhydrous P–T phase relations of an Aleutian high-MgO basalt: An investigation of the role of olivine-liquid reaction in the generation of arc high-alumina basalts. *Contributions to Mineralogy and Petrology* 112: 501–519.
- Drummond MS, Bordon MJ, Boer JZ, Defant MJ, Bellon H, and Feigenson MD (1995) Igneous petrogenesis and tectonic setting of plutonic and volcanic rocks of the Cordillera de Talamanca, Costa Rica–Panama, Central American Arc. *American Journal of Science* 295: 875–919.
- Drummond MS and Defant MJ (1990) A model for trondjemite–tonalite–dacite genesis and crustal growth via slab melting. *Journal of Geophysical Research* 95: 21503–21521.
- Ducea MN and Saleeby JB (1996) Buoyancy sources for a large, unrooted mountain range, the Sierra Nevada, California: Evidence from xenolith thermobarometry. *Journal of Geophysical Research* 101: 8229–8244.
- Dunn RA and Toomey DR (1997) Seismological evidence for three-dimensional melt migration beneath the East Pacific Rise. *Nature* 388: 259–262.
- Earthref database—website for Earth Science reference data and models, <http://earthref.org/> (accessed June 2006).
- Eggins S (1993) Origin and differentiation of picritic arc magmas, Ambae (Aoba), Vanuatu. *Contributions to Mineralogy and Petrology* 114: 79–100.
- Eiler J, Crawford A, Elliott T, Farley KA, Valley JV, and Stolper EM (2000) Oxygen isotope geochemistry of oceanic arc lavas. *Journal of Petrology* 41: 229–256.
- Elkins Tanton LT, Grove TL, and Donnelly-Nolan J (2001) Hot shallow mantle melting under the Cascades volcanic arc. *Geology* 29: 631–634.
- Ellam RM and Hawkesworth C (1988a) Elemental and isotopic variations in subduction related basalts: Evidence for a three component model. *Contributions to Mineralogy and Petrology* 98: 72–80.
- Ellam RM and Hawkesworth CJ (1988b) Is average continental crust generated at subduction zones? *Geology* 16: 314–317.
- Elliott T (2003) Tracers of the slab. In: Eiler J (ed.) *Inside the Subduction Factory (Geophysical Monograph 138)*, pp. 23–45. Washington DC: American geophysical Union.
- Elliott T, Plank T, Zindler A, White W, and Bourdon B (1997) Element transport from slab to volcanic front at the Mariana Arc. *Journal of Geophysical Research* 102: 14991–15019.
- England P, Engdahl R, and Thatcher W (2003) Systematic variation in the depths of slabs beneath arc volcanoes. *Geophysical Journal International* 156(2): 377–408.
- Erikson EH Jr. (1977) Petrology and petrogenesis of the Mount Stuart Batholith—Plutonic equivalent of the high-alumina basalt association? *Contributions to Mineralogy and Petrology* 60: 183–207.
- Falloon TJ and Danyushevsky LV (2000) Melting of refractory mantle at 1.5, 2.0 and 2.5 GPa under H₂O undersaturated conditions: Implications for the petrogenesis of high-Ca boninites and the influence of subduction components on mantle melting. *Journal of Petrology* 41: 257–283.
- Falloon TJ and Green DH (1986) Glass inclusions in magnesian olivine phenocrysts from Tonga: Evidence for highly refractory parental magmas in the Tongan arc. *Earth and Planetary Science Letters* 81: 95–103.
- Falloon TJ, Green DH, and McCulloch MT (1989) 14: Petrogenesis of high-Mg and associated lavas from the north Tonga Trench. In: Crawford AJ (ed.) *Boninites*, pp. 357–395. London: Unwin Hyman.
- Feineman MD and DePaolo DJ (2002) A diffusion-decay model for steady-state U-series disequilibrium in the mantle with implications for island arc lavas. *Eos, Transactions American Geophysical Union* 83(47) Fall Meeting Supplement.
- Fenner CN (1929) The crystallization of basalts. *American Journal of Science* XVIII: 223–253.
- Fenner CN (1937) A view of magmatic differentiation. *Journal of Geology* 45: 158–168.
- Fliedner M and Klemperer SL (1999) Structure of an island arc: Wide-angle seismic studies in the eastern Aleutian Islands, Alaska. *Journal of Geophysical Research* 104: 10667–10694.
- Furukawa Y (1993a) Depth of the decoupling plate interface and thermal structure under arcs. *Journal of Geophysical Research* 98: 20005–20013.

- Furukawa Y (1993b) Magmatic processes under arcs and formation of the volcanic front. *Journal of Geophysical Research* 98: 8309–8319.
- Furukawa Y and Tatsumi Y (1999) Melting of a subducting slab and production of high-Mg andesite magmas: Unusual magmatism in SW Japan at 13 approximately 15 Ma. *Geophysical Research Letters* 26(15): 2271–2274.
- Gaetani GA and Grove TL (1998) The influence of water on melting of mantle peridotite. *Contributions to Mineralogy and Petrology* 131: 323–346.
- Garrido CJ, Kelemen PB, and Hirth G (2001) Variation of cooling rate with depth in lower crust formed at an oceanic spreading ridge: Plagioclase crystal size distributions in gabbros from the Oman ophiolite. *Geochemistry, Geophysics, Geosystems* 2, Paper number 2000GC000136.
- Gast PW (1968) Trace element fractionation and the origin of tholeiitic and alkaline magma types. *Geochimica et Cosmochimica Acta* 32: 1057–1089.
- George MT, Harris NBW, Butler RWH, Treloar PJE, and Searle MPE (1993) The tectonic implications of contrasting granite magmatism between the Kohistan island arc and the Nanga Parbat–Haramosh Massif, Pakistan Himalaya. *Himalayan Tectonics, Seventh Himalaya–Karakoram–Tibet Workshop* 74: 173–191.
- George R, Turner S, Hawkesworth C, et al. (2003) Melting processes and fluid and sediment transport rates along the Alaska–Aleutian arc from an integrated U–Th–Ra–Be isotope study. *Journal of Geophysical Research* 108(B5): 2252.
- Georoc database, <http://www.georoc.mpch-mainz.gwdg.de/> (accessed June 2006).
- Gill J (1981) *Orogenic Andesites and Plate Tectonics*. Berlin: Springer.
- Gill J and Condomines M (1992) Short-lived radioactivity and magma genesis. *Science* 257: 1368–1376.
- Gill JB (1974) Role of underthrust oceanic crust in the genesis of a Fijian calc-alkaline suite. *Contributions to Mineralogy and Petrology* 43: 29–45.
- Gill JB (1978) Role of trace element partition coefficients in models of andesite genesis. *Geochimica et Cosmochimica Acta* 42: 709–724.
- Gill JB and Williams RW (1990) Th isotope and U series studies of subduction-related volcanic rocks. *Geochimica et Cosmochimica Acta* 54: 1427–1442.
- Gough SJ, Searle MP, Waters DJ, and Khan MA (2001) Igneous crystallization, high pressure metamorphism, and subsequent tectonic exhumation of the Jijal and Kamila complexes, Kohistan. *Abstracts: 16th Himalaya–Karakoram–Tibet Workshop Austria, Journal of Asian Earth Sciences* 19: 23–24.
- Grantz A, Thomas H, Stern T, and Sheffey N (1963) Potassium–argon and lead–alpha ages for stratigraphically bracketed plutonic rocks in the Talkeetna Mountains, Alaska. *US Geological Survey Professional Paper* 475–B: B56–B59.
- Green DH (1976) Experimental testing of “equilibrium” partial melting of peridotite under water-saturated, high-pressure conditions. *Canadian Mineralogist* 14: 255–268.
- Green DH and Ringwood AE (1967) The genesis of basaltic magmas. *Contributions to Mineralogy and Petrology* 15: 103–190.
- Green TH and Ringwood AE (1966) Origin of the calc-alkaline igneous rock suite. *Earth and Planetary Science Letters* 1: 307–316.
- Greene AR, Kelemen PB, DeBari SM, Blusztajn J, and Clift P (2003) A detailed geochemical study of island arc crust: The Talkeetna arc section, south-central Alaska. *Journal of Petrology* (submitted).
- Gromet LP and Silver LT (1987) REE variations across the Peninsular Ranges batholith: Implications for batholithic petrogenesis and crustal growth in magmatic arcs. *Journal of Petrology* 28: 75–125.
- Grove TL, Elkins Tanton LT, Parman SW, Chatterjee N, Müntener O, and Gaetani GA (2003) Fractional crystallization and mantle melting controls on calc-alkaline differentiation trends. *Contributions to Mineralogy and Petrology* 145(5): 515–533.
- Grove TL and Kinzler RJ (1986) Petrogenesis of andesites. *Annual Review of Earth and Planetary Sciences* 14: 417–454.
- Grove TL, Gerlach DC, and Sando TW (1982) Origin of calc-alkaline series lavas at Medicine Lake Volcano by fractionation, assimilation and mixing. *Contributions to Mineralogy and Petrology* 80: 160–182.
- Grove TL, Kinzler RJ, Baker MB, Donnelly-Nolan JM, and Leshner CE (1988) Assimilation of granite by basaltic magma at Burnt Lava flow, Medicine Lake volcano, California: Decoupling of heat and mass transfer. *Contributions to Mineralogy and Petrology* 99: 320–343.
- Grove TL, Parman SW, Bowring SA, Price RC, and Baker MB (2001) The role of H₂O-rich fluids in the generation of primitive basaltic andesites and andesites from the Mt. Shasta region N. California. *Contributions to Mineralogy and Petrology* 142: 375–396.
- Gust DA and Perfit MR (1987) Phase relations of a high-Mg basalt from the Aleutian island arc: Implications for primary island arc basalts and high-Al basalts. *Contributions to Mineralogy and Petrology* 97: 7–18.
- Hanson CR (1989) The northern suture in the Shigar Valley, Baltistan, northern Pakistan. *Tectonics of the Western Himalayas, GSA Special Papers* 232: 203–215.
- Harris PG (1957) Zone refining and the origin of potassic basalts. *Geochimica et Cosmochimica Acta* 12: 195–208.
- Hart SR, Blusztajn J, Dick HJB, Meyer PS, and Muehlenbachs K (1999) The fingerprint of seawater circulation in a 500-meter section of ocean crust gabbros. *Geochimica et Cosmochimica Acta* 63: 4059–4080.
- Hauff F, Hoernle K, Bogaard PVD, Alvarado G, and Garbe-Schonberg D (2000) Age and geochemistry of basaltic complexes in western Costa Rica: Contributions to the geotectonic evolution of Central America. *Geochemistry, Geophysics, Geosystems* 1, 41pp., Paper no. 1999GC000020.
- Hauri EH (1995) Major element variability in the Hawaiian mantle plume. *Nature* 382: 415–419.
- Hawkesworth CJ, Gallagher K, Hergt JM, and McDermott F (1993a) Mantle and slab contributions in arc magmas. *Annual Review of Earth and Planetary Sciences* 21: 175–204.
- Hawkesworth CJ, Gallagher K, Hergt JM, and McDermott F (1993b) Trace element fractionation processes in the generation of island arc basalts. *Philosophical Transactions of the Royal Society Series A* 342: 179–191.
- Hawkesworth CJ, Turner SP, McDermott F, Peate DW, and van Calsteren P (1997) U–Th isotopes in arc magmas: Implications for element transfer from the subducted crust. *Science* 276: 551–555.
- Herrstrom EA, Reagan MK, and Morris JD (1995) Variations in lava composition associated with flow of asthenosphere beneath southern Central America. *Geology* 23: 617–620.
- Herzberg CT, Fyfe WS, and Carr MJ (1983) Density constraints on the formation of the continental Moho and crust. *Contributions to Mineralogy and Petrology* 84: 1–5.
- Hildreth W and Moorbath S (1988) Crustal contributions to arc magmatism in the Andes of central Chile. *Contributions to Mineralogy and Petrology* 98: 455–489.
- Hirose K (1997) Melting experiments on lherzolite KLB-1 under hydrous conditions and generation of high-magnesian andesitic melts. *Geology* 25: 42–44.
- Hirschmann MM, Baker MB, and Stolper EM (1998) The effect of alkalis on the silica content of mantle-derived melts. *Geochimica et Cosmochimica Acta* 62: 883–902.
- Hirschmann MM and Stolper EM (1996) A possible role for garnet pyroxenite in the origin of the “garnet signature” in MORB. *Contributions to Mineralogy and Petrology* 124: 185–208.
- Hofmann AW (1988) Chemical differentiation of the Earth: The relationship between mantle, continental crust, and oceanic crust. *Earth and Planetary Science Letters* 90: 297–314.
- Holbrook WS, Lizarralde D, McGeary S, Bangs N, and Diebold J (1999) Structure and composition of the Aleutian island arc and implications for continental crustal growth. *Geology* 27: 31–34.
- Holmes A (1937) *The Age of the Earth*. London: Holmes, Arthur, Thomas Nelson & Sons.
- Honegger K, Dietrich V, Frank W, Gansser A, Thoni M, and Trommsdorff V (1982) Magmatism and metamorphism in the Ladakh Himalayas (the Indus–Tsangpo suture zone). *Earth and Planetary Science Letters* 60: 253–292.
- Hughes SS and Taylor EM (1986) Geochemistry, petrogenesis, and tectonic implications of central High Cascade mafic platform lavas. *Geological Society of America Bulletin* 97: 1024–1036.
- Irvine TN and Baragar WR (1971) A guide to the chemical classification of the common volcanic rocks. *Canadian Journal of Earth Sciences* 8: 523–548.
- Ishikawa T and Nakamura E (1994) Origin of the slab component in arc lavas from across-arc variation of B and Pb isotopes. *Nature* 370: 205–208.
- Iwamori H (1994) ²³⁸U–²³⁰Th–²²⁶Ra and ²³⁵U–²³¹Pa disequilibria produced by mantle melting with porous and channel flows. *Earth and Planetary Science Letters* 125: 1–16.
- Iwamori H (1997) Heat sources and melting in subduction zones. *Journal of Geophysical Research* 102: 14803–14820.
- Jan MQ (1977) The Kohistan basic complex: A summary based on recent petrological research. *Bulletin of the Centre of Excellence in Geology, University of Peshawar* 9–10(1): 36–42.
- Jan MQ (1988) Relative abundances of minor and trace elements in mafic phases from the southern part of the Kohistan Arc. *Geological Bulletin University of Peshawar* 21: 15–25.
- Jan MQ and Howie RA (1981) The mineralogy and geochemistry of the metamorphosed basic and ultrabasic rocks of the Jijal Complex, Kohistan, NW Pakistan. *Journal of Petrology* 22(1): 85–126.
- Jan MQ and Karim A (1995) Coronas and high-P veins in metagabbros of the Kohistan island arc, northern Pakistan: Evidence for crustal thickening during cooling. *Journal of Metamorphic Geology* 13(3): 357–366.
- Jan MQ, Wilson RN, and Windley BF (1982) Paragonite paragenesis from the garnet granulites of the Jijal Complex, Kohistan N. Pakistan. *Mineralogical Magazine* 45(337): 73–77.
- Jarrard RD (1986) Relations among subduction parameters. *Reviews of Geophysics* 24: 217–284.
- Johnson KTM and Dick HJB (1992) Open system melting and temporal and spatial variation of peridotite and basalt at the Atlantis II Fracture Zone. *Journal of Geophysical Research* 97: 9219–9241.

- Johnson KTM, Dick HJB, and Shimizu N (1990) Melting in the oceanic upper mantle: An ion microprobe study of diopsides in abyssal peridotites. *Journal of Geophysical Research* 95: 2661–2678.
- Johnson MC and Plank T (1999) Dehydration and melting experiments constrain the fate of subducted sediments. *Geochemistry, Geophysics, Geosystems* 1: Paper no. 1999GC000014.
- Johnston AD and Wyllie PJ (1988) Constraints on the origin of Archean trondhjemites based on phase relationships of Nuk gneiss with H₂O at 15 kbar. *Contributions to Mineralogy and Petrology* 100: 35–46.
- Jull M and Kelemen PB (2001) On the conditions for lower crustal convective instability. *Journal of Geophysical Research* 106: 6423–6446.
- Jull M, Kelemen PB, and Sims K (2002) Consequences of diffuse and channelled porous melt migration on U-series disequilibria. *Geochimica et Cosmochimica Acta* 66: 4133–4148.
- Kamenetsky VS, Crawford AJ, Eggins S, and Muhe R (1997) Phenocryst and melt inclusion chemistry of near-axis seamounts, Valu Fa Ridge, Lau Basin: Insight into mantle wedge melting and addition of subduction components. *Earth and Planetary Science Letters* 151: 205–223.
- Kawamoto T (1996) Experimental constraints on differentiation and H₂O abundance of calc-alkaline magmas. *Earth and Planetary Science Letters* 144: 577–589.
- Kawamoto T and Holloway JR (1997) Melting temperature and partial melt chemistry of H₂O saturated mantle peridotite to 11 Gigapascals. *Science* 276: 240–243.
- Kawate S and Arima M (1998) Petrogenesis of the Tanzawa plutonic complex, central Japan: Exposed felsic middle crust of the Izu-Bonin-Mariana arc. *The Island Arc* 7: 342–358.
- Kay RW (1978) Aleutian magnesian andesites: Melts from subducted Pacific ocean crust. *Journal of Volcanology and Geothermal Research* 4: 117–132.
- Kay RW (1980) Volcanic arc magmas: Implications of a melting-mixing model for element recycling in the crust-upper mantle system. *Journal of Geology* 88: 497–522.
- Kay RW and Kay SM (1988) Crustal recycling and the Aleutian arc. *Geochimica et Cosmochimica Acta* 52: 1351–1359.
- Kay RW and Kay SM (1991) Creation and destruction of lower continental crust. *Geologische Rundschau* 80: 259–278.
- Kay RW and Kay SM (1993) Delamination and delamination magmatism. *Tectonophysics* 219: 177–189.
- Kay SM and Kay RW (1985) Role of crystal cumulates and the oceanic crust in the formation of the lower crust of the Aleutian Arc. *Geology* 13: 461–464.
- Kay SM and Kay RW (1994) Aleutian magmas in space and time. In: Plafker G and Berg HC (eds.) *The Geology of Alaska: The Geology of North America*, vol. G-1, pp. 687–722. Boulder, CO: Geological Society of America.
- Kay SM, Kay RW, and Citron GP (1982) Tectonic controls on tholeiitic and calc-alkaline magmatism in the Aleutian Arc. *Journal of Geophysical Research* 87: 4051–4072.
- Kay SM, Kay RW, and Perfit MR (1990) Calc-alkaline plutonism in the intra-oceanic Aleutian arc, Alaska. In: Kay SM and Rapela CW (eds.) *Plutonism from Antarctica to Alaska. Geological Society of America Special Papers*, vol. 241, pp. 233–255. Boulder, CO: Geological Society of America.
- Kelemen PB (1986) Assimilation of ultramafic rock in subduction-related magmatic arcs. *Journal of Geology* 94: 829–843.
- Kelemen PB (1990) Reaction between ultramafic rock and fractionating basaltic magma. I: Phase relations, the origin of calc-alkaline magma series, and the formation of discordant dunite. *Journal of Petrology* 31: 51–98.
- Kelemen PB (1995) Genesis of high Mg# andesites and the continental crust. *Contributions to Mineralogy and Petrology* 120: 1–19.
- Kelemen PB and Aharonov E (1998) Periodic formation of magma fractures and generation of layered gabbros in the lower crust beneath oceanic spreading ridges. In: Buck WR, Delaney PT, Karson JA, and Lagabriele Y (eds.) *Faulting and Magmatism at Mid-Ocean Ridges. Geophysical Monograph Series*, vol. 106, pp. 267–289. Washington, DC: American Geophysical Union.
- Kelemen PB and Ghiorso MS (1986) Assimilation of peridotite in calc-alkaline plutonic complexes: Evidence from the Big Jim Complex, Washington Cascades. *Contributions to Mineralogy and Petrology* 94: 12–28.
- Kelemen PB, Hart SR, and Bernstein S (1998) Silica enrichment in the continental upper mantle lithosphere via melt/rock reaction. *Earth and Planetary Science Letters* 164: 387–406.
- Kelemen PB, Hirth G, and Shimizu N (1995a) Be and B partitioning in high pressure pelites, metabasalts, and peridotites: Potential sources for Be and B in arc magmas. In: Barnes HL (ed.) *V. M. Goldschmidt Conference Program and Abstracts*, vol. 60, May 24–26, 1995. State College, PA: Geochemical Society.
- Kelemen PB, Hirth G, Shimizu N, Spiegelman M, and Dick HJB (1997a) A review of melt migration processes in the asthenospheric mantle beneath oceanic spreading centers. *Philosophical Transactions of the Royal Society Series A* 355: 283–318.
- Kelemen PB, Joyce DB, Webster JD, and Holloway JR (1990a) Reaction between ultramafic rock and fractionating basaltic magma. II: Experimental investigation of reaction between olivine tholeiite and harzburgite at 1150–1050 °C and 5 kb. *Journal of Petrology* 31: 99–134.
- Kelemen PB, Joyce DB, Webster JD, and Holloway JR (1990b) Reaction between ultramafic rock and fractionating basaltic magma. II: Experimental investigation of reaction between olivine tholeiite and harzburgite at 1150–1050 °C and 5 kb. *Journal of Petrology* 31: 99–134.
- Kelemen PB, Koga K, and Shimizu N (1997b) Geochemistry of gabbro sills in the crust-mantle transition zone of the Oman ophiolite: Implications for the origin of the oceanic lower crust. *Earth and Planetary Science Letters* 146: 475–488.
- Kelemen PB, Rilling JL, Parmentier EM, Mehl L, and Hacker BR (2003a) Thermal structure due to solid-state flow in the mantle wedge beneath arcs. In: Eiler J (ed.) *Inside the Subduction Factory (Geophysical Monograph 138)*, pp. 293–311. Washington DC: American geophysical Union.
- Kelemen PB, Shimizu N, and Dunn T (1993) Relative depletion of niobium in some arc magmas and the continental crust: Partitioning of K, Nb, La, and Ce during melt/rock reaction in the upper mantle. *Earth and Planetary Science Letters* 120: 111–134.
- Kelemen PB, Shimizu N, and Salters VJM (1995b) Extraction of mid-ocean-ridge basalt from the upwelling mantle by focused flow of melt in dunite channels. *Nature* 375: 747–753.
- Kelemen PB, Yagodinski GM, and Scholl DW (2003b) Along strike variation in lavas of the Aleutian island arc: Implications for the genesis of high Mg# andesite and the continental crust. In: Eiler J (ed.) *Inside the Subduction Factory (Geophysical Monograph 138)*, pp. 223–276. Washington DC: American geophysical Union.
- Kemp AIS and Hawkesworth CJ (2003) Granitic perspectives on the generation and secular evolution of the continental crust. In: Holland HD and Turekian KK (eds.) *Treatise on Geochemistry*, vol. 3, pp. 349–410. Oxford: Elsevier.
- Kepezhinskas P, McDermott F, Defant MJ, et al. (1997) Trace element and Sr–Nd–Pb isotopic constraints on a three-component model of Kamchatka Arc petrogenesis. *Geochimica et Cosmochimica Acta* 61: 577–600.
- Keppler H (1996) Constraints from partitioning experiments on the composition of subduction-zone fluids. *Nature* 380: 237–240.
- Kerr BC and Klemperer S (2002) Wide-angle imaging of the Mariana Subduction Factory. *Eos, Transactions American Geophysical Union* 83(47) Fall Meeting Supplement.
- Khan MA, Jan MQ, Weaver BL, Treloar PJE, and Searle MPE (1993) Evolution of the lower arc crust in Kohistan N, Pakistan: Temporal arc magmatism through early, mature and intra-arc rift stages. *Himalayan Tectonics, Seventh Himalaya-Karakoram-Tibet Workshop* 74: 123–138.
- Khan MA, Jan MQ, Windley BF, Tarney J, and Thirlwall MF (1989) The Chilas mafic-ultramafic igneous complex: The root of the Kohistan island arc in the Himalaya of northern Pakistan. *Tectonics of the Western Himalayas. Geological Society of America Special Papers*, vol. 232, pp. 75–94.
- Kincaid C and Sacks IS (1997) Thermal and dynamical evolution of the upper mantle in subduction zones. *Journal of Geophysical Research* 102: 12295–12315.
- Kinzler RJ and Grove TL (1992) Primary magmas of mid-ocean ridge basalts. 2: Applications. *Journal of Geophysical Research* 97: 6907–6926.
- Kinzler RJ and Grove TL (1993) Corrections and further discussion of the primary magmas of mid-ocean ridge basalts, 1 and 2. *Journal of Geophysical Research* 98: 22339–22347.
- Klein E and Langmuir CH (1987) Global correlations of ocean ridge basalt chemistry with axial depth and crustal thickness. *Journal of Geophysical Research* 92: 8089–8115.
- Kogiso T, Tatsumi Y, and Nakano S (1997) Trace element transport during dehydration processes in the subducted oceanic crust. 1: Experiments and implications for the origin of ocean island basalts. *Earth and Planetary Science Letters* 148: 193–205.
- Korenaga J and Kelemen PB (1997) The origin of gabbro sills in the Moho transition zone of the Oman ophiolite: Implications for magma transport in the oceanic lower crust. *Journal of Geophysical Research* 102: 27729–27749.
- Korenaga J and Kelemen PB (2000) Major element heterogeneity in the mantle source of the North Atlantic igneous province. *Earth and Planetary Science Letters* 184: 251–268.
- Kuno H (1950) Petrology of Hakone volcano and the adjacent areas, Japan. *Geological Society of America Bulletin* 61: 957–1020.
- Kuno H (1968) Origin of andesite and its bearing on the island arc structure. *Bulletin of Volcanology* 32(1): 141–176.
- Kushiro I (1969) The system forsterite–diopside–silica with and without water at high pressures. *American Journal of Science* 267–A: 269–294.
- Kushiro I (1974) Melting of hydrous upper mantle and possible generation of andesitic magma: An approach from synthetic systems. *Earth and Planetary Science Letters* 22: 294–299.
- Kushiro I (1975) On the nature of silicate melt and its significance in magma genesis: Regularities in the shift of the liquidus boundaries involving olivine, pyroxene, and silica minerals. *American Journal of Science* 275: 411–431.

- Kushiro I (1990) Partial melting of mantle wedge and evolution of island arc crust. *Journal of Geophysical Research* 95: 15929–15939.
- Kushiro I and Yoder HS Jr. (1972) Origin of calc-alkalic peraluminous andesite and dacites. *Carnegie Institution Year Book* 71: 411–413.
- Lambert IB and Wyllie PJ (1972) Melting of gabbro (quartz eclogite) with excess water to 35 kilobars, with geological applications. *Journal of Geology* 80: 693–708.
- Langmuir CH, Bender JF, Bence AE, Hanson GN, and Taylor SR (1977) Petrogenesis of basalts from the famous area. Mid-Atlantic Ridge. *Earth and Planetary Science Letters* 36: 133–156.
- Larsen ES Jr. (1948) *Batholith and Associated Rocks of Corona, Elsinore, and San Luis Rey Quadrangles Southern California*. Cambridge, MA: Harvard University.
- Lassiter JC and Hauri EH (1998) Osmium-isotope variations in Hawaiian lavas: Evidence for recycled oceanic lithosphere in the Hawaiian plume. *Earth and Planetary Science Letters* 164: 483–496.
- Leeman WP (1987) Boron geochemistry of volcanic arc magmas: Evidence for recycling of subducted oceanic lithosphere. *Eos, Transactions American Geophysical Union* 68: 462.
- Leeman WP (1996) Boron and other fluid-mobile elements in volcanic arc lavas: Implications for subduction processes. In: Platt JP (ed.) *Subduction Top to Bottom. Geophysical Monograph Series*, vol. 96, pp. 269–276. Washington, DC: American Geophysical Union.
- Lundstrom C (2000) Models of U-series disequilibria generation in MORB: The effects of two scales of melt porosity. *Physics of the Earth and Planetary Interiors* 121: 189–204.
- Lundstrom CC, Gill J, and Williams Q (2000) A geochemically consistent hypothesis for MORB generation. *Chemical Geology* 162: 105–126.
- Lundstrom CC, Gill J, Williams Q, and Perfit MR (1995) Mantle melting and basalt extraction by equilibrium porous flow. *Science* 270: 1958–1961.
- Lundstrom CC, Sampson DE, Perfit MR, Gill J, and Williams Q (1999) Insights into mid-ocean ridge basalt petrogenesis: U-series disequilibria from the Siqueiros Transform, Lamont Seamounts, and East Pacific Rise. *Journal of Geophysical Research* 104: 13035–13048.
- Macdonald R, Hawkesworth CJ, and Heath E (2000) The Lesser Antilles volcanic chain: a study in arc magmatism. *Earth-Science Reviews* 49: 1–76.
- Marsh BD (1976) Some Aleutian andesites: Their nature and source. *Journal of Geology* 84: 27–45.
- Martin H (1986) Effect of steeper Archean geothermal gradient on geochemistry of subduction-zone magmas. *Geology* 14: 753–756.
- Martin H (1999) Adakitic magmas: Modern analogues of Archean granitoids. *Lithos* 46: 411–429.
- Martin G, Johnson B, and Grant U (1915) Geology, and mineral resources of Kenai Peninsula, Alaska. *US Geological Survey Bulletin Report B* 0587: 1–243.
- Matteini M, Mazzuoli R, Omarini R, Cas R, and Maas R (2002) The geochemical variations of the upper cenozoic volcanism along the Calama–Olacapato–El Toro transversal fault system in central Andes (~24 °S): petrogenetic and geodynamic implications. *Tectonophysics* 345: 211–227.
- Maury RC, Defant MJ, and Joron JL (1992) Metasomatism of the sub-arc mantle inferred from trace elements in Philippine xenoliths. *Nature* 360: 661–663.
- McBirney AR, Taylor HP, and Armstrong RL (1987) Paricutin re-examined: A classic example of crustal assimilation in calc-alkaline magma. *Contributions to Mineralogy and Petrology* 95: 4–20.
- McCullough MT and Gamble JA (1991) Geochemical and geodynamical constraints on subduction zone magmatism. *Earth and Planetary Science Letters* 102: 358–374.
- McKenzie D (1985) ^{230}Th – ^{238}U disequilibrium and the melting processes beneath ridge axes. *Earth and Planetary Science Letters* 72: 149–157.
- McLennan SM and Taylor SR (1985) *The Continental Crust: Its Composition and Evolution: An Examination of the Geochemical Record Preserved in Sedimentary Rocks*. Oxford: Blackwell Scientific.
- Miller DJ and Christensen NI (1994) Seismic signature and geochemistry of an island arc: A multidisciplinary study of the Kohistan accreted terrane, northern Pakistan. *Journal of Geophysical Research* 99: 11623–11642.
- Miller DM, Goldstein SL, and Langmuir CH (1994) Cerium/lead and lead isotope ratios in arc magmas and the enrichment of lead in the continents. *Nature* 368: 514–520.
- Millholland M, Graubard C, Mattinson J, and McClelland W (1987) U–Pb age of zircons from the Talkeetna formation, Johnson River area, Alaska. *Isochron/West* 50: 9–11.
- Miller DM, Langmuir CH, Goldstein SL, and Franks AL (1992) The importance of parental magma composition to calc-alkaline and tholeiitic evolution: Evidence from Umnak Island in the Aleutians. *Journal of Geophysical Research* 97(B1): 321–343.
- Miyashiro A (1974) Volcanic rock series in island arcs and active continental margins. *American Journal of Science* 274: 321–355.
- Monzier M, Robin C, Hall ML, et al. (1997) Les Adakites d'Equateur: References modele preliminaire. *Comptes Rendus de l'Académie des Sciences Series IIA* 324: 545–552.
- Morris JD, Leeman WP, and Tera F (1990) The subducted component in island arc lavas: Constraints from Be isotopes and B–Be systematics. *Nature* 344: 31–35.
- Müntener O, Kelemen PB, and Grove TL (2001) The role of H₂O and composition on the genesis of igneous pyroxenites: An experimental study. *Contributions to Mineralogy and Petrology* 141: 643–658.
- Myers JD, Frost CD, and Angevine CL (1986a) A test of a quartz eclogite source for parental Aleutian magmas: A mass balance approach. *Journal of Geology* 94: 811–828.
- Myers JD, Marsh BD, and Sinha AK (1985) Strontium isotopic and selected trace element variations between two Aleutian volcano centers (Adak and Atka): Implications for the development of arc volcanic plumbing systems. *Contributions to Mineralogy and Petrology* 91: 221–234.
- Myers JD, Marsh BD, and Sinha AK (1986b) Geochemical and strontium isotopic characteristics of parental Aleutian Arc magmas: Evidence from the basaltic lavas of Atka. *Contributions to Mineralogy and Petrology* 94: 1–11.
- Mysen B and Wheeler K (2000) Solubility behavior of water in haploandesitic melts at high pressure and high temperature. *American Mineralogist* 85: 1128–1142.
- Newberry R, Burns L, and Pessel P (1986) Volcanogenic massive sulfide deposits and the missing complement to the calc-alkaline trend: Evidence from the Jurassic Talkeetna island arc of southern Alaska. *Economic Geology* 81: 951–960.
- Newman S, Macdougall JD, and Finkel RC (1984) ^{230}Th – ^{238}U disequilibrium in island arcs: Evidence from the Aleutians and the Marianas. *Nature* 308: 268–270.
- Newman S, MacDougall JD, and Finkel RC (1986) Petrogenesis and ^{230}Th – ^{238}U disequilibrium at Mt. Shasta, California and in the Cascades. *Contributions to Mineralogy and Petrology* 93: 195–206.
- Nicholls IA (1974) Liquids in equilibrium with peridotite mineral assemblages at high water pressures. *Contributions to Mineralogy and Petrology* 45: 289–316.
- Nicholls IA and Ringwood AE (1973) Effect of water on olivine stability in tholeiites and the production of silica-saturated magmas in the island-arc environment. *Journal of Geology* 81: 285–300.
- Nichols GT, Wyllie PJ, and Stern CR (1994) Subduction zone melting of pelagic sediments constrained by melting experiments. *Nature* 371: 785–788.
- Nokleberg W, Platker G, and Wilson F (1994) Geology of south-central Alaska. *The Geology of Alaska. The Geology of North America*, vol. G-1, pp. 311–366. Boulder, CO: Geological Society of America.
- Nye CJ (1983) *Petrology and Geochemistry of Okmok and Wrangell Volcanoes, Alaska*, p. 215. PhD Thesis, University of California at Santa Cruz.
- Nye CJ and Reid MR (1986) Geochemistry of primary and least fractionated lavas from Okmok Volcano, Central Aleutians: Implications for arc magmatogenesis. *Journal of Geophysical Research* 91: 10271–10287.
- Nye CJ and Reid MR (1987) Corrections to Geochemistry of primary and least fractionated lavas from Okmok volcano, central Aleutians: Implications for magmatogenesis. *Journal of Geophysical Research* 92: 8182.
- O'Hara MJ and Mathews RE (1981) Geochemical evolution in an advancing, periodically replenished, periodically tapped, continuously fractionated magma chamber. *Journal of the Geological Society* 138: 237–277.
- Osborn EF (1959) Role of oxygen pressure in the crystallization and differentiation of basaltic magma. *American Journal of Science* 257: 609–647.
- Ozawa K (2001) Mass balance equations for open magmatic systems: Trace element behavior and its application to open system melting in the upper mantle. *Journal of Geophysical Research* 106: 13407–14434.
- Ozawa K and Shimizu N (1995) Open-system melting in the upper mantle: Constraints from the Hayachine-Miyamori ophiolite, northeastern Japan. *Journal of Geophysical Research* 100(No. B11): 22315–22335.
- Palfy J, Smith P, Mortensen J, and Friedman R (1999) Integrated ammonite biochronology and U–Pb geochronometry from a basal Jurassic section in Alaska. *Geological Society of America Bulletin* 111: 1537–1549.
- Parkinson IJ and Arculus RJ (1999) The redox state of subduction zones: Insights from arc peridotites. *Chemical Geology* 160: 409–423.
- Patino LC, Carr MJ, and Feigenson MD (2000) Local and regional variations in Central American arc lavas controlled by variations in subducted sediment input. *Contributions to Mineralogy and Petrology* 138: 265–283.
- Pavlis T (1983) Pre-cretaceous crystalline rocks of the western Chugach Mountains, Alaska: Nature of the basement of the Jurassic Peninsular terrane. *Geological Society of America Bulletin* 94: 1329–1344.
- Peacock SM (1996) Thermal and petrologic structure of subduction zones. In: Bebout GE, Scholl DW, Kirby SH, and Platt JP (eds.) *Subduction Zones, Top to Bottom. Geophysics Monograph Series*, vol. 96, pp. 119–133. Washington, DC: American Geophysical Union.

- Peacock SM (2003) Thermal structure and metamorphic evolution of subducting slabs. In: Eiler J (ed.) *Inside the Subduction Factory (Geophysical Monograph 138)*, pp. 7–22. Washington DC: American geophysical Union.
- Peacock SM, Rushmer T, and Thompson AB (1994) Partial melting of subducting oceanic crust. *Earth and Planetary Science Letters* 121: 227–244.
- Pearce JA (1982) Trace element characteristics of lavas from destructive plate boundaries. In: Thorpe RS (ed.) *Andesites: Orogenic Andesites and Related Rocks*, pp. 526–547. Chichester: Wiley.
- Pearce JA and Peate DW (1995) Tectonic implications of the composition of volcanic arc magmas. *Annual Review of Earth and Planetary Sciences* 23: 251–285.
- Pearce JA, van der Laan SR, Arculus RJ, et al. (1992) 38 Boninite and Harzburgite from Leg 125 (Bonin–Mariana Forearc): A case study of magmatogenesis during the initial stages of subduction. *Proceedings of the Ocean Drilling Program, Scientific Results* 125: 623–659.
- PetDB website—Petrological Database of the Ocean Floor, <http://www.petdb.org/> (accessed June 2006).
- Petterson MG, Crawford MB, and Windley BF (1993) Petrogenetic implications of neodymium isotope data from the Kohistan Batholith, North Pakistan. *Journal of the Geological Society* 150(Part 1): 125–129.
- Petterson MG and Windley BF (1985) Rb–Sr dating of the Kohistan arc-batholith in the Trans-Himalaya of North Pakistan, and tectonic implications. *Earth and Planetary Science Letters* 74(1): 45–57.
- Petterson MG and Windley BF (1992) Field relations, geochemistry and petrogenesis of the Cretaceous basaltic Jutal dykes, Kohistan, northern Pakistan. *Journal of the Geological Society* 149(part 1): 107–114.
- Petterson MG, Windley BF, and Sullivan M (1991) A petrological, chronological, structural and geochemical review of Kohistan Batholith and its relationship to regional tectonics. *Physics and Chemistry of the Earth* 17(Part II): 47–70.
- Pichavant M, Mysen BO, and Macdonald R (2002) Source and H₂O content of high-MgO magmas in island arc settings: An experimental study of a primitive calc-alkaline basalt from St. Vincent, Lesser Antilles arc. *Geochimica et Cosmochimica Acta* 66: 2193–2209.
- Pickett DA and Saleeby JB (1993) Thermobarometric constraints on the depth of exposure and conditions of plutonism and metamorphism at deep levels of the Sierra Nevada Batholith, Tehachapi Mountains, California. *Journal of Geophysical Research* 98: 609–629.
- Pickett DA and Saleeby JB (1994) Nd, Sr, and Pb isotopic characteristics of Cretaceous intrusive rocks from deep levels of the Sierra Nevada Batholith, Tehachapi Mountains, California. *Contributions to Mineralogy and Petrology* 118: 198–215.
- Plafker G, Nokleberg WJ, and Lull JS (1989) Bedrock geology and tectonic evolution of the Wrangellia, Peninsular, and Chugach terranes along the trans-Alaska crustal transect in the Chugach Mountains and Southern Copper River Basin, Alaska. *Journal of Geophysical Research* 94(B4): 4255–4295.
- Plank T (2003) Constraints from Th/La on the evolution of the continents. *Journal of Petrology* (submitted).
- Plank T and Langmuir CH (1988) An evaluation of the global variations in the major element chemistry of arc basalts. *Earth and Planetary Science Letters* 90: 349–370.
- Plank T and Langmuir CH (1993) Tracing trace elements from sediment input to volcanic output at subduction zones. *Nature* 362: 739–743.
- Plank T and Langmuir CH (1998) The chemical composition of subducting sediment and its consequences for the crust and mantle. *Chemical Geology* 145: 325–394.
- Presnall DC and Hoover JD (1984) Composition and depth of origin of primary mid-ocean ridge basalts. *Contributions to Mineralogy and Petrology* 87: 170–178.
- Ramsay WRH, Crawford AJ, and Foden JD (1984) Field setting, mineralogy, chemistry and genesis of arc picrites, New Georgia, Solomon Islands. *Contributions to Mineralogy and Petrology* 88: 386–402.
- Ranero CR and von Huene R (2000) Subduction erosion along the Middle America convergent margin. *Nature* 404: 748–755.
- Rapp RP, Shimizu N, Norman MD, and Applegate GS (1999) Reaction between slab-derived melts and peridotite in the mantle wedge: Experimental constraints at 3.8 GPa. *Chemical Geology* 160: 335–356.
- Rapp RP and Watson EB (1995) Dehydration melting of metabasalt at 8–32 kbar: Implications for continental growth and crust-mantle recycling. *Journal of Petrology* 36(4): 891–931.
- Rapp RP, Watson EB, and Miller CF (1991) Partial melting of amphibolite/eclogite and the origin of Archean trondhjemites and tonalites. *Precambrian Research* 51: 1–25.
- Reagan MK and Gill JB (1989) Coexisting calcalkaline and high-niobium basalts from Turrialba Volcano, Costa Rica: Implications for residual titanates in arc magma sources. *Journal of Geophysical Research* 94: 4619–4633.
- Reagan MK, Morris JD, Herrstrom EA, and Murrell MT (1994) Uranium series and beryllium isotope evidence for an extended history of subduction modification of the mantle below Nicaragua. *Geochimica et Cosmochimica Acta* 58: 4199–4212.
- Regelous M, Collerson KD, Ewart A, and Wendt JI (1997) Trace element transport rates in subduction zones: Evidence from Th, Sr and Pb isotope data for Tonga–Kermadec arc lavas. *Earth and Planetary Science Letters* 150: 291–302.
- Richardson C and McKenzie D (1994) Radioactive disequilibria from 2D models of melt generation by plumes and ridges. *Earth and Planetary Science Letters* 128: 425–437.
- Ringuette L, Martignole J, and Windley BF (1999) Magmatic crystallization, isobaric cooling, and decompression of the garnet-bearing assemblages of the Jijal Sequence (Kohistan Terrane, western Himalayas). *Nature* 27(2): 139–142.
- Ringwood AE (1966) The chemical composition and origin of the Earth. In: Hurley PM (ed.) *Advances in Earth Science*, pp. 287–356. Cambridge, MA: MIT Press.
- Ringwood AE (1974) The petrological evolution of island arc systems. *Journal of the Geological Society* 130: 183–204.
- Rioux M, Mattinson J, Hacker B, and Grove M (2002a) Growth and evolution of the accreted Talkeetna arc, southcentral Alaska: Solutions to the arc paradox. *Geological Society of America Abstracts with Programs* 34: 269–270.
- Rioux M, Mattinson J, Hacker B, and Grove M (2002b) Growth and evolution of the accreted Talkeetna arc, southcentral Alaska: Solutions to the “arc paradox.” *Eos, Transactions American Geophysical Union, Fall Meeting Abstracts* 83: 1482.
- Rioux M, Mehl L, Hacker B, Mattinson J, Gans P, and Wooden J (2001a) Understanding island arc evolution through U–Pb and ⁴⁰Ar–³⁹Ar geochronology of the Talkeetna arc, south-central Alaska. *Eos, Transactions American Geophysical Union, Fall Meeting Abstracts* 82: 120.
- Rioux M, Mehl L, Hacker B, Mattinson J, and Wooden J (2001b) Understanding island arc thermal structure through U–Pb and ⁴⁰Ar–³⁹Ar geochronology of the Talkeetna arc section, south central Alaska. *Geological Society of America Abstracts with Programs* 33: 256–257.
- Roeske S, Mattinson J, and Armstrong R (1989) Isotopic ages of glaucophane schists on the Kodiak Islands, southern Alaska, and their implications for the Mesozoic tectonic history of the Border Ranges fault system. *Geological Society of America Bulletin* 101: 1021–1037.
- Rogers G, Saunders AD, Terrell DJ, Verma SP, and Marriner GF (1985) Geochemistry of Holocene volcanic rocks associated with ridge subduction in Baja California, Mexico. *Nature* 315: 389–392.
- Roggensack K, Hervig RL, McKnight SB, and Williams SN (1997) Explosive basaltic volcanism from Cerro Negro volcano: Influence of volatiles on eruptive style. *Science* 277: 1639–1642.
- Rowland AD and Davies HJ (1999) Buoyancy rather than rheology controls the thickness of the overriding mechanical lithosphere at subduction zones. *Geophysical Research Letters* 26: 3037–3040.
- Rudnick RL (1995) Making continental crust. *Nature* 378: 571–577.
- Rudnick RL and Fountain DM (1995) Nature and composition of the continental crust: a lower crustal perspective. *Reviews of Geophysics* 33(3): 267–309.
- Rudnick RL, McDonough WF, and Orpin A (1994) Northern Tanzania peridotite xenoliths: A comparison with Kapvaal peridotites and inferences on metasomatic reactions. In: Meyer HOA, Leonards O, and Othon H (eds.) *Kimberlites, Related Rocks and Mantle Xenoliths: Vol. 1. Proceedings of the 5th International Kimberlite Conference, CRPM-Special Publication, Araxa, Brazil*, vol. 1A, pp. 336–353. Rio de Janeiro, Brazil: Companhia de Pesquisa de Recursos Minerais.
- Rudnick RL and Presper T (1990) Geochemistry of intermediate- to high-pressure granulites. In: Vielzeuf D and Vidal P (eds.) *Granulites and Crustal Evolution. NATO ASI Series C: Mathematical and Physical Sciences*, vol. 311, pp. 523–550. Dordrecht, Boston: D. Reidel Publishing Company.
- Ryan JG and Langmuir CH (1992) The systematics of boron abundances in young volcanic rocks. *Geochimica et Cosmochimica Acta* 57: 1489–1498.
- Ryan JG, Leeman WP, Morris JD, and Langmuir CH (1989) B/Be and Li/Be systematics and the nature of subducted components in the Mantle. *Eos, Transactions American Geophysical Union* 70: 1388.
- Ryerson FJ (1985) Oxide solution mechanisms in silicate melts: Systematic variations in the activity coefficient of SiO₂. *Geochimica et Cosmochimica Acta* 49: 637–649.
- Ryerson FJ and Watson EB (1987) Rutile saturation in magmas: Implications for Ti–Nb–Ta depletion in island-arc basalts. *Earth and Planetary Science Letters* 86: 225–239.
- Saal AE, Van Orman JA, Hauri EH, Langmuir CH, and Perfit MR (2002) An alternative hypothesis for the origin of the high ²²⁶Ra excess in MORBs. *Eos, Transactions American Geophysical Union* 83(47), Fall Meeting Supplement.
- Schiano P, Birck JL, and Allégre CJ (1997) Osmium–strontium–neodymium–lead isotopic covariations in midocean ridge basalt glasses and the heterogeneity of the upper mantle. *Earth and Planetary Science Letters* 150: 363–379.
- Schiano P, Clochiatti R, Shimizu N, Maury RC, Jochum KP, and Hofmann AW (1995) Hydrous, silica-rich melts in the sub-arc mantle and their relationship with erupted arc lavas. *Nature* 377: 595–600.

- Schmidt MW and Poli S (1998) Experimentally based water budgets for dehydrating slabs and consequences for arc magma generation. *Earth and Planetary Science Letters* 163(1–4): 361–379.
- Scholl DW, Vallier TL, and Stevenson AJ (1987) Geologic evolution and petroleum geology of the Aleutian Ridge. In: Scholl DW, Grantz A, and Vedder JG (eds.) *Geology and Resource Potential of the Continental Margin of Western North America and Adjacent Ocean Basins. Beaufort Sea to Baja California, Circum-Pacific Council for Energy and Mineral Resources. Earth Science Series*, vol. 6, pp. 123–155. Houston, TX: Circum-Pacific Council for Energy and Mineral Resources.
- Shah MT and Shervais JW (1999) The Dir-Utror metavolcanic sequence, Kohistan arc terrane, northern Pakistan. *Journal of Asian Earth Sciences* 17(4): 459–475.
- Shaw DM (1970) Trace element fractionation during anatexis. *Geochimica et Cosmochimica Acta* 34: 237–243.
- Shimoda G, Tatsumi Y, Nohda S, Ishizaka K, and Jahn BM (1998) Setouchi high-Mg andesites revisited: Geochemical evidence for melting of subducting sediments. *Earth and Planetary Science Letters* 160: 479–492.
- Sigmarsson O, Chmiele J, Morris J, and Lopez-Escobar L (2002) Origin of $^{226}\text{Ra}/^{230}\text{Th}$ disequilibria in arc lavas from southern Chile and implications for magma transfer time. *Earth and Planetary Science Letters* 196: 189–196.
- Sigmarsson O, Condomines M, Morris JD, and Harmon RS (1990) Uranium and ^{10}Be enrichments by fluids in Andean arc magmas. *Nature* 346: 163–165.
- Sigmarsson O, Martin H, and Knowles J (1998) Melting of a subducting oceanic crust from U–Th disequilibria in austral Andean lavas. *Nature* 394: 566–569.
- Silver LT and Chappell BW (1988) The Peninsular Ranges batholith: An insight into the evolution of the Cordilleran batholiths of southwestern North America. *Transactions of the Royal Society of Edinburgh: Earth and Environmental Science* 79: 105–121.
- Sims KW, Goldstein SJ, Blichert-Toft J, et al. (2002) Chemical and isotopic constraints on the generation and transport of magma beneath the East Pacific Rise. *Geochimica et Cosmochimica Acta* 66: 3481–3504.
- Singer BS, Myers JD, and Frost CD (1992a) Mid-Pleistocene basalts from the Segum Volcanic Center, Central Aleutian arc, Alaska: Local lithospheric structures and source variability in the Aleutian arc. *Journal of Geophysical Research* 97: 4561–4578.
- Singer BS, Myers JD, and Frost CD (1992b) Mid-Pleistocene lavas from the Segum Island volcanic center, central Aleutian arc: Closed-system fractional crystallization of a basalt to rhyodacite eruptive suite. *Contributions to Mineralogy and Petrology* 110: 87–112.
- Sisson TW and Bronto S (1998) Evidence for pressure-release melting beneath magmatic arcs from basalt at Galunggung, Indonesia. *Nature* 391: 883–886.
- Sisson TW and Grove TL (1993a) Experimental investigations of the role of H_2O in calc-alkaline differentiation and subduction zone magmatism. *Contributions to Mineralogy and Petrology* 113: 143–166.
- Sisson TW and Grove TL (1993b) Temperatures and H_2O contents of low MgO high-alumina basalts. *Contributions to Mineralogy and Petrology* 113: 167–184.
- Sisson TW and Layne GD (1993) H_2O in basalt and basaltic andesite glass inclusions from four subduction-related volcanoes. *Earth and Planetary Science Letters* 117: 619–635.
- Sobolev AV and Chaussidon M (1996) H_2O concentrations in primary melts from supra-subduction zones and mid-ocean ridges. *Earth and Planetary Science Letters* 137: 45–55.
- Sobolev AV and Danyushevsky LV (1994) Petrology and geochemistry of boninites from the north termination of the Tonga Trench: Constraints on the generation conditions of primary high-Ca boninite magmas. *Journal of Petrology* 35: 1183–1211.
- Sobolev AV, Hofmann AW, and Nikogosian IK (2000) Recycled oceanic crust observed in 'ghost plagioclase' within the source of Mauna Loa lavas. *Nature* 404: 986–990.
- Sobolev AV and Shimizu N (1992) Superdepleted melts and ocean mantle permeability. *Doklady Rossiyskoy Akademii Nauk* 326(2): 354–360.
- Spiegelman M and Elliot T (1992) Consequences of melt transport for uranium series disequilibrium in young lavas. *Earth and Planetary Science Letters* 118: 1–20.
- Spiegelman M, Kelemen PB, and Aharonov E (2001) Causes and consequences of flow organization during melt transport: The reaction infiltration instability. *Journal of Geophysical Research* 106: 2061–2078.
- Spiegelman M and McKenzie D (1987) Simple 2-D models for melt extraction at mid-ocean ridges and island arcs. *Earth and Planetary Science Letters* 83: 137–152.
- Stalder R, Foley SF, Brey GP, and Horn I (1998) Mineral-aqueous fluid partitioning of trace elements at 900–1200 °C and 3.0–5.7 GPa: New experimental data for garnet, clinopyroxene and rutile and implications for mantle metasomatism. *Geochimica et Cosmochimica Acta* 62: 1781–1801.
- Stern CR and Kilian R (1996) Role of the subducted slab, mantle wedge and continental crust in the generation of adakites from the Andean Austral Volcanic Zone. *Contributions to Mineralogy and Petrology* 123: 263–281.
- Stern CR and Wyllie PJ (1973) Melting relations of basalt–andesite–rhyolite H_2O and a pelagic red clay at 30 kb. *Contributions to Mineralogy and Petrology* 42: 313–323.
- Stern RJ and Bloomer SH (1992) Subduction zone infancy: Examples from the Eocene Izu–Bonin–Mariana and Jurassic California arcs. *Geological Society of America Bulletin* 104: 1621–1636.
- Stolper E and Newman S (1992) The role of water in the petrogenesis of Mariana Trough magmas. *Earth and Planetary Science Letters* 121: 293–325.
- Sullivan MA, Windley BF, Saunders AD, Haynes JR, and Rex DC (1993) A palaeogeographic reconstruction of the Dir Group: Evidence for magmatic arc migration within Kohistan N. Pakistan. *Himalayan Tectonics, Seventh Himalaya–Karakoram–Tibet Workshop* 74: 139–160.
- Sun SS and McDonough WF (1989) Chemical and isotopic systematics of oceanic basalts: Implications for mantle composition and processes. *Geological Society Special Publication* 42: 313–345.
- Suyehiro K, Takahashi N, Arie Y, et al. (1996) Continental crust, crustal underplating, and low-Q upper mantle beneath an oceanic island arc. *Science* 272: 390–392.
- Tahirkheli RAKE (1979) Geotectonic evolution of Kohistan. In: Tahirkheli RAKE and Jan MQE (eds.) *Geology of Kohistan, Karakoram Himalaya, Northern Pakistan, Geological Bulletin University of Peshawar*, vol. 11, pp. 113–130. Peshawar, Pakistan: University of Peshawar.
- Tatsumi Y (1981) Melting experiments on a high-magnesian andesite. *Earth and Planetary Science Letters* 54: 357–365.
- Tatsumi Y (1982) Origin of high-magnesian andesites in the Setouchi volcanic belt, southwest Japan. II: Melting phase relations at high pressures. *Earth and Planetary Science Letters* 60: 305–317.
- Tatsumi Y (2000) Continental crust formation by delamination in subduction zones and complementary accumulation of the enriched mantle I component in the mantle. *Geochimistry, Geophysics, Geosystems* 1: 1–17.
- Tatsumi Y (2001) Geochemical modelling of partial melting of subducting sediments and subsequent melt–mantle interaction: Generation of high-Mg andesites in the Setouchi volcanic belt, southwest Japan. *Geology* 29(4): 323–326.
- Tatsumi Y and Eggins S (1995) *Subduction Zone Magmatism*. Oxford: Blackwell.
- Tatsumi Y and Ishizaka K (1981) Existence of andesitic primary magma: An example from southwest Japan. *Earth and Planetary Science Letters* 53: 124–130.
- Tatsumi Y and Ishizaka K (1982) Origin of high-magnesian andesites in the Setouchi volcanic belt, southwest Japan. I: Petrographical and chemical characteristics. *Earth and Planetary Science Letters* 60: 293–304.
- Tatsumi Y and Kogiso T (1997) Trace element transport during dehydration processes in the subducted oceanic crust. 2: Origin of chemical and physical characteristics in arc magmatism. *Earth and Planetary Science Letters* 148: 207–221.
- Tatsumi Y, Sakuyama M, Fukuyama H, and Kushiro I (1983) Generation of arc basalt magmas and thermal structure of the mantle wedge in subduction zones. *Journal of Geophysical Research* 88: 5815–5825.
- Taylor SR (1977) Island arc models and the composition of the continental crust. In: Talwani M and Pitman WC (eds.) *Island Arcs, Deep Sea Trenches, and Back-Arc Basins. Geophysical Monograph Series*, vol. 1, pp. 325–335. Washington, DC: American Geophysical Union.
- Tepper JH, Nelson BK, Bergantz GW, and Irving AJ (1993) Petrology of the Chilliwack batholith, North Cascades, Washington: generation of calc-alkaline granitoids by melting of mafic lower crust with variable water fugacity. *Contributions to Mineralogy and Petrology* 113: 333–351.
- The Aleutian Arc website—website hosted by the Department of Geology and Geophysics, University of Wyoming, <http://www.gg.uwyo.edu/aleutians/index.htm> (accessed June 2006).
- Thomas RB, Hirschmann MM, Cheng H, Reagan MK, and Edwards RL (2002) ($^{231}\text{Pa}/^{235}\text{U}$)–($^{230}\text{Th}/^{238}\text{U}$) of young mafic volcanic rocks from Nicaragua and Costa Rica and the influence of flux melting on U-series systematics of arc lavas. *Geochimica et Cosmochimica Acta*, 66: 4287–4309.
- Tomascak PB, Ryan JG, and Defant MJ (2000) Lithium isotope evidence for light element decoupling in the Panama subarc mantle. *Geology* 28: 507–510.
- Treloar PJ (1995) Pressure–temperature–time paths and the relationship between collision, deformation and metamorphism in the north-west Himalaya. *Geological Journal* 30: 333–348.
- Treloar PJ, O'Brien PJ, and Khan MA (2001) Exhumation of early Tertiary, coesite-bearing eclogites from the Kaghan valley, Pakistan Himalaya, Abstracts: 16th Himalaya–Karakoram–Tibet Workshop, Austria. *Journal of Asian Earth Sciences* 19: 68–69.
- Treloar PJ, Petterson MG, Jan MQ, and Sullivan MA (1996) A re-evaluation of the stratigraphy and evolution of the Kohistan Arc sequence, Pakistan Himalaya: Implications for magmatic and tectonic arc-building processes. *Journal of the Geological Society* 153: 681–693.
- Turcotte DL (1989) Geophysical processes influencing the lower continental crust. In: Mereu RF, Mueller S, and Fountain DM (eds.) *Properties and Processes of*

- Earth's Lower Crust. Geophysical Monograph Series*, vol. 51, pp. 321–329. Washington, DC: American Geophysical Union.
- Turner S, Blundy J, Wood B, and Hole M (2000b) Large ^{230}Th excesses in basalts produced by partial melting of spinel lherzolite. *Chemical Geology* 162: 127–136.
- Turner S, Bourdon B, and Gill J (2003) Insights into magma genesis at convergent margins from U-series isotopes, Chapter 7. In: Bourdon B, Henderson G, Lundstrom C, and Turner S (eds.) *Uranium Series Geochemistry. Review of Mineralogy and Geochemistry*, vol. 52, pp. 255–312. Washington, DC: Mineralogical Society of America and Geochemical Society.
- Turner S, Bourdon B, Hawkesworth C, and Evans P (2000a) ^{226}Ra – ^{230}Th evidence for multiple dehydration events, rapid melt ascent and the timescales of differentiation beneath the Tonga–Kermadec island arc. *Earth and Planetary Science Letters* 179: 581–593.
- Turner S, Evans P, and Hawkesworth CJ (2001) Ultrafast source-to-surface movement of melt at island arcs from ^{226}Ra – ^{230}Th systematics. *Science* 292: 1363–1366.
- Turner S and Foden J (2001) U, Th and Ra disequilibria, Sr, Nd and Pb isotope and trace element variations in Sunda arc lavas: Predominance of a subducted sediment component. *Contributions To Mineralogy and Petrology* 142: 43–57.
- Turner S, Hawkesworth C, Rogers N, et al. (1997) ^{238}U – ^{230}Th disequilibria, magma petrogenesis, and flux rates beneath the depleted Tonga–Kermadec island arc. *Geochimica et Cosmochimica Acta* 61: 4855–4884.
- Turner SP, George RMM, Evans PJ, Hawkesworth CJ, and Zellmer GF (2000c) Timescales of magma formation, ascent and storage beneath subduction-zone volcanoes. *Philosophical Transactions of the Royal Society Series A* 358: 1443–1464.
- Ulmer P (2001) Partial melting in the mantle wedge: The role of H_2O in the genesis of mantle derived, arc-related, magmas. *Physics of the Earth and Planetary Interiors*. 127: 215–232.
- van Keken PE, Kiefer B, and Peacock SM (2002) High resolution models of subduction zones: Implications for mineral dehydration reactions and the transport of water into the deep mantle. *Geochemistry, Geophysics, Geosystems* 3: pp. 2001GC000256.
- Van Orman J, Saal A, Bourdon B, and Hauri E (2002) A new model for U-series isotope fractionation during igneous processes, with finite diffusion and multiple solid phases. *Eos, Transactions American Geophysical Union* 83(47) Fall Meeting Supplement.
- Vannucchi P, Scholl DW, Meschede M, and McDougall-Reid K (2001) Tectonic erosion and consequent collapse of the Pacific margin of Costa Rica: Combined implications from ODP Leg 170, seismic offshore data, and regional geology of the Nicoya Peninsula. *Tectonics* 20: 649–668.
- Vernieres J, Godard M, and Bodinier J-L (1997) A plate model for the simulation of trace element fractionation during partial melting and magma transport in the Earth's upper mantle. *Journal of Geophysical Research* 102: 24771–24784.
- von Huene R and Scholl DW (1991) Observations at convergent margins concerning sediment subduction, subduction erosion, and the growth of continental crust. *Reviews of Geophysics* 29: 279–316.
- von Huene R and Scholl DW (1993) The return of sialic material to the mantle indicated by terrigenous material subducted at convergent margins. *Tectonophysics* 219: 163–175.
- Watson EB and Lupulescu A (1993) Aqueous fluid connectivity and chemical transport in clinopyroxene-rich rocks. *Earth and Planetary Science Letters* 117: 279–294.
- Weaver BL and Tarney J (1984) Empirical approach to estimating the composition of the continental crust. *Nature* 310: 575–577.
- White C and McBirney AR (1978) Some quantitative aspects of orogenic volcanism in the Oregon Cascades. *Geological Society of America Memoir* 153: 369–388.
- Wilcox RE (1944) Rhyolite-basalt complex on Gardiner River, Yellowstone Park, Wyoming. *Geological Society of America Bulletin* 55: 1047–1080.
- Winkler GR, Silberman ML, Grantz A, Miller RJ, and MacKevett JEM (1981) Geologic map and summary geochronology of the Valdez Quadrangle, Southern Alaska. *US Geological Survey Open File Report* 80–892-A.
- Wood BJ, Blundy JD, and Robinson JAC (1999) The role of clinopyroxene in generating U-series disequilibrium during mantle melting. *Geochimica et Cosmochimica Acta* 63: 1613–1620.
- Yamamoto H (1993) Contrasting metamorphic P–T–t paths of the Kohistan granulites and tectonics of the western Himalayas. *Journal of the Geological Society* 150(Part 5): 843–856.
- Yamamoto H and Yoshino T (1998) Superposition of replacements in the mafic granulites of the Jijal Complex of the Kohistan Arc, northern Pakistan: Dehydration and rehydration within deep arc crust. *Lithos* 43(4): 219–234.
- Yogodzinski GM, Kay RW, Volynets ON, Koloskov AV, and Kay SM (1995) Magnesian andesite in the western Aleutian Komandorsky region: Implications for slab melting and processes in the mantle wedge. *Geological Society of America Bulletin* 107(5): 505–519.
- Yogodzinski GM and Kelemen PB (1998) Slab melting in the Aleutians: Implications of an ion probe study of clinopyroxene in primitive adakite and basalt. *Earth and Planetary Science Letters* 158: 53–65.
- Yogodzinski GM and Kelemen PB (2000) Geochemical diversity in primitive Aleutian magmas: Evidence from an ion probe study of clinopyroxene in mafic and ultramafic xenoliths. *Eos, Transactions American Geophysical Union* 81: F1281.
- Yogodzinski GM, Lees JM, Churikova TG, Dorendorf F, Woerner G, and Volynets ON (2001) Geochemical evidence for the melting of subducting oceanic lithosphere at plate edges. *Nature* 409: 500–504.
- Yogodzinski GM, Volynets ON, Koloskov AV, Seliverstov NI, and Matvenkov VV (1994) Magnesian andesites and the subduction component in a strongly calc-alkaline series at Piip Volcano, Far Western Aleutians. *Journal of Petrology* 35(1): 163–204.
- Yoshino T and Satish-Kumar M (2001) Origin of scapolite in deep-seated metagabbros of the Kohistan Arc, NW Himalayas. *Contributions to Mineralogy and Petrology* 140(5): 511–531.
- You CF, Spivack AJ, Gieskes JM, Rosenbauer R, and Bischoff JL (1995) Experimental study of boron geochemistry: Implications for fluid processes in subduction zones. *Geochimica et Cosmochimica Acta* 59: 2435–2442.
- You CF, Spivack AJ, Smith JH, and Gieskes JM (1993) Mobilization of boron in convergent margins: Implications for the boron geochemical cycle. *Geology* 21: 207–210.
- Zegers TE and van Keken PE (2001) Middle Archean continent formation by crustal delamination. *Geology* 29: 1083–1086.
- Zhao D, Horiuchi S, and Hasegawa A (1992) Seismic velocity structure of the crust beneath the Japan Islands. *Tectonophysics* 212(3–4): 289–301.
- Zhao D, Yingbiao X, Weins DA, Dorman L, Hildebrand J, and Webb S (1997) Depth extent of the Lau back-arc spreading center and its relation to subduction processes. *Science* 278: 254–257.

